

Sand demand of the Eastern Scheldt

morphology around the barrier



Prepared for:
Waterdienst

Sand demand of the Eastern Scheldt

morphology around the barrier

B.J.A. Huisman
A.P. Luijendijk

Report

February 2009

Client	Waterdienst						
Title	Sand demand of the Eastern Scheldt						
Abstract							
<p>In 2008, Deltares was requested by 'Rijkswaterstaat - De Waterdienst' (Dutch governmental centre for water management) to perform a study investigating the reduction of the inter-tidal areas in the Eastern Scheldt. This report presents the evaluation of potential measures for the Eastern Scheldt barrier, which should enhance the import of sediment or the tidal prism inside the basin. For this purpose, the morphology around the barrier is studied, as sufficient sediment should be able to reach the barrier if sediment import is to be enhanced. The assessment in this report includes:</p> <ul style="list-style-type: none"> • review of information in literature on the morphological system of the Eastern Scheldt • assessment of time development of scour holes near to the barrier (with bathymetry data) • set up of a wave model to compute wave forces • derivation of tidal data from the operational model 'MATROOS' • set up of a model to compute wave induced longshore sediment transport along the coasts of Walcheren and Schouwen • set up of a morphological point model to compute tide driven (net) sediment transports in the Eastern Scheldt delta <p>Five measures were assessed (1: 'filling and covering the scour hole(s)', 2: 'adjusting the barrier structure', 3: 'opening land heads', 4: 'manipulation of the barrier operation', 5: 'directly or indirectly (by means of a pipeline) nourishing sediment into the basin'), of which filling the scour hole was considered in combination with a large nourishment. The first and the last one are regarded the alternatives with most potential to be effective (on the basis of morphological considerations).</p>							
References			Deltares, 2008				
Ver	Author		Date	Remarks	Review		Approved by
1.0	B.J.A. Huisman A.P. Luijendijk		16-12-2008	Draft	K.J. Bos		W.M.K. Tilmans
1.1	B.J.A. Huisman A.P. Luijendijk		<i>Bilin</i> 25-02-2009	Final	K.J. Bos <i>[Signature]</i>		W.M.K. Tilmans <i>[Signature]</i>
Project number			Z4581				
Keywords			Eastern Scheldt, Storm surge barrier, Morphology, Sand Nourishment				
Number of pages			40				
Classification			None				
Status			Final				

Contents

1	Introduction	3
1.1	Background.....	3
1.2	Scope of work.....	3
1.3	Aim of the present report.....	4
1.4	Outline.....	4
2	Problem analysis.....	5
2.1	Introduction	5
2.2	History of the Eastern Scheldt.....	5
2.3	Morphologic changes after completion of the Delta Works.....	7
2.4	Main questions.....	10
3	Data and modelling	11
3.1	Introduction	11
3.2	Wave modelling	11
3.3	Tide modelling.....	13
3.4	Historical development of the Eastern Scheldt delta.....	14
3.4.1	Historical development of the Eastern Scheldt outer delta.....	14
3.4.2	Scour holes near to the barrier	16
4	Morphological modelling.....	18
4.1	Introduction	18
4.2	Coastal sediment transport.....	18
4.3	Tidal sediment transport	20
4.4	Interpretation of transport capacities	22
5	Analysis.....	24
5.1	Introduction	24
5.2	Question 1 : Aspects that restrict the import of sediment at the barrier.....	24
5.3	Question 2: Measures that improve sediment import.....	25
5.3.1	Possible measures.....	25
5.3.2	Estimated effect of measures.....	26
5.3.3	Timeframe of measures	29
5.4	Question 3: Sediment transport potential	29
5.4.1	Potential sources of sediment.....	29
5.4.2	Evaluation of sediment transport potential.....	30
5.5	Evaluation of measures	30
5.6	How to proceed.....	31

6 Conclusions..... 33

6.1 Conclusions 33

6.2 Recommendations 33

References

Tables

Figures

Appendices

1 Introduction

1.1 Background

In 2008, Deltares was requested by 'Rijkswaterstaat - De Waterdienst' (Dutch governmental centre for water management) to perform a study which investigates the reduction of the inter-tidal areas in the Eastern Scheldt (see Figure 1.1). This project includes an assessment of morphological processes near to the inter-tidal flats (item 1, including monitoring of a trial nourishment), a description of the large scale morphology (item 2) and a study of the sediment transport processes near to the Eastern Scheldt barrier (item 3).

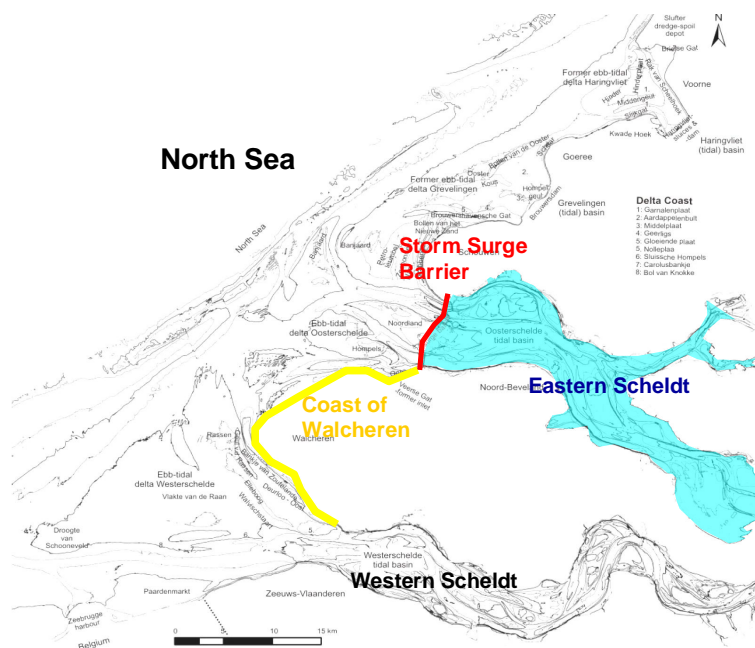


Figure 1.1 Eastern Scheldt

This report makes an assessment of item 3, sediment transport processes near to the Eastern Scheldt barrier.

1.2 Scope of work

In this report the following is discussed:

- 1) Problem analysis
- 2) Modelling techniques and data sources
- 3) Morphological computations
- 4) Analysis

Problem analysis

In the problem analysis the history of the Eastern Scheldt is summarised. From this analysis it follows that due to the construction of the barrier the tidal flow velocities inside the basin decreased and it is expected to have blocked sediment transports into the basin. Consequently, the shoals inside the basin deteriorate (crest is eroded), which

results in a reduction of the ecological value of the Eastern Scheldt inner basin. Furthermore, the changes inside the inner basin may also have safety consequences (e.g. on wave attack). This relation is translated to a limited number of questions:

- Which aspects determine the constraint of the import of sand through the Eastern Scheldt barrier?
- Which measures can be taken to take away these constraints?
- What is globally the maximum sand import that can be achieved with these measures (in Mm³/yr)?

Modelling techniques and data sources

In order to analyse some of the 'main questions', data is required on local hydraulic conditions and sediment transports. For this purpose a number of data sources and numerical models were used to derive the hydraulic conditions (like SWAN, MATROOS). Furthermore, available information on the morphology of the Eastern Scheldt was assessed.

Morphological computations

Data from these models were used to assess sediment transport capacities in the vicinity of the Eastern Scheldt Barrier. This holds for two items, namely the longshore sediment transport along the coasts of Walcheren and Schouwen and computations of sediment transport capacities (due to combined tidal currents and waves) at several locations in the tidal channels and on the tidal flats.

Analysis

An analysis is made of the 'main questions', for which the computed sediment transports were used. Furthermore, the current status of the project and required modelling and measurements to assess the (most promising) measures are discussed.

1.3 Aim of the present report

The objective of the study in this report is to analyse the sediment transport near to the Eastern Scheldt Storm Surge barrier, as well as to assess the status of the current knowledge and to discern items that need to be studied in more detail.

1.4 Outline

The problem analysis is described in Chapter 2. Required hydraulic data and modelling are described in Chapter 3. Chapter 4 provides a description of sediment transport computations near to the Eastern Scheldt barrier. These data are used in Chapter 5 to analyse the questions that arose from the problem analysis. Finally, conclusions and recommendations are presented in Chapter 6.

2 Problem analysis

2.1 Introduction

In this chapter a description of the development of the Eastern Scheldt (Section 2.2) is provided. The ecological problem (reduction of inter-tidal areas as a consequence of a sediment deficit), that has been caused by the completion of the Delta works is then described in Section 2.3 and analysed. A number of measures to the barrier, as given in WL | Delft Hydraulics (2007), to compensate or alleviate the problems are also presented in this section. In Section 2.4 the main questions that emerge from the problem analysis are summarised.

2.2 History of the Eastern Scheldt

The topography of the Eastern Scheldt and the other estuaries in the delta area, as it existed before the delta works, was the result of fairly gradual natural processes (except for sudden changes that took place during storm surges). Although human interventions, like the construction of dikes and dams and the execution of dredging activities, also had an increasing impact on the topography of channels and inter-tidal areas. The bottom of the Eastern Scheldt mainly exists of fine sand ($150 \mu\text{m} - 200 \mu\text{m}$), which could easily be transported by the water in the past, as flow velocities inside the channels were up to 1 m/s or 2 m/s (average tide). The gradual morphological changes in the past are illustrated in Figure 2.1, which show the development of inter-tidal areas and channels in the period 1827-1953.

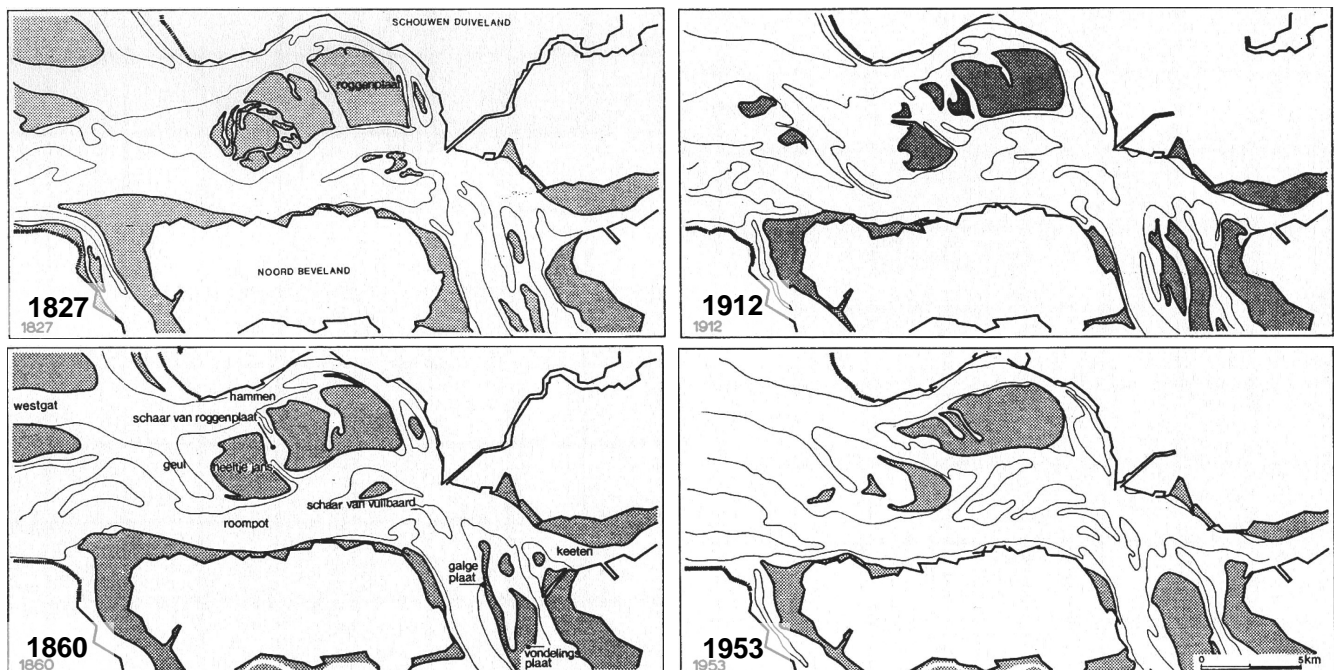


Figure 2.1 Development of channels and inter-tidal areas of the Eastern Scheldt (before construction of the storm surge barrier)

In 1953 a large part of the South-West of the Netherlands was flooded in a major storm. More than 1850 people drowned and significant damage was done to the properties

inside the polders. Therefore a special 'delta commission' was appointed, which gave a number of advices between 1953 and 1955 amongst which the closure of several tidal channels.

In the framework of the Deltaplan, the Grevelingendam (1964) and the Volkerakdam (1969) were constructed, after which the tidal volume through the opening of the Eastern Scheldt increased significantly. Consequently, additional tidal prism that had to flow through the Eastern Scheldt entrance, the flow velocities in the Eastern Scheldt basin increased. These higher flow velocities resulted in a deepening and re-location of the tidal channels during the 1960s and 1970s. Sediment was moved from the central part and the entrance of the Eastern Scheldt to the more eastern part of the basin and the outer delta of the Eastern Scheldt seaward of the entrance (see Figure 2.2 central panel).

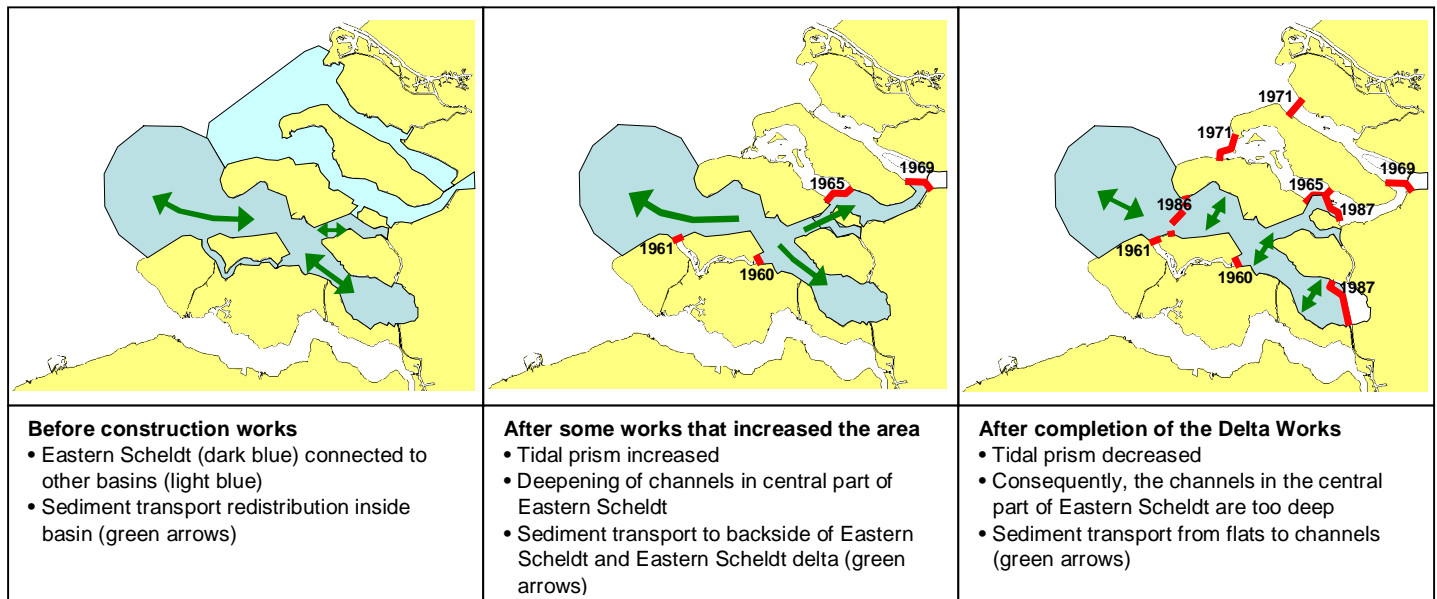


Figure 2.2 Eastern Scheldt area before construction works (left) after some works that increased the area (middle) and after completion of the Delta Works (right)

Later on the tidal prism and flow velocities in the channels were reduced due to compartmenting of the Eastern Scheldt inner basin (Zandkreekdam (1960), Veerse Gatdam (1961), Philipsdam (1987) and Oesterdam (1986)). Furthermore, the construction of the Eastern Scheldt barrier (1986, see Figure 2.2 right panel) reduced the tidal prism inside the Eastern Scheldt basin. This was caused by the reduction of the cross-sectional area at the location of the storm surge barrier. The part of the storm surge barrier that can be closed is built only in the main tidal channels (Roompot, Hammen and Schaar), while the rest of the storm surge barrier is a closed dam. Furthermore, the flow is hindered by the storm surge barrier itself, as the foundation and bottom protection of the storm surge barrier were constructed (for a large part) as a sill above the initial bed level of the channels (see Figure 2.3).

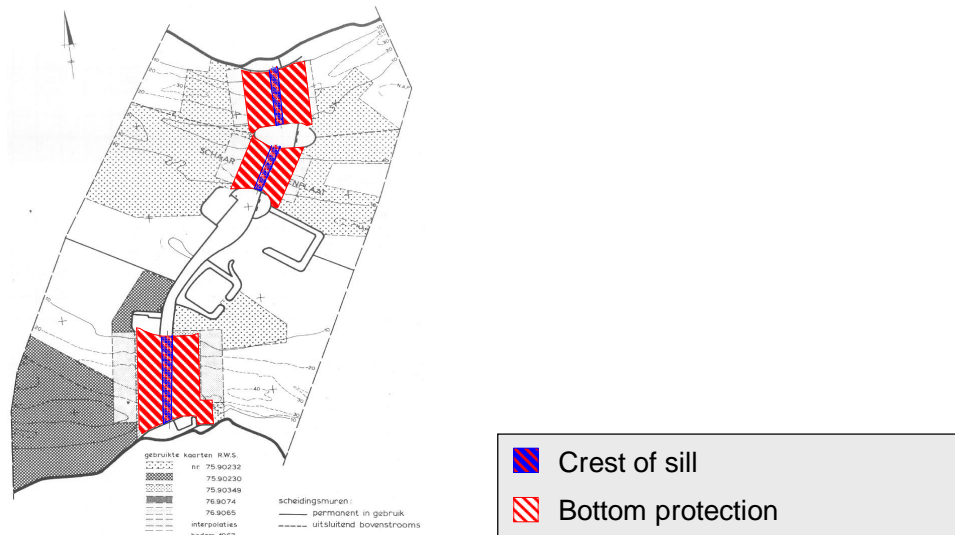


Figure 2.3 Eastern Scheldt storm surge barrier with bottom protection (top-view)

Consequently, the cross-sectional area after construction of the Eastern Scheldt storm surge barrier is approximately 18,000 m² (below NAP), while the cross-sectional area before construction was about 80,000 m². Maximum flow velocities inside the channels now vary between 0.5 m/s and 1.5 m/s for an averaged tide in the western part of the Eastern Scheldt basin (Oosterlaan & Zagers, 1996).

So, two causes for the decrease in tidal range and flow velocities can be depicted. Firstly the decrease of tidal prism due to closure of parts of the basin and secondly due to the reduced cross-sectional area at the entrance of the Eastern Scheldt basin as a result of the construction of the storm surge barrier. Table 2.1 (RWS-RIKZ, 2003) presents some of the changes in the hydraulic characteristics of the Eastern Scheldt basin as a result of the construction of the Eastern Scheldt storm surge barrier.

		Before Eastern Scheldt works	After Eastern Scheldt works
Total area	[km ²]	452	351
Water area	[km ²]	362	304
Inter-tidal area	[km ²]	183	118
Cross-sectional area of storm surge barrier	[m ²]	80000	17900
Vertical tide, Yerseke	[m]	3.7	3.25
Maximum flow velocity	[m s ⁻¹]	1.5	1.0
Residence time	[days]	5-50	10-150
Average tidal prism	[10 ⁶ m ³]	1230	880
Total water volume	[10 ⁶ m ³]	3050	2750

Table 2.1 Dynamic characteristics of the Eastern Scheldt basin, before and after the construction works in the Eastern Scheldt (source: RWS-RIKZ, 2003)

2.3 Morphologic changes after completion of the Delta Works

The changes in the hydraulic characteristics have an impact on the morphology of the Eastern Scheldt basin. As the morphology of the inter-tidal areas and tidal channels (see Figure 2.4) depends on the tide.

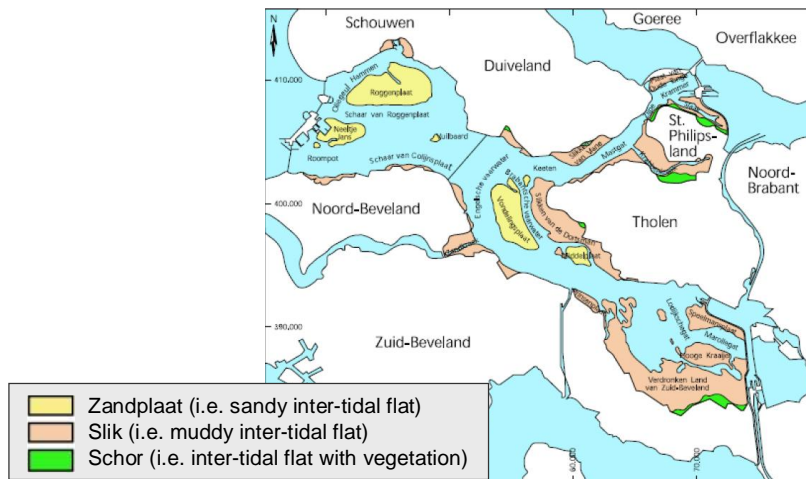


Figure 2.4 Eastern Scheldt basin: most important inter-tidal areas (i.e. platen, schorren en slikken) (source: [RWS-RIKZ, 2004])

At present, as a consequence of the reduction in the maximum flow velocities, the tidal channels of the Eastern Scheldt basin are not in equilibrium. It is expected that the tidal channels will fill up over time. On the basis of empirical relations between tidal prism and cross-sectional area in the tidal channels, it is estimated by Rijkswaterstaat (abbreviated as RWS) that the cross-sectional area of the tidal channels may reduce by 25% (with respect to the present situation). This corresponds with a sand volume of 400 to 600 million m³. So, additional sand is required to reach an equilibrium (often referred to as ‘Zandhonger’ or ‘Sand demand’ of the Eastern Scheldt).

Because these channels are not filled up by sand from the outer delta, it is expected that they slowly consume sand from the inter-tidal areas. In RWS-RIKZ (2004) it is noted that for the changed tidal flow conditions and the reduced tidal range (after the completion of the Delta works) the inter-tidal areas are slowly eroding. The eroded material settles on the edges of the inter-tidal areas and partly in the deeper channels (see Figure 2.5).

Note that this (i.e. morphologic change in the inner basin) was already envisaged (RWS-1) at the time of completion of the Delta Works (with the Eastern Scheldt barrier, Oesterdam and Philipsdam), as it was expected that the tidal current would transport less sand (which would result in a reduction of the build up of the inter-tidal flats **inside the Eastern Scheldt inner basin**). **The reduction of the inter-tidal flats, however, was stronger than foreseen.**

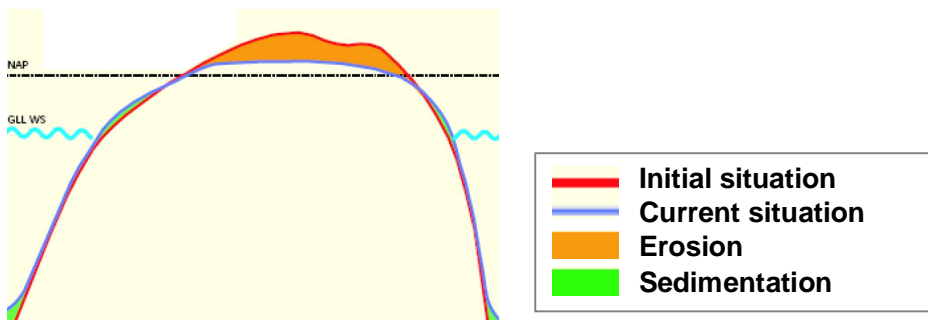


Figure 2.5 Schematic representation of erosion of the inter-tidal areas of the Eastern Scheldt (source : [RWS-RIKZ, 2004])

As a consequence of the reduction in the tidal range and the erosion of the sand banks and shoals, the area of inter-tidal flats in the Eastern Scheldt basin is reducing. Figure 2.6 presents the changes since 1983 (before completion of the Delta Works) of the timeframe that inter-tidal flats are dry.

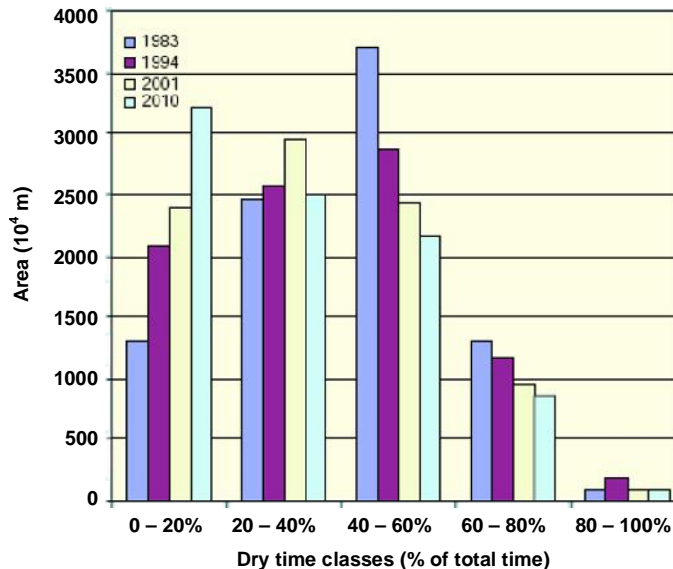


Figure 2.6 Changes in timeframe for which inter-tidal areas are dry

The timeframe for which the inter-tidal flats are dry is of importance to the ecological value of an inter-tidal area. If this timeframe is smaller, birds will have less time to forage for food. Furthermore, a decrease in dry time of the inter-tidal flats is unfavourable for some of the bottom organisms, like cockles, which is a major food source for these birds.

Morphological changes as a consequence of the completion of the Delta Works (i.e. due to construction of the Eastern Scheldt works) were also envisaged for the outer delta. It was expected that coast parallel sandbanks would appear as a result of the decrease in tidal prism. These sandbanks would develop on the edges of the former outer delta at a distance of about 3 to 8 km offshore (Stolk, 1989). It was expected that, in the period 1959 – 1976 before the construction of the Eastern Scheldt works (Eastern Scheldt barrier, Oesterdam and Philipsdam), the morphological changes in the outer delta were small. In R1367 (1980) a general deepening in the order of 1-3 cm/yr is estimated. A more recent study by RIKZ (RWS-RIKZ, 2000-1) indicated that the rate of sediment loss for the outer delta of the Eastern Scheldt was $6.5 \cdot 10^6 \text{ m}^3/\text{yr}$ over the period 1965-1995. In RWS-RIKZ (2000-2) a detailed assessment is made of the recent changes in the Eastern Scheldt outer delta. It was put forward in this report that the sandbanks and inter-tidal flats have been stabilised, but also that in recent years again some regression is found. In general the area of inter-tidal flats in the outer delta has increased, although this does not weigh up to the decrease of inter-tidal flat area in the Eastern Scheldt basin.

2.4 Main questions

This translates into the following questions:

- I. *Which aspects determine the constraint of the import of sand through the Eastern Scheldt barrier?*

This question focuses on the hydraulic and morphologic processes near to the Eastern Scheldt storm surge barrier. The historical development of the Eastern Scheldt estuary is assessed and the current hypothesis for the constraint in sediment transport through the Eastern Scheldt barrier are discussed.

- II. *Which measures may be taken to take away these constraints?*
Or : *In which way can the sand import be increased?*
 Which civil-technical measures should be taken?
 What are the global costs of realisation?

This question focuses on the measures that can be applied near to or directly to the storm surge barrier to increase the sediment transport. A summary of measures (of which some presented in WL | Delft Hydraulics, 2007) is given. Furthermore, a rough indication of the potential effect of such measures is presented.

- III. *What is globally the maximum sand import that can be achieved with these measures (in Mm³/yr)?*

This question focuses on the capability of the outer delta to support the sand demand of the Eastern Scheldt. This involves the availability of sediment and the potential capacity to transport the sand towards the barrier. With respect to sediment transport capacity, the wave driven longshore transport along the coasts of Walcheren and Schouwen and the sediment transport over the channels and inter-tidal flats due to tidal flow are assessed. The sediment transport potential will be compared to the sediment demand of the Eastern Scheldt basin.

3 Data and modelling

3.1 Introduction

In this chapter the hydraulic data and modelling techniques are discussed and the available information on the morphology of the Eastern Scheldt outer delta are assessed. The hydraulic data are required for the assessment of the sediment transports in Chapter 4. In Section 3.2 the assessment of (normal) wave climate conditions is discussed, while Section 3.3 discusses the derivation of tidal data from an operational model (MATROOS). In Section 3.4 some background is provided on the historical development of the Eastern Scheldt outer delta on the basis of available literature. Furthermore, in this section also the historical development of the bathymetry at the inlets of the Eastern Scheldt (Hammen, Schaar and Roompot) is evaluated, focussing in particular on the development of the scour hole at the Roompot.

3.2 Wave modelling

The following steps were performed to derive representative nearshore (normal) wave conditions:

- Selection of offshore data point with wave measurements
- Schematisation of measured offshore wave data to a limited number of representative conditions;
- Transformation (i.e. wave propagation towards the coast) of waves from offshore to the area of interest near to the Eastern Scheldt Barrier and along the coasts of Walcheren and Schouwen.

Selection of offshore data point

For the derivation of representative normal wave conditions, a data point with a long series of wave measurements is required. At some locations on the North Sea such wave measurements over a long period (tens of years) are available. In this study offshore wave and wind data from the 'Europlatform' were used, as this is the 'nearest data point where also measurements of the wave directions are available. For the analyses, 21 years (1979 to 2002) of wave height measurements and 22 years of wind data (1983 to 2005) at the 'Europlatform' were used. Besides using all data, this data set was also split in four parts to represent the four seasons. So, five different model periods were modelled:

- All year
- Winter (from 21 December to 20 March)
- Spring (from 21 March to 20 June)
- Summer (from 21 June to 20 September)
- Autumn (from 21 September to 20 December)

However, as it is too time consuming to simulate the wave propagation towards the coast over a long period of time, these data had to be schematised. For this purpose the time series of wave conditions is schematised to a limited number of typical wave conditions, which are representative for the total time series of wave conditions.

Schematisation of wave measurements

First of all, a distinction was made between sea (local wind generated) and swell (propagating from elsewhere) waves. To make this distinction a typical relation between H_s and T_p was used to split the sea and swell waves (eq. 3-1).

$$H_s = \left(\frac{1}{4.5} T_p \right)^B + C \quad (3-1)$$

Above relation has been established on the basis of a relationship for the maximum steepness of wind-sea waves, as found in the Joint North Sea Wave Project (JONSWAP). For the maximum steepness of the waves in wind-sea, a coefficient for 'B' of 2 and a coefficient for 'C' of 0 were found in the JONSWAP project. For the 'Europlatform' a line with a more or less similar shape was used to divide sea and swell waves ($B = 1.8$, and $C = -0.45$) with an additional constraint for the minimal peak wave period (T_p) for swell (should be $>5s$). In Figure 3.1 (see annex) a plot of the wave measurements at the 'Europlatform' and the applied splitting line between sea and swell are presented.

Secondly, a schematisation was made for the wind-sea and for the swell data separately. This was done by bunching measurements in bins with more or less similar wave conditions. For each of these 'wave bins' the corresponding wind measurements were also bunched. More elaborately, the procedure can be described as follows:

1. the wave measurements are bunched in bins with a characteristic range of wave height, wave period and wave direction. In this study, the measured waves smaller than 0.35m were ignored.
2. For each bin typical wind conditions (wind speed and wind direction) were computed from the wind measurements that correspond with (were measured at the same time as) the wave measurements in that bin.
3. The number of measurements in each bin is a measure for the duration of a condition.

The bin sizes for the wave height, wave period, wave direction, wind speed and wind direction are presented in Table 3.1. The bin size of the wave height bins was 1.5m, with an exception for the first class which ranged from 0.35 to 1m. Wave directions were divided in 30° sectors. For the wave period three bins were used, ranging respectively from 1-5 s, 5-10s and larger than 10s.

Class		I	II	III	IV	V	VI	VII	VIII	IX	X	XI	XII
Significant wave height	(H_s) [m]	0.35-1	1-2.5	2.5-4	4-5.5	5.5-7	>7						
Peak wave period	(T_p) [s]	1-5	5-10	>10									
Wave direction	(dir) [$^\circ$ N]	15 - 45	45 - 75	75 - 105	105 - 135	135 - 165	165 - 195	195 - 225	225 - 255	255 - 285	285 - 315	315 - 345	345 - 15

Table 3.1 : Classification of normal wave conditions at offshore location (Europlatform)

Besides schematising the wave climate for the full year, a schematisation of the wave conditions was also made for four seasons (winter, spring, summer, autumn). The schematised normal wave climates are presented in Tables 3.2 to 3.6.

Transformation of waves from offshore to nearshore

The schematised wave climate is representative only for the offshore location. Therefore the propagation of waves towards the coast should be modelled to attain normal wave conditions at relevant nearshore locations. For this purpose SWAN model simulations were carried out for all five climate scenarios (all year, winter, spring, summer, autumn). The SWAN model is a model that computes the transformation of waves due to a number of physical processes, like wave breaking, whitecapping, shoaling and refraction.

In the wave computations a constant waterlevel at mean sea level (excluding surge, tide and sea level rise) was applied. Note that these water levels are not expected to have a significant impact on the SWAN results for most of the selected locations (which have considerable water depth). The structures (e.g. the Eastern Scheldt storm surge barrier) were schematised as a closed boundary with zero reflection.

Model computations were performed for two typical bathymetries, namely:

- Bathymetry data of the Dutch coast for 2004 (supplemented with 2003 data) were used. Figure 3.2 presents an overview of the applied wave grids and 2004 bathymetry, while in Figure 3.3a a detail of the bathymetry data for 2004 is presented for the Eastern Scheldt delta.
- A bathymetry that was extracted from the database of the operational model 'MATROOS' (for a large part measured in 1999). The 'MATROOS' bathymetry was used in the wave computations to attain wave data that were computed for a similar model bathymetry as the tidal data from 'MATROOS'. Figure 3.3b presents the 'MATROOS' bathymetry for the Eastern Scheldt delta.

From these SWAN computations it followed that most of the computed wave conditions are very similar for both bathymetries. This is illustrated by Figures 3.4a to 3.5b, which present the computed wave height and mean wave direction for both bathymetries for a moderate condition (Figures 3.4a and 3.4b) and a typical winter storm (Figures 3.5a and 3.5b).

The yearly averaged wave climates in the Eastern Scheldt delta are presented for both bathymetries in Figures 3.6a and 3.6b by means of wave roses. Figures 3.7a to 3.7e present wave roses at the coasts of Walcheren and Schouwen both for a full year as well as for each season (2004 bathymetry).

3.3 Tide modelling

Tidal data is required for the assessment of the sediment transport capacity at some locations in the Eastern Scheldt delta in Section 4.3. Setting up and calibrating a numerical model that computes tidal flow velocities and storm surges was, however, beyond the scope of this project. Therefore, tidal data was derived from an operational model ('MATROOS').

For the assessment of the sediment transport capacity in Section 4.3 the flow velocities (in x and y direction) were derived from 'MATROOS'. Note that even though the data in 'MATROOS' have been calibrated for water levels only, it is expected that the accuracy of the flow velocity data is sufficient for the assessment in this study. For this purpose,

maps of flow velocities (for a certain time step) were derived from 'MATROOS' for a time period of two months. For each of the considered locations in Section 4.3 a time series with water level and flow velocities (in two directions) was extracted.

In Figures 3.8a and 3.8b examples of the tidal flow velocities (as computed by 'MATROOS') during ebb and flood are presented. Figure 3.9 presents an example of the tidal flow velocities (as derived from 'MATROOS') for one of the locations close to the Eastern Scheldt storm surge barrier.

3.4 Historical development of the Eastern Scheldt delta

3.4.1 Historical development of the Eastern Scheldt outer delta

The historical development of the Eastern Scheldt outer delta has been assessed in Alkyon (2008). In that study a sediment balance was made for the South-West coast of the Netherlands on the basis of bathymetrical data (over the period 1964-2004). Two aspects were considered by Alkyon:

- An estimate of the development of the sediment volumes of the former ebb-tidal delta(s)
- long-term morphological changes over the period 1964 to 2004 (see Figure 3.15 on next page)

Development of sediment volumes

For the estimate of the sediment volumes the bathymetry data has been corrected (by Alkyon) by filtering it for small but systematic shifts in the measured depths (for areas where changes are small). As these shifts can have a significant influence on the computed sediment volumes. From this analyses the yearly volume change of the Eastern Scheldt (over the period 1980-2004) was estimated at -1.2 to 0.4 million m³ a year.

Morphological changes in the outer delta

Furthermore, the long-term morphological changes of the Eastern Scheldt were assessed from the bathymetry data in Alkyon (2008). It was concluded that the morphological developments on the ebb-tidal delta of the Eastern Scheldt from 1964 to 2004 are dominated by the adaptations to the changes in the tidal flow. These adaptations were the result of the construction works inside the Eastern Scheldt (i.e. barrier and closure works) which altered the tidal prism. In addition to the adaptation the 'normal' morphological developments on the ebb-tidal delta continued. These normal changes comprise the development, migration and diminishing of tidal channels, the formation and migration of swash bars and the formation and levelling of ebb and flood chutes and their associated shields. An overview of the morphological developments on the ebb-tidal delta of the Eastern Scheldt is presented in Figure 3.15. The areas coloured blue represent areas with persistent erosion, while the orange colour represents persistent sedimentation.

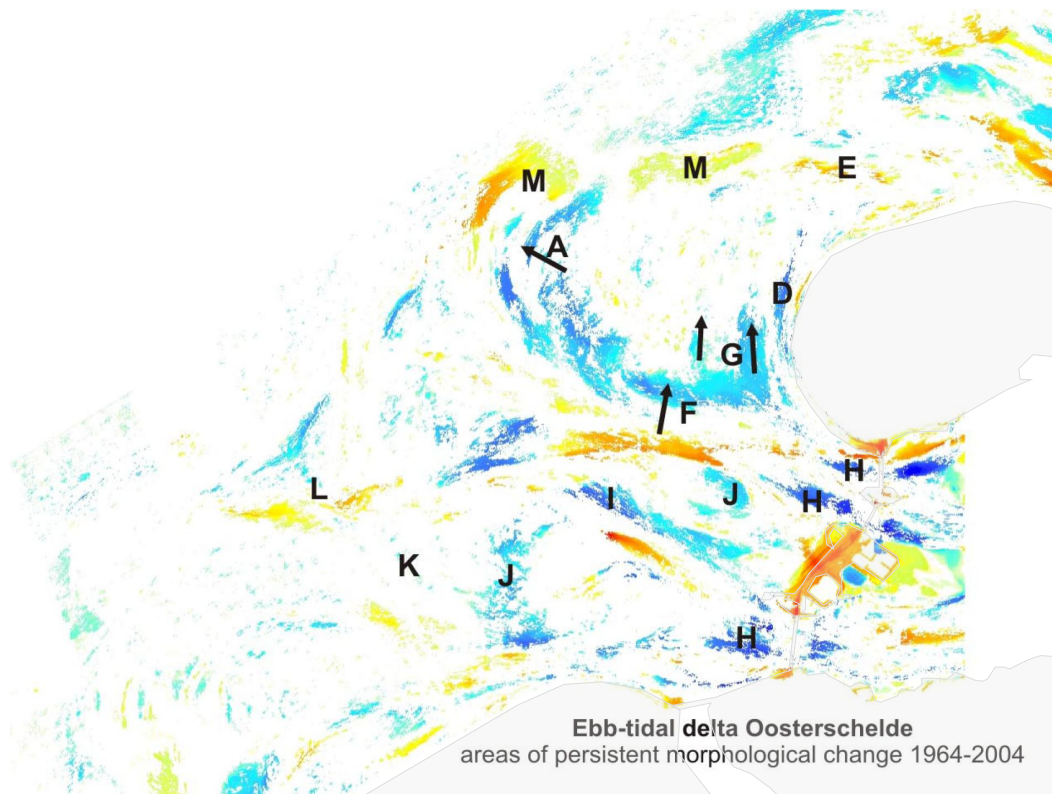


Figure 3.15 Persistent large-scale trends on the ebb-tidal delta of the Eastern Scheldt (source : Alkyon, 2008)

The lettering in Figure 3.15 reads as follows:

- A:** Seaward migration of tidal channels on the Banjaard;
- B:** Landward migration of swash bars on the sub-tidal flats Banjaard, Petroleum Bol, Zeehondenplaat and Bollen van het Nieuwe Zand;
- C:** Development of a (flood) chute from the Brouwershavensche Gat into the sub-tidal flat Banjaard;
- D:** Northward extension of the tidal channel Krabbengat, and along with that development;
- E:** Northward translation of the ebb-shield of the tidal channel Krabbegat, the Bollen van het Nieuwe Zand;
- F:** The migration of the tidal channel Geul van van de Banjaard towards the north, that is accompanied by the erosion of the southern margin of the sub-tidal flat Banjaard and the deposition along the northern side of the sub-tidal flat Noordland.
- G:** The development of two ebb chutes from the tidal channel Geul van de Banjaard into the sub-tidal flat Banjaard;
- H:** The development of deep scour holes in the tidal channels near the entrances to the storm-surge barrier;
- I:** The seaward extension of the tidal channel Oude Roompot, that was accompanied by a redistribution of the sub-tidal flats (especially Hompels), which surrounded the tidal channel. As a result the tidal channel Oude Roompot is currently connected to the tidal channel Westgat;
- J:** A decrease of the maximum height of the tidal flats directly west of the storm-surge barrier (Noorland and Hompels);
- K:** A slight increase in depth and a change in orientation of the nameless entrance channels towards the Roompot and Westgat;

L: The development of a new flood chute and diminishing of the old flood chute on the seaward fringe of the ebb-tidal delta. This development is associated with the extension of the shield of the chute;

On the ebb-tidal delta of the Eastern Scheldt it is difficult to distinguish between the effects of human interferences in the inlet and the normal "natural" morphological changes. This is partly due to the restricted nature of the human interference (the tidal basin still acts as such) and partly due to the natural developments on this ebb-tidal delta which are relative large.

Most of the 'normal' changes on the ebb-tidal delta of the Eastern Scheldt are semi-cyclic developments that involve the formation, growth and migration followed by the demise of morphological elements like channels, swash bars and ebb or flood chutes. Developments with a relatively long lifecycle, do show up in the bathymetry data. Some of the seaward channel migration on the western end of the Banjaard does show up, because the lifecycle of these channels exceeds tens of years. The Banjaard sub-tidal flat complex has shifted further north, following the northern migration of the tidal channel of the Geul van de Banjaard and the evolution of the ebb-chutes.

The human induced changes are related to the reorientation of the tidal flow and the reduction of the tidal volume of the basin. Overall the channels have shifted slightly to the north to north-northeast, although the position of the Roompot tidal channel on the southern side of the ebb-tidal delta has remained stable. The closure of the Grevelingen inlet (north of the Eastern scheldt outer delta) has resulted in an increase of the ebb tidal area at the north side that is influenced by the tidal flow of the Eastern Scheldt. The formation of the scour holes near the entrance of the storm-surge barrier temporarily provided some sediment to the outer delta. The depth of the rest of the ebb-tidal delta and the cross-sectional area of the channels decreased, thus forming a sink for sediment.

3.4.2 Scour holes near to the barrier

On the basis of in-house data an assessment was made of the development of the scour holes at all three inlets of the Eastern Scheldt over the period 1986 to 2000. These are presented in Figures 3.10 to 3.12 (for Hammen, Schaar and Roompot respectively). The following was concluded:

- After the construction of the Eastern Scheldt storm surge barrier large scour holes developed in all three inlets. These scour holes were already present in 1986 for each of the scour holes.
- Significant scour took place in the period between 1986 and 1990.
- After 1990 the depth of the scour hole progressed on slower pace at most locations, except for the seaward part of the Roompot of which the depth still increased at a large pace after 1990.
- Noticeable is that the depth decreased at the seaward side of the Roompot in the 2000 bathymetry, which may be due to a landslide of rock.
- For the seaward sides of the Hammen and the Geul van Roggeplaat, as well as for the basin side of the Roompot the depth seems to be progressing at a slow pace.

As can be seen from Figures 3.12a and 3.12b, conclusions can differ if another cross-section is analysed. Therefore the scour hole of the Roompot was studied in more

detail, as it is the largest inlet of the Eastern Scheldt with the largest sediment transport capacity of all. For this purpose the 'Rijkswaterstaat-Zeeland' provided bathymetry samples of the Roompot (seaward of the barrier) for the period between 1985 and 2008 (see Figures 3.13a to 3.13d). From these data the trend in the development of the depth of the scour hole over time could be found (see Figure 3.14). The following was concluded:

- For the Roompot, large scour occurred in the period between 1985 and 1996.
- After 1996 only limited progression in the depth of the scour hole can be seen, but the area of the scour hole still increased.
- Currently the depth of the scour hole in the Roompot is almost stable (it is only slowly getting deeper), while the area of the scour hole still grows over time.

4 Morphological modelling

4.1 Introduction

In this chapter the hydraulic conditions from Chapter 3 are used to compute sediment transport capacities in the Eastern Scheldt outer delta. The sediment transport capacities are used in the analysis to answer the 'main questions' in Chapter 5 (especially question 3). Section 4.2 describes the assessment of the longshore sediment transport along the coasts of Walcheren and Schouwen. After that, the sediment transport capacity (due to combined tidal currents and waves) at several locations in the tidal channels and on the shoals is assessed in Section 4.3.

4.2 Coastal sediment transport

The first type of morphological model that has been set up is a model that computes wave driven sediment transports along the coasts of Walcheren and Schouwen. These transports occur close to the coast (in the last hundreds of meters from the shoreline). These transports give an indication of the potential of sediment transport close to the coast as a result of wave driven currents. Note that cross-shore sediment transports are not included in the computations.

1D model setup

For the computations of the wave-driven longshore sediment transport the 1D shoreline model UNIBEST-CL+ has been used. For the current project the sediment transport formula of 'Bijker' (1971) was applied. A description of this model and the 'Bijker' transport formula is included in Appendix A.

The coastline has been set up in RD coordinates, for which data was used from 'Google Earth' satellite images (see Figure 4.1). In the longshore sediment computations a representative median grain diameter (D50) of 250 μm was used. Revetments and groynes were also schematised in the model.

Along the coast a large number of cross-shore profiles (rays) were defined for which bathymetry data from 'vaklodingen' (2004) and 'JARKUS' were used. For each of these rays the nearshore wave climates from SWAN (reference is made to Section 3.2) were used as a boundary condition in the UNIBEST-CL+ model. Longshore sediment transport computations were performed for five time periods:

- All year
- Winter
- Spring
- Summer
- Autumn

Longshore sediment transport

The computations of the longshore sediment transport along the coasts of Walcheren and Schouwen indicate that the sediment transport varies significantly over the length of the coast (see Figure 4.2). In general sediment transport is larger along the north-western shores of Walcheren (between West- and Oostkapelle) than for Schouwen and

the northern side of Walcheren. Typically the following (net) longshore sediment transport patterns can be distinguished from the modelling:

- North of Westkapelle the computed longshore sediment transport increases along the coast from zero at Westkapelle to about 80,000 m³/yr (to be interpreted within a range of 50,000 to 100,000 m³/yr) north of Oostkapelle. On the basis of the longshore sediment transports only (without cross-shore transport and the effect of the tide), significant erosion is expected between Westkapelle and Domburg.
- From Oostkapelle to the Onrustpolder the computed longshore sediment transport decreases from about 80,000 m³/yr to 10,000 m³/yr. On the basis of the computed longshore sediment transports, sedimentation is expected in this area, which is expected to be concentrated North-West of Vrouwenpolder. Note that locally coastal retreat is observed, which is due to cross-shore transport and the relocation of a local tidal channel at the Onrustpolder (resulting in a steeper beach profile and cross-shore sediment transport).
- Sediment transport at the head of Schouwen is directed Southward between Nieuw-Haamstede and Westenschouwen and ranges between 0 to 10,000 m³/yr at Nieuw-Haamstede and 10,000 to 40,000 m³/yr halfway Nieuw-Haamstede and Westenschouwen. Between Westenschouwen and the Eastern Scheldt barrier the longshore sediment transport decreases to about 10,000 m³/yr.

The computed longshore sediment transport per season has been presented in Figure 4.3. From this figure it can be distinguished that:

- At the north-western side of Walcheren (between Westkapelle and Oostkapelle), about 80 percent of the sediment transport occurs during the autumn and winter season.
- For the other (less exposed) parts of the shoreline (south-western side of Schouwen and the beaches from Oostkapelle to the Onrustpolder) the longshore sediment transports per season are more equally distributed over the seasons with only slightly larger transports in winter.

Besides the net longshore sediment transports (net result in one direction) also the gross transports¹ have been computed for some locations close to the Eastern Scheldt barrier. From this analysis it was found that the computed gross longshore sediment transport for the north-western side of Walcheren (at Domburg) is about 50% larger than the net transport (so a gross north-eastern transport that is 150% of the net transport and a gross south-western transport that is 50% of the net transport). At the northern side of Walcheren the difference between the net and the gross transport becomes smaller, as a larger part of the waves comes from one side. At Vrouwenpolder the gross transport to the east is about 25% larger than the net transport, while at the Onrustpolder the gross and net longshore sediment transport are about equal (transport only in one direction).

At Schouwen the gross sediment transport close to the barrier is about similar to the net transport, while at Nieuw-Haamstede the gross-transport can be in the order of 20,000 m³/yr which is about 4 times the computed net transport.

¹ A gross sediment transport is the total sediment transport in one direction over a certain time period. So, the difference between the gross transports (in both directions) is the net transport

Coastline changes

On the basis of longshore sediment transport, a general tendency towards sedimentation is expected between Vrouwenpolder and the Onrustpolder. However, from the 'Kustlijnkaarten 2007' (RWS-RIKZ, 2006) a mixed pattern of coastline accretion and retreat was observed for this area (over this period). For this reason it is expected that a significant part of the sediment that is transported along the coast of Walcheren is transported in offshore direction (cross-shore transport) towards the tidal channels. At the coast of Schouwen a general tendency towards retreat is presented in the 'Kustlijnkaarten 2007'. It is expected that for the areas with decreasing sediment transport (between Westenschouwen and the barrier) a large part of the sediment is transported in offshore direction.

Impact of different coastline orientation

Another question that may be raised is what the maximum longshore sediment transport would be if the coast orientation is altered, for example by a large nourishment (like planned for 'De Banjaard'). It is, however, very difficult to determine the longshore sediment transport for a situation that is significantly changed, as the waves will be different for a different beach orientation and even the morphologic system may change. The local wave energy will, however, be of the same order as for the undisturbed situation. Therefore the maximum transport capacity (due to wave driven processes alone) will be limited by this wave energy, and is then independent of the amount of sediment that is available. For a moderately exposed area North of Vrouwenpolder the transport is expected not to exceed 100,000 m³/yr in any case. In such a situation the tide driven transport (additional to the wave driven sediment transport) is expected to contribute significantly more to the total sediment transport. More on tide driven transport in Section 4.3.

4.3 Tidal sediment transport

Tidal flow velocities are the main driving factor for sediment transport on the shoals and in the tidal channels. To provide insight into the potential sediment transport capacity in the tidal channels and on the shoals of the Eastern Scheldt delta (which is relevant for 'Question 3' in Chapter 5), a point model was used. With this model an estimate has been made of the sediment transport capacities for 69 locations in the Eastern Scheldt delta (see Figure 4.4), which gives an impression of the local sediment transport and transport directions. Furthermore, a part of the delta was segmented with lines, along which the computed sediment transport was integrated to obtain an indication of the sediment transport through the segments.

Morphological point model

The point model used in this study is the SPCM model, which has been used in other projects and contains similar sediment transport formulae as in Delft3D. Such a point model computes the sediment transport (both suspended and bed transport) at a certain location on the basis of the local hydraulic conditions. The results provide an estimate of the local sediment transport capacity, although these transports should not be mistaken for the actual transports. As the following is assumed in the model:

- Stationary flow (same flow velocity over a significant distance)
- Small bed level gradients (almost flat bottom)
- Unlimited availability of sediment
- Sediment already in suspension

For the Eastern Scheldt delta it is expected that the model can give a good indication of sediment transport capacity in the tidal channels and on the tidal flats, as these intertidal flats and channels are generally quite large (compared to the water depth) and have mild slopes. On the transition between a flat and a channel (with steep slopes) the computed sediment transport capacity may differ to some extent from the actual transport. As the transport capacity on the transition slopes may in some cases be influenced by accelerating or decelerating flow and/or local turbulence as a result of bed level gradients. Furthermore, there will be some uncertainty in the results near to the Eastern Scheldt barrier due to local turbulence and large bed level gradients. However, despite the drawbacks of such a model it is expected to provide results that are sufficiently accurate to assess the questions in Chapter 5. In Figure 4.4 the 69 locations that were investigated with the point model are presented.

Model setup

In the point model the 'Van Rijn 1993' transport formula has been used, which is a commonly used formula for morphological computations (Van Rijn, 1993). In the model the following data were used:

- Tide data were derived from the operational tidal flow model 'MATROOS', which is discussed in Section 3.3.
- For the sediment a median grain diameter (D_{50}) of 250 μm was used.
- Wave data for each location were derived from the wave model with the 1999 'MATROOS' bathymetry discussed in Section 3.2. For each wave condition the local sediment transport for the whole timeseries was computed, which were afterwards combined by taking a weighed average on the basis of their durations.

Sediment transport capacity

The results of the computations are presented in two ways:

- Sediment transport capacity at the 69 locations (for 10° directional sectors)
- Integrated sediment transport through the segments (input for a sediment balance)

From the computed sediment transports (per timestep) from the SPCM model the magnitude and direction of the net sediment transport capacities were computed. A way to present the sediment transport for each location is to bunch the sediment transport capacities in different directional bins. In this case 36 directional bins were made for which the (gross) transport was computed. In Figure 4.5a a map overview of the local sediment transport capacities and transport directions for all locations is provided. It is stressed that this figure does not present the actual sediment transports, but the transport capacity if sufficient sand is available, which is for example not the case at the barrier itself. Note that a number of typical transport roses can be distinguished (see Figure 4.5b), as for some locations the transport is in all directions (due to a wide variation in flow directions). This occurs most often on the shoals while in the channels the transport capacity is directed in one or two (often opposing) directions.

To obtain an indication of the sediment transports through channels or on shoals, a part of the delta was segmented with lines along which the sediment transport was integrated (see Figure 4.6). In this way the net sediment transport from one section to another can be estimated. For this purpose, about 5 or 6 computations were made on each line segment. For each of the computations the component of the net transport that is normal to that segment was computed. These were integrated by multiplying the

sediment transport ($\text{m}^3/\text{m}/\text{yr}$) by the length of the segment (m). In Figure 4.6 the computed integrated net transport for each of the segments is presented. It should be noted that some of the computed net sediment transports on the shoals (dashed arrows) are expected to be somewhat smaller than computed with the model.

4.4 Interpretation of transport capacities

On the basis of the computed sediment transport capacities in Figures 4.2, 4.5a and 4.6 an interpretation was made of the sediment transport patterns in the Eastern Scheldt delta. This interpretation is presented in Figure 4.7. Note that at some locations only the direction of the sediment transport was estimated, these estimates are presented with dashed arrows. The main (interpreted) aspects of the sediment transport pattern in Figure 4.7 are:

- Indication that the barrier is an obstruction for sediment transport
Note that close to the storm surge barrier the sediment transport capacity is generally away from the barrier, which is expected to be due to the asymmetry of the horizontal tide (the flow velocities are larger away from the barrier than towards the barrier, see also Figures 3.8a and 3.8b for an illustration of the jet 'downstream' of the barrier). Although some physical aspects (like local turbulence, bottom gradients and limited availability of sediment at the hard structure of the barrier) were not included in the point model, it is still regarded as a strong indication that sediment transport through the storm surge barrier is significantly hindered. Furthermore, in reality there is no sediment available locally at the barrier and the steep slopes will hinder sediment transport even more, which makes the hypothesis that the barrier blocks the sediment stronger. The computed sediment transport capacities at the barrier itself should therefore not be regarded to be 'actual' transports, but potential transports if sufficient sediment was available. Although this will have to be verified with more detailed modelling (2DH and/or 3D morphological model) in a later stage.
- Sand entering the Roompot is expected to be transported to the North-West
As no significant part of the sediment is expected to move through the barrier, it is expected that there is a net sediment transport along the northern coast of Walcheren (shores and tidal channels) which ends up in the Roompot. From the Roompot this sediment is expected to move in north-western direction. Where it is expected to be moved further northward or onto the shoals. Note that a large capacity to transport sediment away from the barrier was also found at the scour hole on the inner basin side of the Roompot (from the scour hole into the inner basin), although it can be smaller than computed due to the effect of the slope of the scour.
- Sediment transport at Hammen and Schaar is much smaller than for the Roompot
Sediment transports at the Hammen and the Schaar are expected to be smaller than for the Roompot and generally directed away from the barrier, which may result in a slow increase of the local scour holes.
- A significant part of the sediment that is transported along the coasts moves offshore in the Eastern Scheldt outer delta. Note that the Eastern Scheldt outer delta can benefit from this sediment and that at other locations sand is transported towards the coast.
For this purpose the observed coastal changes (dashed red or green lines) in the 'Kustlijnkaarten' (2007) were compared to the modelled sediment

transports. On the basis of modelled sediment transports alone accretion would be expected at the shores of Vrouwenpolder and Onrustpolder (Northern part of Walcheren) and Westenschouwen, which is not the case. Therefore a significant part of this longshore transported sediment is expected to be moved in offshore direction at these locations (see Section 4.2).

For a large nourishment in front of the Walcheren coast, for example a 'zandmotor' at the Banjaard (RWS-Zeeland, 2008), the following is expected to happen:

- Most sediment is expected to be transported (by the tide) towards the Roompot even for large nourishments, although a part of the sediment for very large nourishments may be transported to the West. As the flow and morphological patterns may change to some extent.
- For the current situation it is expected that most of the sediment at the Roompot is transported in north-western direction and not through the barrier (see Figure 4.7). If more sediment is transported (in the case of a large nourishment at the 'Banjaard') still most of the sediment is expected to be transported to the North-West.
- Note that even for a seriously altered coastline orientation the wave driven longshore transport is not expected to supply more than 100,000 m³/yr of the sediment along the coast of Walcheren (as the wave energy is limited). This is an order of magnitude smaller than the sediment demand of the Eastern Scheldt (approximately 400 to 600 million m³; WL | Delft Hydraulics, 2007). Therefore the tidal flow will have to move most of the sediment, which will be transported to the tidal channel and seaward scour hole of the Roompot.

5 Analysis

5.1 Introduction

This chapter deals with the questions raised in Section 2.4. Sequentially an assessment is made of the causes for the sediment transport blockage due to the barrier (Section 5.2), measures that may improve the situation (Section 5.3), the potential to transport (or provide) sediment in the Eastern Scheldt outer delta (Section 5.4) and an assessment of remaining questions and required work to proceed. The assessment in this chapter is based on the hydraulic and morphologic model results which were provided in Chapter 3 and 4. Which aspects restrict the import of sand through the Eastern Scheldt barrier?

5.2 Question 1 : Aspects that restrict the import of sediment at the barrier

Two causes can be discerned for the constraint of sediment import at the barrier:

- The sediment transport capacity, which is already limited in the natural situation (see Section 5.4).
- Blockage of sediment transport due to the Eastern Scheldt barrier

In this section the current hypothesis on the blockage of sediment by the Eastern Scheldt barrier is discussed. This hypothesis is based on a couple of physical processes that give a strong indication for the blocking of sediment transport by the Eastern Scheldt storm surge barrier. These processes can be subdivided in three categories:

- Asymmetry in flow velocities during ebb and flood tide
- Turbulence generated by the vertical elevation of the barrier
- Effect of the slopes at both sides of the barrier

Tidal flow asymmetry

For a long estuary with a relatively small entrance (compared to the tidal prism), the flow velocities directly seaward of the entrance can be smaller during flood than during ebb. The reason for this is that during flood the water will flow from all directions towards the entrance (Figure 5.2a), while during ebb it is jetted out of the entrance over a smaller area (Figure 5.2b). This was also observed in the tidal flow model results from 'MATROOS' in Section 3.4. Figures 3.8a and 3.8b showed that flow velocities at the seaward side of the barrier are smaller during flood than during ebb.

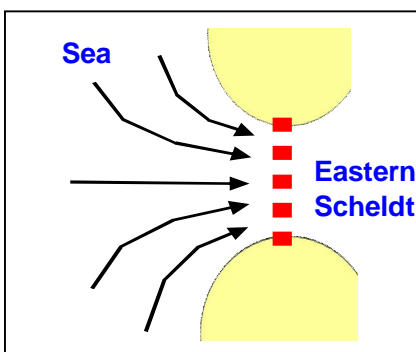


Figure 5.2a Small flow velocities during flood

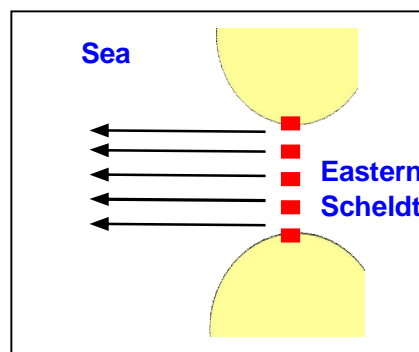


Figure 5.2b Large flow velocities during ebb

This may be a potential cause for (partial) sediment blocking as the water has less capacity to transport sediment if the flow velocities are smaller. Furthermore, it is known that a scour hole exists on both sides of the Eastern Scheldt barrier. Due to this scour hole even less sand may pass through the barrier, as sediment will fall to the bottom of the scour hole (with low flow velocities) during flood and will be pushed back to sea by the large flow velocities that occur during the ebb tide.

Turbulence and slopes

Another aspect that may play a role is the sill at the barrier structure. At ebb tide the flow jets over the sill and creates large turbulence that will erode the scour hole (Figure 5.3). It is expected that during flood the sediment will fall into this scour hole, as the sediment will not be able to move over the steep slopes of the scour hole and the sill of the barrier. At ebb tide this sediment will be transported away from the barrier again.

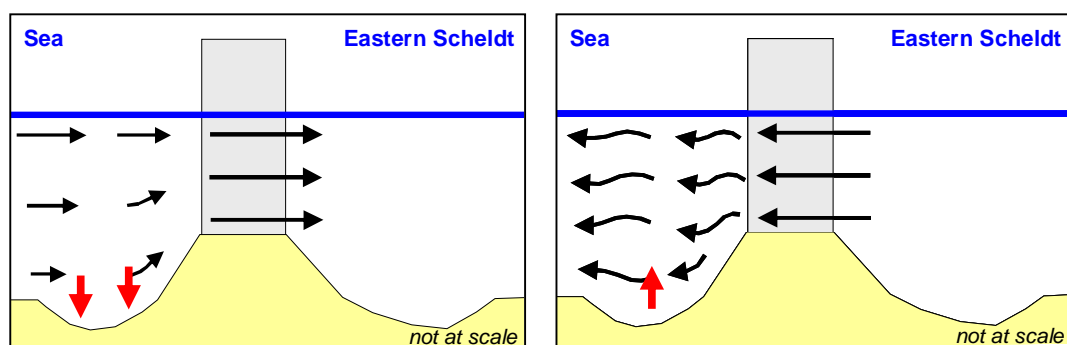


Figure 5.3 Potential flow during flood (left) and turbulence behind structure during ebb tide (right)

5.3 Question 2: Measures that improve sediment import

5.3.1 Possible measures

As mentioned in Section 5.2.2 there are strong indications that the Eastern Scheldt barrier currently blocks (most of) the sediment transport. However, it can be beneficial for the Eastern Scheldt basin if sand is imported through the barrier. Provided that enough sand is available or is nourished in the Eastern Scheldt outer delta. A couple of measures to make the Eastern Scheldt barrier more 'morphologically open' are therefore discerned and discussed.

On the basis of the work of 'Tom Jongeling' (WL | Delft Hydraulics, 2007) a couple of potential measures that can improve the sediment import through the Eastern Scheldt barrier could be discerned:

- Filling one or more scour hole(s) at the seaward side of the Eastern Scheldt barrier and protecting them by means of (rock) filter layers.
- Adjusting barrier structure to reduce the hydraulic resistance.
- Opening the dams at the landward sides of the barrier.
- Manipulation of the opening and closing timeframes of the gates of the barrier during a tidal cycle (operation of the Eastern Scheldt barrier).
- Directly or indirectly (by means of a pipeline from the barrier sluices to the scour hole(s) at the basin side of the barrier) nourishing sediment into the basin.

5.3.2 Estimated effect of measures

A rough indication of the potential effect of above measures is provided in this section.

Filling the scour hole

Reference is made to WL | Delft Hydraulics (2007) where this measure is discussed. With this measure the blocking of sediment, as a result of sediment trapping at the seaward side of the Eastern Scheldt barrier (see Section 5.2.2) is counter-acted. It is expected that sand will be transported more easily towards the barrier structure in that situation, as the flow velocities at the filled scour hole will be larger (due to smaller water depth). Furthermore, it is expected to act as a one way valve, allowing sand to go into the Eastern Scheldt basin but not allowing it to go back (as the scour hole on the inside still exists).

For this purpose the scour hole will have to be filled (partially) and covered with a protecting layer. This can be done by means of geo-containers or sand fill with a protecting rock layer. The costs of such a measure were estimated in WL | Delft Hydraulics (2007) at 50-70 M€ for the sand fill and rock cover option and 60-100 M€ for the geo-container option.

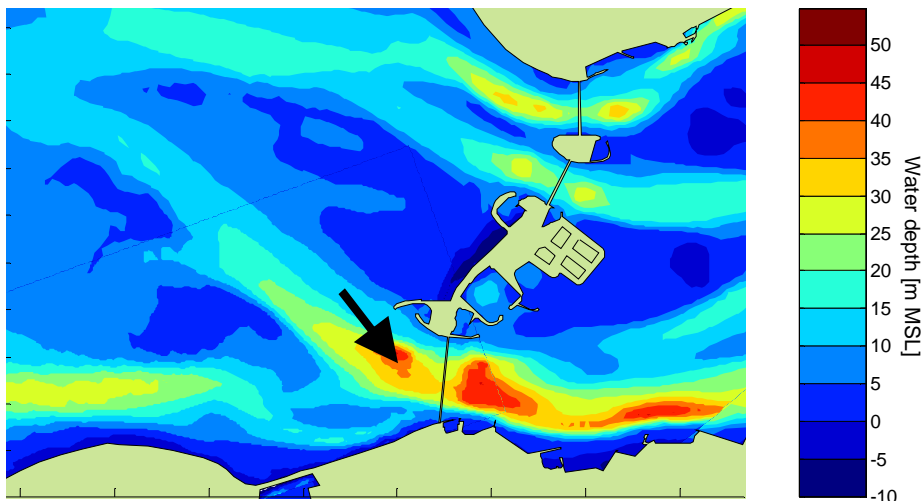


Figure 5.4 Scour holes at the Eastern Scheldt inlets (1999 bathymetry)

Adjusting the barrier structure

Another option is to decrease the resistance of the barrier structure by streamlining it or by enlarging the cross-sectional area. The effect of such measures will be that the tidal prism inside the Eastern Scheldt basin will increase and consequently the flow velocities inside the channels will increase (thus requiring less sand).

Two options with respect to streamlining were considered in WL | Delft Hydraulics (2007). The first one involves smoothing of the sill towards the barrier structure to a slope of 1:10 (currently about 1:3), which will reduce the energy loss (i.e. turbulence) and is expected to allow for a 10% increase in flow capacity (averaged over a tidal cycle). If this is realised with geo-containers, the costs of such a measure were estimated at 40-70 M€ (WL | Delft Hydraulics, 2007). However, note that it should also be assessed then if geo-containers can safely be applied at that location. Secondly, a smaller effect (approximately an increase of 5% in flow capacity) can be obtained by

adjusting the streamlining of the concrete sills and piers. Costs of the second measure are, however, expected to be very high (estimated to be at least 100 M€).



Figure 5.5 Turbulence at the Schaar van Roggenplaat

Opening the dams at the landward sides of the barrier sections

Furthermore, an option with respect to increasing the cross-sectional area can be considered. This involves the opening of the dams at the Landward sides of the barrier sections. Due to this measure the cross-sectional area will be enlarged by about 1000 m² (about 6% larger), which (according to WL | Delft Hydraulics, 2007) will result in some percentages of extra tidal range at Yerseke. Furthermore, sand may be bypassed through these gaps. However, for this purpose the considered areas close to the dams should be restructured and concrete sills will have to be built. The costs for such a measure are high (estimated to be at least 100 M€). In WL | Delft Hydraulics (2007) it is discussed that alternatively the bypassing of the dams can be increased by using hollow blocks for the dams (make the dam permeable). It is, however, uncertain whether such a structure will be effective (what the hydraulic resistance will be). It is therefore not advised to use a permeable dam with hollow blocks.



Figure 5.6 Dams at Noord-Beveland; left situation in 1993, right situation in 2005 (source: RWS-RIKZ)

Although above options may have a positive effect on the tidal prism inside the Eastern Scheldt, making only adjustments to the barrier is not expected to have a significantly large impact on the system to prevent the deterioration of the inter-tidal flats inside the Eastern Scheldt basin. Furthermore, the costs for adjusting the barrier are expected to be very high. Therefore, only a combination with another measure, like (partially) filling the scour hole and covering it, could be more feasible.

Manipulation of the operation of the gates

It is expected that by manipulating the operation of the barrier gates (opening and closing) the flow velocities can be increased in a part of a tidal cycle (WL | Delft Hydraulics, 2007). In this way the flow patterns and sediment transport can be influenced. For example by closing parts of the barrier at ebb and other parts at flood. By closing during flood more sand can then be transported towards the barrier, or the flow velocities close to the coast may be higher resulting in an increase of sediment transport. Although some gain in sediment import may be achieved, this measure has the obvious disadvantage that it reduces the tidal prism inside the basin. Furthermore, more maintenance of the barrier may be required, which is undesirable.

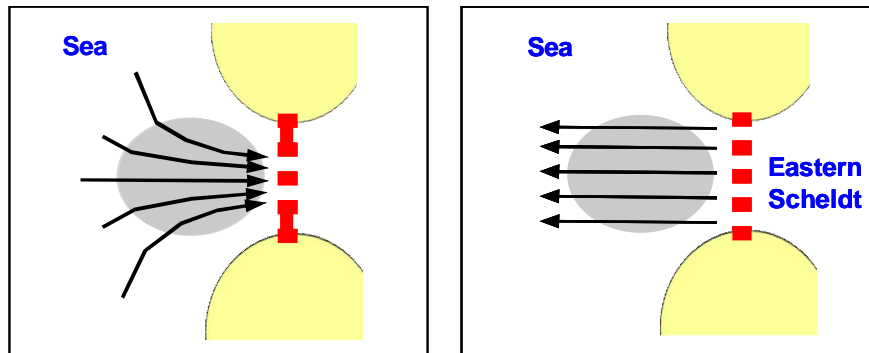


Figure 5.7 Indicative sketch of a possible different operation of the barrier gates during a tidal cycle

Directly or indirectly (by means of a pipeline) nourishing sediment in the basin

The most basic way to bring sediment to the Eastern Scheldt basin is to directly bring sediment to the scour hole(s) at the basin side of the Eastern Scheldt barrier. As it is assumed that sediment transport will be blocked by the barrier, the sediment will then move inside the basin. Where it will initially fill up the tidal channels and over the longer term also be beneficial for the inter-tidal flats.

Additionally, a permanent pipeline for the transport of sediment from outside the Eastern Scheldt to the scour hole on the inside of the barrier. Dredging vessels can then anchor on the seaward side of the barrier (e.g. on the seaward side of the sluices) and pump the sediment into the scour hole on the basin side of the barrier. The costs of such a measure are expected to be significantly smaller than for the other options.

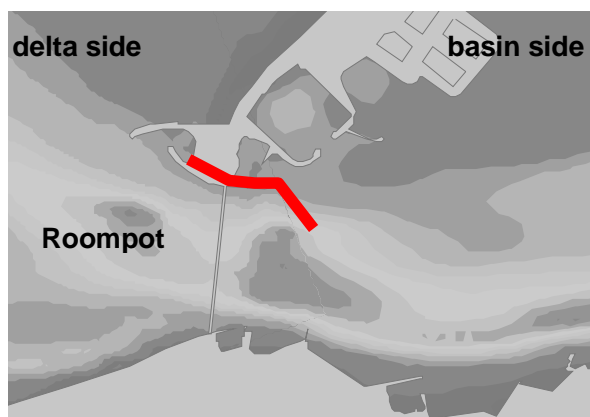


Figure 5.8 Indicative sketch (one of the options) of a pipeline towards the scour hole inside the basin

5.3.3 Timeframe of measures

A disadvantage of above measures, which improve sediment import into the Eastern Scheldt basin, is that it will take a very long time (tens of years) before the imported sediment will have an effect on the inter-tidal flats. Initially, only the tidal channels will be influenced.

A more direct way to raise the crest level of the inter-tidal flats is to nourish sand directly onto the inter-tidal flats. For which it is possible to either use sand from the tidal channels inside the Eastern Scheldt basin (although this sand will on the longer term return to the channels) or from outside the basin (a more permanent solution). The disadvantage of nourishing sand directly onto the inter-tidal flats is that it will be very expensive. In WL | Delft Hydraulics (2007) a rough estimate is given of the costs for purely nourishing sand from outside the Eastern Scheldt onto the inter-tidal flats of 1200-3600 M€. Therefore a combination of one of above measures (for the long term) with direct nourishing (on the short term) is worthwhile to be considered.

5.4 Question 3: Sediment transport potential

This question focuses on the capability of the outer delta to support the sand demand of the Eastern Scheldt. Note that in Chapter 4 the potential capacity of the Eastern Scheldt outer delta to transport sediment towards the barrier has been modelled and interpreted. It is then discussed how the local transport capacity compares to the actual sand demand of the Eastern Scheldt. Finally, the potential measures (in Section 5.3) are evaluated on the basis of our interpretation of the morphology. For which also the expected effect of a large nourishment ('mega suppletie') is discussed.

5.4.1 Potential sources of sediment

If measures are taken to allow the Eastern Scheldt to import sediment through the barrier, sufficient sediment is required near to the Eastern Scheldt barrier. If insufficient sediment is transported (or artificially nourished) in this area, the area seaward of the barrier will start to erode and sediment transport through the barrier will diminish. It is therefore very important to consider the potential capacity in the outer delta (mainly seaward of the Eastern Scheldt barrier) to transport sediment. Besides nourishing, two natural suppliers (transporters) of sediment can be distinguished, which are:

- Wave driven longshore sediment transport along the coasts of Walcheren and Schouwen and Schouwen (<1km from the shoreline)
- Tide driven sediment transport

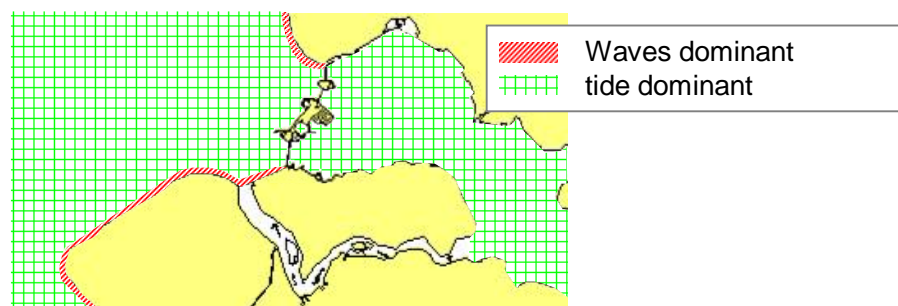


Figure 5.8 Governing sediment transport processes

In Figure 4.7 an interpretation is given of the (wave and tide driven) sediment transports in the Eastern Scheldt outer delta, as well as the observed coastline changes (from the 'Kustlijnkaarten 2007'). This figure has been used for the morphological evaluation of the measures.

5.4.2 Evaluation of sediment transport potential

On the basis of the evaluation of the sediment transport processes in the previous sections, it can be discerned how the transport capacity in the Eastern Scheldt outer delta compares to the sediment demand of the Eastern Scheldt basin. This sediment demand is in the order of 400 to 600 million m³ (see Section 2.3). If a timeframe of 100 years is concerned, the following can be concluded:

- To cope with the demand of the Eastern Scheldt basin over 100 year about 4 to 6 million m³/yr is required. Note that this is a considerable amount of sand (in the order of the total yearly sediment nourishments in the Netherlands).
- This is expected to be of the same order of magnitude as the tide driven transport capacities at the basin sides of the tidal inlets (tidal channels at about 2 kilometres from the barrier). Therefore it is expected that, in principle, sufficient transport capacity is available to make sediment import through the barrier feasible (i.e. contribute significantly).
- The wave driven longshore transport is an order of magnitude smaller than the required sediment import of the basin. It is in the order of 10,000 m³/yr for the current situation. While even for a seriously altered coastline orientation the contribution by wave driven longshore transport is not expected to supply more than 100,000 m³/yr as the wave energy is limited (but the tide driven transport may increase significantly).
- On the basis of the analysis of the sediment transports (Figure 4.7) it is expected that the Roompot has the most potential to transport sediment (most transport capacity). At the Hammen and at the Schaar the transport capacity is about a factor 3 smaller than for the Roompot (smaller inlets).

5.5 Evaluation of measures

The effectiveness of the measures can be evaluated on the basis of above considerations.

Filling the scour hole

Filling (and possibly covering) one or more of the scour hole(s) is expected to provide a suitable way to bypass sediment along the barrier. It is advised to study the filling and covering of the scour hole at the Roompot in combination with a large nourishment on the shoals south-west of the Roompot (e.g at the Banjaard). This combination will be required as it is possible that, as a result of filling the scour hole(s), too much sediment is exported from the Eastern Scheldt outer delta to the inner basin. The required dimensions of the area that is filled are expected to be of influence to the amount of sediment that will enter the basin and should be studied. Other questions that remain are related to the way the scour hole should be filled (e.g. by rock or geocontainers) and what the consequences of such a measure are. However, note that although importing sand through the barrier can provide sediment to the Western part of the basin (mainly inside the channels), it will take a long time before effects can be seen on the inter-tidal flats. Import of sediment should therefore be considered a long-term

measure. A combination with locally nourishing the inter-tidal flats (short-term measure) can therefore be effective.

Directly or indirectly (by means of a pipeline) nourishing sediment in the basin

Another option that is worth taking into consideration is directly or indirectly (by means of a pipeline) nourishing sediment into the basin. Sediment can be dredged outside the 'coastal foundation' and pumped into the basin. This can be regarded a zero or zero+ alternative, as these options have low initial costs. It is advised to study the effects of nourishing sediment into the scour hole(s) at the Eastern Scheldt side of the barrier.

Opening the dams at the landward sides of the barrier sections

On the basis of the sediment transport computations the opening of the dams at the landward sides of the barrier is expected to be a less effective solution, as the current longshore sediment transport at the Onrustpolder is only 10000 m³/yr and will not be in the order of millions of cubic meters in any case. The opening of the landward dams is therefore not expected to contribute enough to attain a significant import of sediment into the basin. Furthermore, the effect on the tidal prism of such a measure will be small.

Adjusting the barrier structure

Adjusting the barrier structure (reducing the hydraulic resistance) is expected to be a very costly solution. It is expected to yield a small increase in tidal flow through the barrier (and tidal range inside the basin), but sediment import through the barrier is not expected to be improved. It is therefore not considered a cost-effective solution.

Manipulation of the operation of the gates

Manipulating the barrier operation is an option that is not considered very practical as the effect is expected to be small and additional maintenance of the barrier is expected. Another impact of such a measure will be that the tidal prism inside the basin will be smaller, which is undesirable. Furthermore, there is the risk of damaging the gates.

Other developments

The effect of a large nourishment in front of the Walcheren coast, for example a 'zandmotor' at the Banjaard (RWS-Zeeland, 2008), on the import of sediment is expected to be small if it is not combined with one of the measures to make the barrier more 'open' to sediment transport (see Section 5.3). As most sediment is expected to be transported towards the Roompot and from there in north-western direction through the tidal channel and not through the barrier (see Figure 4.7). Furthermore, the sediment is not expected to be transported in 'large enough' quantities along the coast by wave driven transport (even for a seriously altered coastline orientation the wave driven longshore transport is an order of magnitude smaller than the sediment demand of the Eastern Scheldt).

5.6 How to proceed

As this is an initial assessment of the sediment transport capacities in the Eastern Scheldt outer delta, not all questions can be answered. This section points out a number of questions for different situations and the required actions to assess these questions.

Making the barrier more 'morphologically open'

If measures are implemented to make the barrier more 'open' to sediment transport, the following questions should be assessed:

- What will happen to the morphology of the Eastern Scheldt outer delta (i.e. transport patterns) if sand is imported into the Eastern Scheldt basin?
- What are the effects on the volume of the Eastern Scheldt outer delta itself? Is a (temporary) reduction in outer delta volume allowed?
- What are the secondary effects of a large scale measure (like filling and covering a scour hole) on the tide inside the Eastern Scheldt basin? Will it be reduced?
- What will be the effect of the sand that is brought into the Eastern Scheldt inner basin (beyond the barrier)? And what timescales should be expected?

Combine measures to the barrier with a large sediment nourishment

If measures to make the barrier more 'open' to sediment transport are combined with a large nourishment (e.g. at the 'Banjaard'), a number of questions still remain.

- What are the effects of the nourishment itself on the tidal flow and sediment transport patterns inside the Eastern Scheldt outer delta? Will it behave as expected for the current situation?
- What part of the nourished sediment will then enter the Eastern Scheldt basin for each of the measures?

Required modelling

To answer these questions morphological simulations with 2D and 3D numerical models will be required for specific combinations of measures (to the barrier) and nourishments. To come to such a model a number of steps should be taken:

- A model will need to be set-up that can hind-cast the tidal flow in the Eastern Scheldt in sufficient detail (especially close to the barrier).
- This model will have to be extended with a morphological module that can hind-cast the long-term morphological development of the Eastern Scheldt basin (modelling over time is to computational intensive for such a large area).
- This model will need to be validated by means of flow and sediment concentration measurements. The following measurements are suggested:
 - Tidal flow measurements at some locations preferably over half a year (and at least 28 days, which is one Spring-Neap cycle). These measurements are required to assess the residual currents. Relevant locations are the shoal South-West of the Roompot scour hole, the Roompot close to the Eastern Scheldt barrier and the tidal channel North-West of the Roompot.
 - Some 13 hour tidal flow measurements should be made over a ray close to the Eastern Scheldt barrier (approximately 1 or 2 kilometres from the barrier) for all three inlets. In this way a detailed flow field near to the barrier can be obtained for a small time interval. This information can then be used to calibrate the long-term measurements at single locations.
 - Taking water samples at the Eastern Scheldt barrier (at different depths, for different phases of the tide) and deriving the sand and mud content of these samples.
 - Additionally sediment concentration measurements can be made at the shoal South-West of the Roompot.

6 Conclusions

6.1 Conclusions

This report contains an initial assessment of the sediment transport capacities in the Eastern Scheldt outer delta, as well as an interpretation of the sediment transport patterns. This information has been applied to a number of currently considered measures that are aimed at making the Eastern Scheldt barrier more 'open' to sediment transport or nourishing sediment into the basin.

Morphology

From the initial analysis of the morphology of the Eastern Scheldt, it was concluded that the sediment transport capacity at the barrier provides a strong indication that it blocks sediment transport. Furthermore, the sediment transport capacities at Hammen and Schaar are smaller than for the Roompot. It is expected that sand is transported through the channels north of Walcheren towards the Roompot, from where it is expected to be transported to the North-West. Sediment that is transported along the coasts is expected to be transported in offshore direction in the Eastern Scheldt outer delta (Note that the Eastern Scheldt outer delta can benefit from this sediment and that at other locations sand is transported towards the coast).

Potentially effective measures

On the basis of the morphological findings, the following combinations of measures are expected to have the best prospects:

- A large nourishment at the northern side of Walcheren (at Vrouwenpolder or at the Banjaard) possibly in combination with filling (and possibly covering) the scour hole at the seaward side of the Roompot. It is expected that a part of this sediment is then transported through the barrier into the Eastern Scheldt basin. Further study will, however, be required to assess the effectiveness of such a measure (i.e. part of the sediment that is imported into the basin).
- Bringing sand from outside the 'coastal foundation' directly or indirectly (by means of a pipeline beyond the barrier) to the scour hole at the Eastern Scheldt basin side of the Roompot.

6.2 Recommendations

In Section 5.5 a number of questions that need to be assessed are mentioned. This section points out a number of questions which are related to:

- the morphology of the Eastern Scheldt outer delta,
- the hydraulic and morphologic impact of measures at the barrier, and
- the hydraulic and morphologic impact of a large nourishment at the 'Banjaard'.
- the effects of the sediment that is imported into the Eastern Scheldt basin

To answer these questions morphological simulations with 2D and 3D numerical models are recommended for specific combinations of measures (to the barrier) and nourishments.

References

Alkyon, 2008

'Morphodynamics of the Delta coast (south-west Netherlands): Quantative analysis and phenomenology of the morphological evolution 1964-2004'

Alkyon, project A1881, January 2008

Deltares, 2008

'projectplan zandhonger Oosterschelde'

Deltares, project Z4581, June 2008

R1367, 1980

'Morfologie voordelta Oosterscheldemonnd'

WL | Delft Hydraulics, verslag onderzoek, augustus 1980

RWS-RIKZ, 2006

'Kustlijnkaarten 2007'

Rijkswaterstaat, Rijksinstituut voor Kust en Zee / RIKZ, rapport RIKZ-2006.019, December 2006

RWS-1

'Ontwerpnota stormvloedkering Oosterschelde. Boek 1: Totaalontwerp'

Min. van Verkeer en Waterstaat, Rijkswaterstaat

RWS-Zeeland, 2008

'Toepassing Zandmotor Banjaard in de ZW Delta'

Saskia Huijs & Leo Adriaanse, memo, 15 oktober 2008

Oosterlaan, W.M.A., Zagers, L.M., 1996

'Veranderingen in de hydrodynamiek en morfologie van het Oosterscheldebekken in de periode 1990-1995'

Universiteit Utrecht, Inst. voor Marien en Atmosferisch Onderzoek, rapport R96-22, november 1996

RWS-RIKZ, 2000-1

'Zandverliezen in het Nederlandse kuststelsel. Advies voor dynamisch handhaven in de 21e eeuw'

Rijkswaterstaat, Rijksinstituut voor Kust en Zee / RIKZ, rapport RIKZ/2000.36, juni 2000

RWS-RIKZ, 2000-2

'Delta 2000. Inventarisatie huidige situatie Deltawateren'

Rijkswaterstaat, Rijksinstituut voor Kust en Zee / RIKZ, rapport RIKZ/2000.047, oktober 2000

RWS-RIKZ, 2003-1

'Veranderende draagkracht van de Oosterschelde voor kokkels'

Rijkswaterstaat, Rijksinstituut voor Kust en Zee / RIKZ, rapport RIKZ 2003.043, november 2003

RWS-RIKZ , 2003-2

‘Verkenning draagkracht Oosterschelde’

Rijksinstituut voor Kust en Zee / RIKZ, rapport RIKZ 2003.049, november 2003

RWS-RIKZ en RIVO, 2003

‘Veranderende draagkracht van de Oosterschelde voor kokkels’

Rijksinstituut voor Kust en Zee / RIKZ, rapport RIKZ 2003.043, november 2003

Stolk, A., 1989

‘Zandsysteem kust, een morfologische karakterisering’

Rijksuniversiteit Utrecht, Vakgroep Fysische Geografie, rapport GEOPRO 1989.02, 1989

Van Rijn, 1993.

‘Principles of sediment transport in rivers, estuaries and coastal seas.’

Aqua Publications, The Netherlands, Van Rijn, L.C., 1993, 7.41–7.43 stochastic predictor

WL | Delft Hydraulics, 2007

‘Zandhonger Oosterschelde, Maatregelen ter vergroting van doorstroomcapaciteit en zanddoorvoer stormvloedkering Oosterschelde’

WL | Delft Hydraulics , Ir. T.H.G. Jongeling, project Q4264, November 2007

Tables

Cond.	Hs	Tp	Peak wave direction	Duration	Cond.	Hs	Tp	Peak wave direction	Duration
	[m]	[s]	[°N]	[Days]		[m]	[s]	[°N]	[Days]
1	0.6	4.4	1	11.04	61	4.5	8.6	356	0.2
2	0.7	4.3	29	11.93	62	4.2	8.3	28	0.036
3	0.6	4.1	59	6.71	63	4.7	8.0	71	0.0052
4	0.7	4.0	90	4.33	64	4.6	8.0	146	0.01
5	0.7	3.8	120	3.51	65	4.2	7.8	179	0.01
6	0.6	3.8	151	3.53	66	4.3	7.5	219	0.089
7	0.7	3.9	183	5.68	67	4.4	7.7	239	0.59
8	0.7	4.0	213	13.34	68	4.5	7.7	270	0.49
9	0.7	4.2	239	18.59	69	4.4	7.8	300	0.34
10	0.7	4.2	269	8.61	70	4.4	8.5	331	0.5
11	0.6	4.3	300	6.65	71	5.6	9.2	350	0.0052
12	0.6	4.4	331	6.95	72	5.8	7.9	210	0.0052
13	1.2	4.7	1	2.84	73	6.0	8.9	240	0.026
14	1.2	4.7	30	3.67	74	5.8	8.0	284	0.0052
15	1.2	4.7	60	2.25	75	5.9	8.9	289	0.0052
16	1.3	4.6	91	2.4	76	5.9	9.4	332	0.042
17	1.2	4.4	120	1.46	77	5.6	10.2	346	0.0052
18	1.3	4.4	152	1.18	78	6.2	10.2	339	0.0052
19	1.3	4.4	184	3.4	79	0.5	5.0	0	0.78
20	1.3	4.6	214	12.31	80	0.5	5.0	28	0.31
21	1.3	4.6	237	12.92	81	0.6	5.0	63	0.1
22	1.3	4.6	268	4.52	82	0.6	5.0	92	0.01
23	1.2	4.7	300	2.53	83	0.5	5.0	122	0.026
24	1.2	4.7	331	2.19	84	0.5	5.0	154	0.0052
25	0.9	5.2	2	0.92	85	0.5	5.0	186	0.031
26	0.9	5.2	27	0.64	86	0.6	5.0	211	0.073
27	0.9	5.2	59	0.22	87	0.6	5.0	243	0.14
28	0.9	5.2	84	0.031	88	0.6	5.0	270	0.14
29	0.9	5.2	123	0.016	89	0.6	5.0	301	0.29
30	0.9	5.1	149	0.036	90	0.6	5.0	331	0.49
31	0.9	5.2	185	0.042	91	0.7	6.0	358	19.44
32	0.9	5.2	215	0.13	92	0.7	5.7	26	3.98
33	0.9	5.2	239	0.53	93	0.7	5.9	60	1.2
34	0.9	5.2	270	0.29	94	0.7	5.9	87	0.6
35	0.9	5.2	301	0.34	95	0.7	5.8	120	0.31
36	0.9	5.2	331	0.5	96	0.6	5.9	152	0.24
37	1.7	6.0	359	16.18	97	0.7	5.8	182	0.51
38	1.6	5.8	29	9.37	98	0.7	5.7	211	0.73
39	1.7	5.7	58	3.9	99	0.7	5.7	242	1.61
40	1.7	5.5	87	1.14	100	0.7	5.8	271	1.68
41	1.6	5.4	118	0.26	101	0.7	5.8	302	3.05
42	1.9	5.5	154	0.26	102	0.7	6.0	334	9.27
43	1.8	5.5	186	1.51	103	1.3	6.7	357	8.72
44	1.8	5.6	217	14.29	104	1.2	6.5	27	1.07
45	1.8	5.7	237	23.92	105	1.2	6.5	60	0.37
46	1.8	5.7	269	8.82	106	1.2	6.6	90	0.2
47	1.7	5.8	301	8.03	107	1.3	6.8	123	0.057
48	1.8	6.1	332	12.6	108	1.4	6.6	148	0.042
49	3.0	7.3	357	2.78	109	1.4	7.2	182	0.1
50	3.0	7.0	29	1.13	110	1.1	6.2	212	0.068
51	2.8	6.7	56	0.36	111	1.1	6.1	240	0.23
52	2.7	6.1	87	0.073	112	1.2	6.4	273	0.35
53	2.8	6.2	123	0.042	113	1.2	6.5	302	0.85
54	3.2	6.4	150	0.036	114	1.3	6.8	335	4.52
55	3.0	6.3	185	0.29	115	2.8	8.7	350	0.016
56	2.9	6.4	217	3.88	116	2.7	8.7	335	0.031
57	3.0	6.7	236	9.99	117	0.7	12.6	344	0.0052
58	3.1	6.7	270	3.58					
59	3.0	6.8	300	2.4					
60	3.0	7.3	332	4.15					

Table 3.2 Schematised normal wave climate (all year)

Cond.	Hs	Tp	Peak wave direction	Duration	Cond.	Hs	Tp	Peak wave direction	Duration
	[m]	[s]	[°N]	[Days]		[m]	[s]	[°N]	[Days]
1	0.6	4.5	1	1.06	61	4.6	8.7	358	0.089
2	0.6	4.4	32	1.58	62	4.3	8.4	31	0.026
3	0.7	4.2	59	1.42	63	4.7	8.0	71	0.0052
4	0.7	4.0	90	1.25	64	4.4	8.4	146	0.0052
5	0.7	3.8	120	1.23	65	4.1	7.3	220	0.021
6	0.6	3.8	150	1.03	66	4.4	7.8	240	0.32
7	0.7	3.8	183	1.71	67	4.5	7.7	271	0.27
8	0.7	3.9	212	3.63	68	4.5	7.9	300	0.18
9	0.7	4.1	239	3.48	69	4.5	8.5	332	0.32
10	0.7	4.2	269	1.7	70	6.3	9.1	240	0.01
11	0.7	4.4	300	1.11	71	5.8	8.0	284	0.0052
12	0.7	4.5	331	1.03	72	5.7	9.3	337	0.01
13	1.3	4.7	360	0.27	73	0.5	5.0	2	0.083
14	1.2	4.8	32	0.69	74	0.6	5.0	30	0.078
15	1.3	4.6	60	0.98	75	0.6	5.0	63	0.031
16	1.3	4.6	90	1.03	76	0.5	5.0	154	0.0052
17	1.2	4.4	119	0.54	77	0.5	5.0	185	0.016
18	1.3	4.3	152	0.37	78	0.5	5.0	211	0.01
19	1.3	4.4	184	1.05	79	0.6	5.0	239	0.021
20	1.4	4.6	213	3.59	80	0.6	5.0	275	0.026
21	1.3	4.7	237	2.93	81	0.5	5.0	302	0.057
22	1.3	4.7	268	0.98	82	0.6	5.0	331	0.11
23	1.3	4.7	301	0.59	83	0.7	6.1	358	3.08
24	1.3	4.8	329	0.45	84	0.7	5.8	27	0.74
25	1.0	5.3	5	0.11	85	0.7	5.9	60	0.32
26	0.9	5.2	30	0.15	86	0.7	5.9	87	0.17
27	0.9	5.2	61	0.083	87	0.7	6.0	121	0.11
28	0.9	5.2	78	0.01	88	0.7	6.1	150	0.083
29	1.0	5.4	107	0.0052	89	0.7	5.8	184	0.19
30	0.9	5.1	154	0.026	90	0.7	5.6	209	0.2
31	1.0	5.3	189	0.01	91	0.7	5.7	243	0.37
32	0.9	5.3	214	0.031	92	0.7	5.9	270	0.29
33	0.9	5.2	238	0.14	93	0.7	5.8	302	0.57
34	1.0	5.2	271	0.052	94	0.7	6.0	334	1.68
35	0.9	5.2	299	0.073	95	1.3	6.8	357	1.65
36	0.9	5.3	331	0.073	96	1.3	6.6	29	0.35
37	1.7	6.1	358	2.69	97	1.2	6.5	60	0.23
38	1.7	5.8	32	2.88	98	1.2	6.5	91	0.13
39	1.7	5.8	58	1.99	99	1.2	6.7	120	0.036
40	1.7	5.5	87	0.6	100	1.5	6.9	152	0.01
41	1.6	5.4	119	0.14	101	1.3	7.2	182	0.078
42	2.0	5.6	156	0.099	102	1.2	6.2	211	0.021
43	1.8	5.6	186	0.62	103	1.2	6.0	239	0.089
44	1.9	5.6	216	4.39	104	1.3	6.6	271	0.12
45	1.9	5.7	237	7.62	105	1.3	6.7	303	0.22
46	1.9	5.7	269	2.63	106	1.3	6.8	334	0.99
47	1.8	5.8	301	2.28	107	2.7	8.7	348	0.01
48	1.8	6.1	331	2.72	108	2.7	8.6	332	0.016
49	3.0	7.3	357	0.64					
50	2.9	7.0	34	0.51					
51	2.8	6.9	56	0.28					
52	2.7	6.2	89	0.052					
53	2.7	6.0	124	0.016					
54	3.1	6.2	151	0.021					
55	3.1	6.3	184	0.14					
56	3.0	6.5	218	1.3					
57	3.0	6.7	236	4.55					
58	3.1	6.7	269	1.62					
59	3.1	6.8	300	0.95					
60	3.1	7.4	332	1.28					

Table 3.3 Schematised normal wave climate (Winter)

Cond.	Hs	Tp	Peak wave direction	Duration	Cond.	Hs	Tp	Peak wave direction	Duration
	[m]	[s]	[°N]	[Days]		[m]	[s]	[°N]	[Days]
1	0.6	4.4	2	4.53	61	4.6	7.3	223	0.01
2	0.7	4.3	28	4.34	62	4.6	7.9	237	0.047
3	0.6	4.2	59	1.74	63	4.4	7.8	273	0.026
4	0.6	4.1	90	1.11	64	4.1	7.8	311	0.0052
5	0.6	4.0	120	0.49	65	4.2	8.9	339	0.021
6	0.6	4.0	151	0.7	66	0.6	5.0	2	0.31
7	0.6	3.9	183	1.25	67	0.5	5.0	31	0.078
8	0.7	4.1	214	3.2	68	0.6	5.0	61	0.042
9	0.7	4.2	238	5.56	69	0.6	5.0	92	0.01
10	0.6	4.3	268	2.06	70	0.5	5.0	122	0.026
11	0.6	4.3	301	1.84	71	0.7	5.0	194	0.0052
12	0.6	4.3	331	1.97	72	0.6	5.0	213	0.036
13	1.2	4.7	2	1.18	73	0.6	5.0	242	0.052
14	1.2	4.7	28	1.36	74	0.6	5.0	268	0.063
15	1.3	4.7	56	0.23	75	0.6	5.0	301	0.12
16	1.2	4.5	90	0.21	76	0.6	5.0	330	0.14
17	1.2	4.5	119	0.099	77	0.7	6.0	358	7.17
18	1.3	4.5	153	0.073	78	0.7	5.7	25	1.3
19	1.3	4.4	184	0.36	79	0.7	5.8	60	0.4
20	1.3	4.6	216	2.21	80	0.7	5.7	86	0.23
21	1.3	4.6	235	2.74	81	0.6	5.8	120	0.1
22	1.3	4.6	267	0.95	82	0.6	5.8	152	0.1
23	1.3	4.7	300	0.46	83	0.6	5.7	180	0.12
24	1.2	4.7	333	0.58	84	0.7	5.8	213	0.27
25	0.9	5.2	2	0.4	85	0.7	5.7	241	0.61
26	0.9	5.2	26	0.19	86	0.7	5.8	272	0.69
27	0.9	5.2	59	0.042	87	0.7	5.8	302	1.07
28	0.9	5.2	93	0.01	88	0.7	6.1	334	3.35
29	0.9	5.1	132	0.01	89	1.2	6.6	357	2.53
30	0.9	5.2	137	0.01	90	1.2	6.4	27	0.25
31	0.9	5.3	178	0.0052	91	1.2	6.5	59	0.068
32	0.9	5.1	215	0.047	92	1.4	7.1	87	0.021
33	0.9	5.2	237	0.17	93	1.5	6.9	128	0.021
34	0.9	5.2	269	0.1	94	1.3	6.6	147	0.031
35	0.9	5.2	301	0.1	95	1.8	7.3	176	0.0052
36	0.9	5.2	330	0.16	96	1.1	5.9	214	0.01
37	1.7	6.0	0	5.67	97	1.1	6.1	240	0.094
38	1.6	5.7	26	3.04	98	1.2	6.5	275	0.073
39	1.6	5.7	57	0.53	99	1.2	6.6	300	0.16
40	1.3	5.6	90	0.078	100	1.3	6.8	336	1.25
41	1.5	5.7	115	0.031	101	2.9	8.9	353	0.0052
42	1.7	5.3	153	0.021	102	0.7	12.6	344	0.0052
43	1.6	5.5	185	0.1					
44	1.7	5.6	218	2.41					
45	1.7	5.6	235	4.22					
46	1.7	5.7	270	0.95					
47	1.7	5.8	302	1.04					
48	1.8	6.0	334	2.91					
49	3.0	7.3	358	0.82					
50	2.8	6.8	29	0.15					
51	2.8	6.4	51	0.01					
52	3.0	6.5	90	0.0052					
53	2.6	6.7	131	0.0052					
54	2.7	5.8	189	0.021					
55	2.9	6.4	218	0.39					
56	3.0	6.6	234	0.63					
57	2.9	6.6	270	0.22					
58	2.9	6.7	298	0.14					
59	2.9	7.3	334	0.73					
60	4.3	8.7	356	0.036					

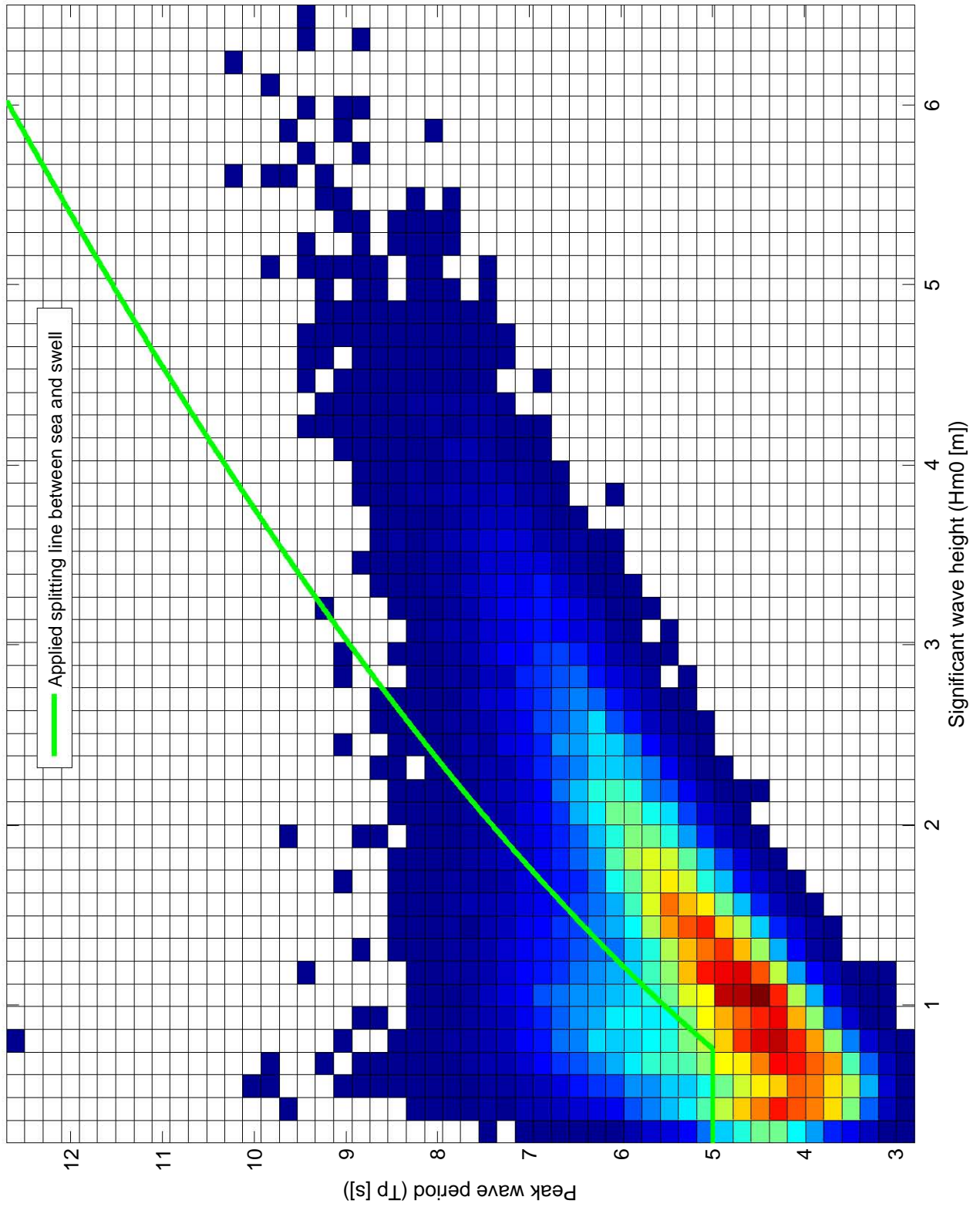
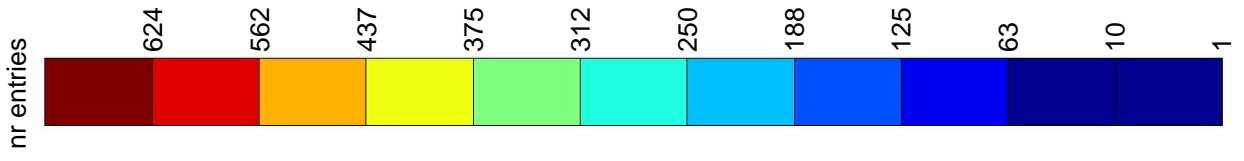
Table 3.4 Schematised normal wave climate (Spring)

Cond.	Hs	Tp	Peak wave direction	Duration	Cond.	Hs	Tp	Peak wave direction	Duration
	[m]	[s]	[°N]	[Days]		[m]	[s]	[°N]	[Days]
1	0.6	4.4	1	3.95	61	0.5	5.0	359	0.28
2	0.7	4.2	29	4.14	62	0.5	5.0	27	0.089
3	0.6	4.1	58	1.71	63	0.5	5.0	67	0.021
4	0.6	4.0	89	0.77	64	0.5	5.0	174	0.0052
5	0.6	3.8	118	0.39	65	0.6	5.0	214	0.01
6	0.6	3.8	151	0.4	66	0.6	5.0	243	0.057
7	0.6	3.9	183	0.91	67	0.6	5.0	267	0.026
8	0.7	4.0	215	3.02	68	0.5	5.0	301	0.073
9	0.7	4.1	238	6.95	69	0.5	5.0	331	0.18
10	0.7	4.2	269	3.45	70	0.7	6.0	358	5.42
11	0.6	4.2	300	2.62	71	0.7	5.7	27	1.15
12	0.6	4.4	331	2.69	72	0.7	5.8	59	0.31
13	1.2	4.7	1	1.09	73	0.6	5.8	90	0.078
14	1.2	4.7	28	1.13	74	0.7	6.1	119	0.036
15	1.2	4.7	56	0.26	75	0.5	5.6	158	0.026
16	1.2	4.5	90	0.11	76	0.5	5.9	182	0.083
17	1.1	4.3	116	0.042	77	0.6	5.6	212	0.11
18	1.3	4.4	152	0.099	78	0.6	5.6	241	0.37
19	1.3	4.4	183	0.32	79	0.7	5.7	270	0.48
20	1.3	4.5	217	2.4	80	0.7	5.7	303	0.96
21	1.3	4.6	237	4.54	81	0.7	5.9	334	2.76
22	1.3	4.6	269	1.12	82	1.3	6.6	357	2.39
23	1.2	4.7	299	0.82	83	1.2	6.4	27	0.16
24	1.2	4.7	331	0.75	84	1.2	7.1	69	0.031
25	0.9	5.2	1	0.29	85	1.2	6.2	88	0.016
26	0.9	5.2	26	0.17	86	1.0	5.7	222	0.01
27	0.9	5.2	58	0.052	87	1.1	5.9	235	0.016
28	0.9	5.4	84	0.0052	88	1.1	6.2	274	0.063
29	0.9	5.3	187	0.01	89	1.2	6.4	303	0.29
30	0.9	5.2	216	0.026	90	1.3	6.6	335	1.37
31	0.9	5.2	241	0.16					
32	0.9	5.2	273	0.089					
33	0.9	5.2	303	0.12					
34	0.9	5.2	332	0.15					
35	1.6	5.9	358	4.18					
36	1.5	5.6	27	1.25					
37	1.4	5.3	58	0.19					
38	1.3	5.4	86	0.021					
39	1.7	5.4	118	0.021					
40	1.6	5.7	150	0.016					
41	1.7	5.3	189	0.12					
42	1.8	5.6	219	2.18					
43	1.8	5.6	236	5.67					
44	1.7	5.6	269	2.11					
45	1.6	5.7	302	1.83					
46	1.7	6.1	333	3.47					
47	2.9	7.1	354	0.25					
48	2.9	7.3	21	0.042					
49	2.9	6.2	190	0.016					
50	2.9	6.3	219	0.41					
51	2.8	6.4	234	0.94					
52	3.0	6.5	270	0.25					
53	2.9	6.7	302	0.31					
54	3.1	7.2	331	0.81					
55	4.2	8.4	347	0.016					
56	4.0	8.2	21	0.0052					
57	4.0	7.3	226	0.0052					
58	4.3	7.7	269	0.026					
59	4.1	7.8	305	0.01					
60	4.3	8.2	329	0.083					

Table 3.5 Schematised normal wave climate (Summer)

Cond.	Hs	Tp	Peak wave direction	Duration	Cond.	Hs	Tp	Peak wave direction	Duration
	[m]	[s]	[°N]	[Days]		[m]	[s]	[°N]	[Days]
1	0.6	4.5	1	1.51	61	4.8	7.6	145	0.0052
2	0.7	4.3	31	1.87	62	4.2	7.8	179	0.01
3	0.7	4.1	60	1.84	63	4.3	7.6	218	0.057
4	0.7	4.0	91	1.21	64	4.3	7.6	239	0.22
5	0.7	3.8	121	1.41	65	4.5	7.7	270	0.17
6	0.7	3.8	152	1.42	66	4.4	7.8	298	0.15
7	0.7	3.9	182	1.82	67	4.3	8.4	330	0.083
8	0.7	4.0	212	3.49	68	5.6	9.2	350	0.0052
9	0.7	4.2	239	2.59	69	5.8	7.9	210	0.0052
10	0.7	4.2	269	1.4	70	5.8	8.8	240	0.016
11	0.7	4.4	300	1.08	71	5.9	8.9	289	0.0052
12	0.7	4.5	330	1.27	72	5.9	9.5	330	0.031
13	1.3	4.8	359	0.31	73	5.6	10.2	346	0.0052
14	1.2	4.7	34	0.48	74	6.2	10.2	339	0.0052
15	1.2	4.7	62	0.78	75	0.6	5.0	359	0.11
16	1.3	4.6	92	1.04	76	0.6	5.0	23	0.063
17	1.3	4.4	120	0.78	77	0.7	5.0	62	0.01
18	1.3	4.4	151	0.63	78	0.4	5.0	190	0.0052
19	1.3	4.5	184	1.67	79	0.6	5.0	204	0.016
20	1.4	4.6	211	4.11	80	0.7	5.0	254	0.0052
21	1.3	4.7	239	2.72	81	0.6	5.0	272	0.021
22	1.3	4.7	267	1.48	82	0.6	5.0	298	0.036
23	1.2	4.7	299	0.66	83	0.7	5.0	329	0.073
24	1.3	4.8	328	0.41	84	0.7	6.1	360	3.77
25	0.9	5.2	1	0.12	85	0.7	5.7	26	0.8
26	0.9	5.2	27	0.13	86	0.7	5.9	59	0.17
27	0.9	5.2	56	0.042	87	0.7	6.0	84	0.12
28	0.9	5.1	81	0.0052	88	0.6	5.5	120	0.057
29	0.9	5.1	185	0.016	89	0.7	5.7	152	0.026
30	0.9	5.2	212	0.026	90	0.7	5.7	182	0.11
31	0.9	5.2	243	0.063	91	0.7	5.7	212	0.15
32	0.9	5.2	265	0.042	92	0.7	5.7	243	0.26
33	0.9	5.2	299	0.047	93	0.7	5.8	270	0.22
34	0.9	5.2	330	0.12	94	0.7	5.6	302	0.45
35	1.7	6.2	358	3.63	95	0.7	6.0	334	1.48
36	1.7	5.8	30	2.19	96	1.3	6.8	358	2.14
37	1.7	5.6	58	1.19	97	1.2	6.4	26	0.31
38	1.7	5.5	86	0.44	98	1.1	6.2	57	0.047
39	1.7	5.3	118	0.063	99	1.1	6.6	88	0.036
40	1.8	5.5	153	0.12	100	1.4	7.0	182	0.021
41	1.8	5.5	185	0.67	101	1.2	6.6	209	0.026
42	1.9	5.6	215	5.32	102	1.2	6.1	247	0.036
43	1.9	5.7	238	6.41	103	1.2	6.4	275	0.099
44	1.8	5.7	270	3.12	104	1.3	6.6	304	0.18
45	1.8	5.8	301	2.88	105	1.4	6.9	335	0.91
46	1.8	6.1	331	3.49	106	2.8	8.8	338	0.016
47	3.0	7.5	357	1.07					
48	3.0	7.0	26	0.43					
49	2.8	6.3	59	0.073					
50	2.7	5.9	79	0.016					
51	3.1	6.2	121	0.021					
52	3.2	6.5	149	0.016					
53	2.9	6.4	185	0.11					
54	2.9	6.4	217	1.79					
55	3.0	6.7	237	3.86					
56	3.1	6.7	271	1.48					
57	3.1	6.9	299	1					
58	3.0	7.3	332	1.33					
59	4.4	8.5	355	0.063					
60	4.0	7.6	23	0.0052					

Table 3.6 Schematised normal wave climate (Autumn)



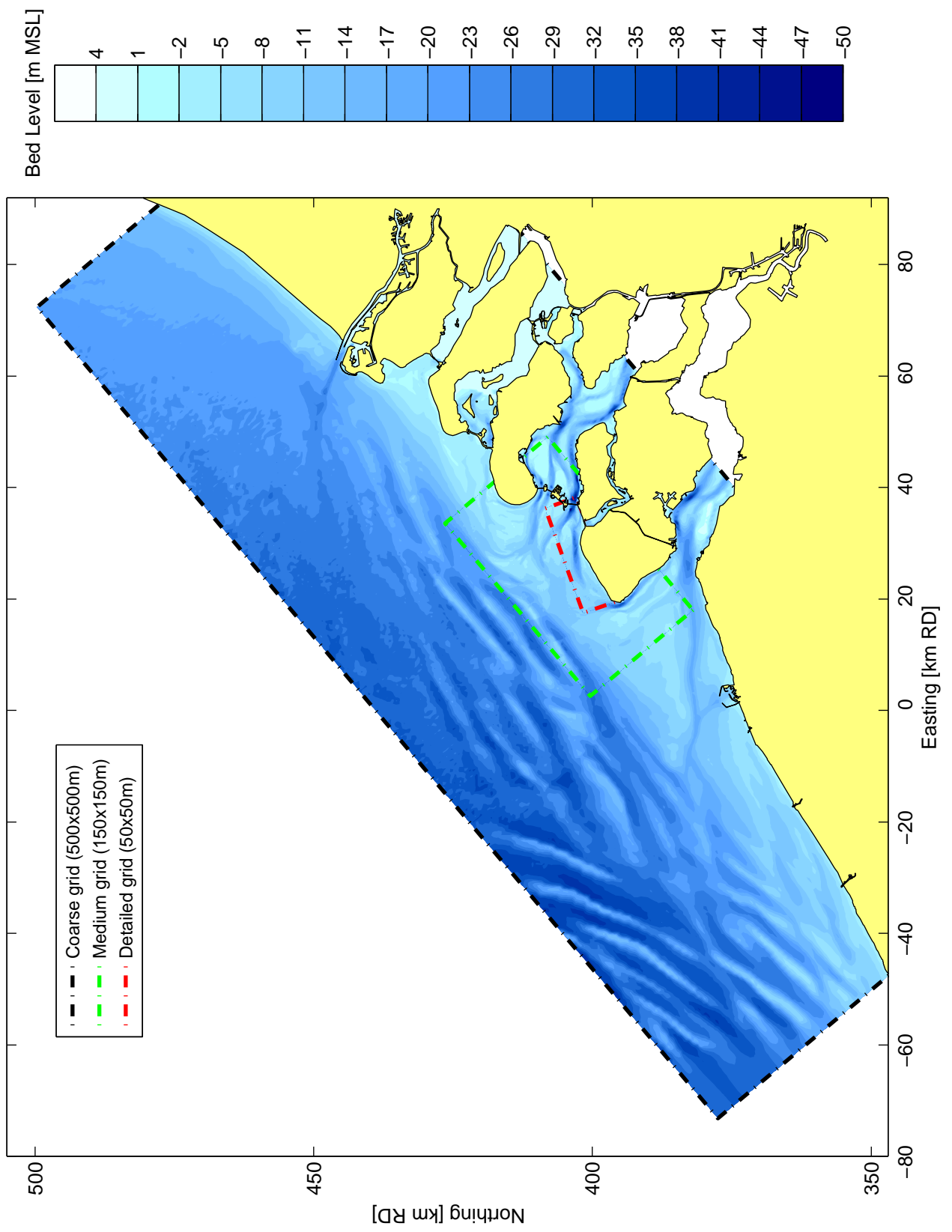
Scatter plot in terms of entries of wave data and splitting line of sea and swell data

Zandhonger Oosterschelde

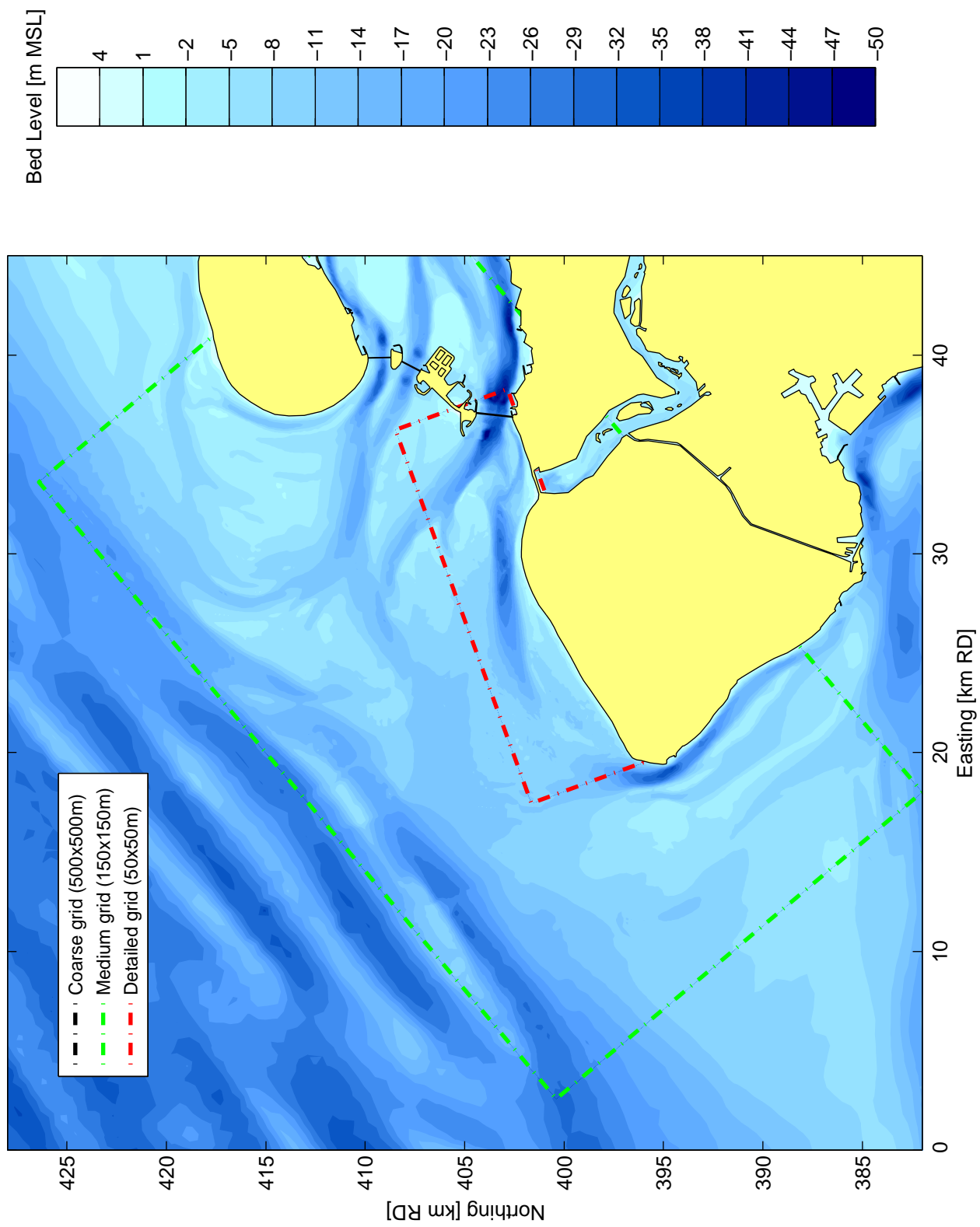
Deltares

Z4581

Fig. 3.1



Bathymetry and grid of the SWAN model (bathymetry data 2004)		
	Zandhonger Oosterschelde	
Deltares	z4581	Fig.3.2



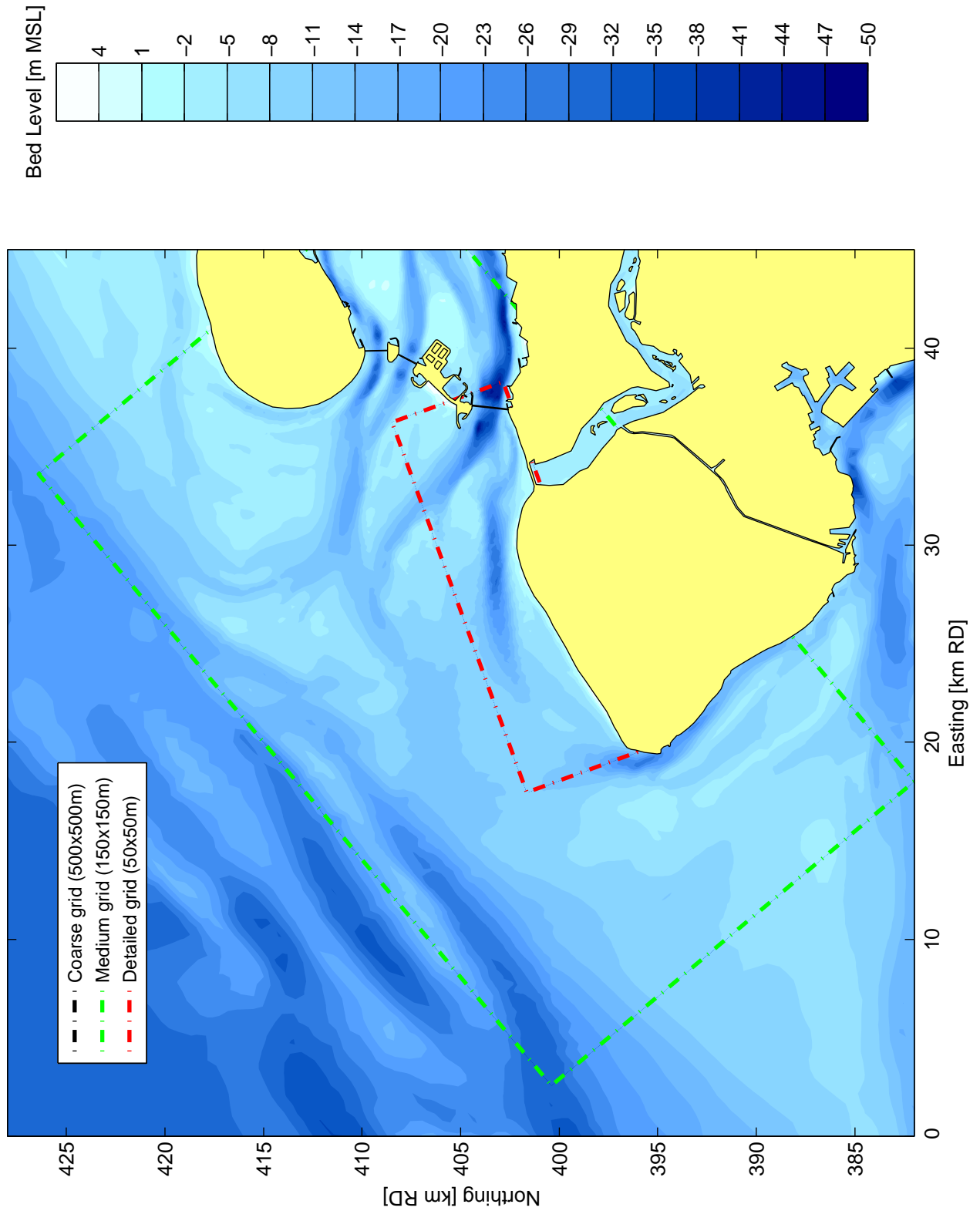
Detail of Eastern Scheldt bathymetry in the SWAN model
(bathymetry data 2004)

Zandhonger Oosterschelde

Deltares

z4581

Fig.3.3a



Detail of Eastern Scheldt bathymetry in the SWAN model
(bathymetry data 1999 from MATROOS)

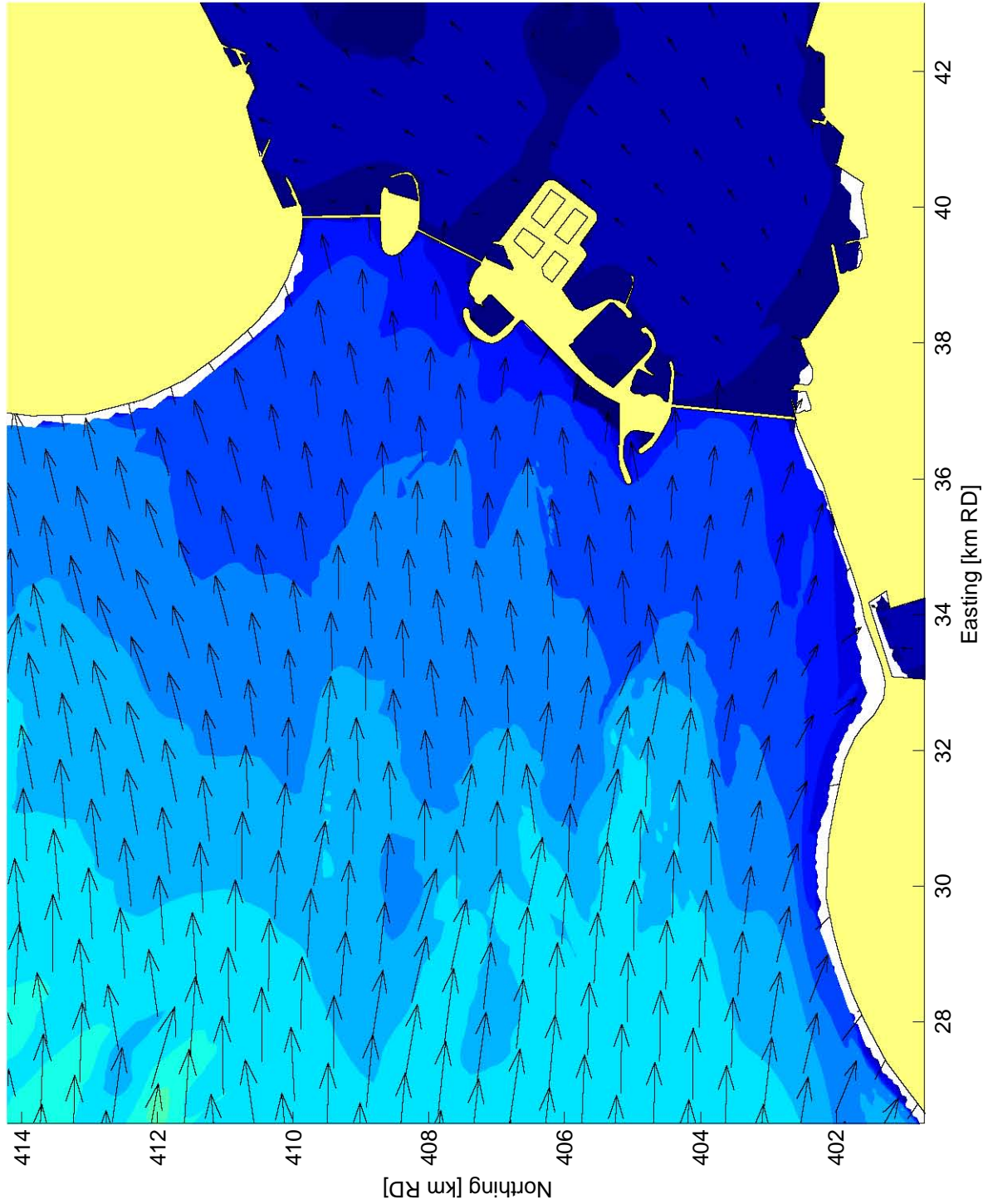
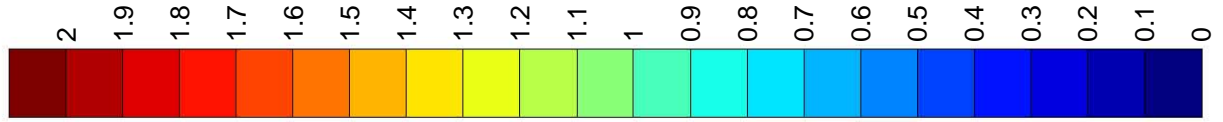
Zandhonger Oosterschelde

Deltares

z4581

Fig.3.3b

Significant wave height (m)



Normal wave condition 45 for the Eastern Scheldt delta (bathymetry 2004)
 (offshore : $H_s = 1.8\text{m}$, $T_p = 5.7\text{s}$, $\text{dir} = 237^\circ\text{N}$, ~ 25 days/yr)

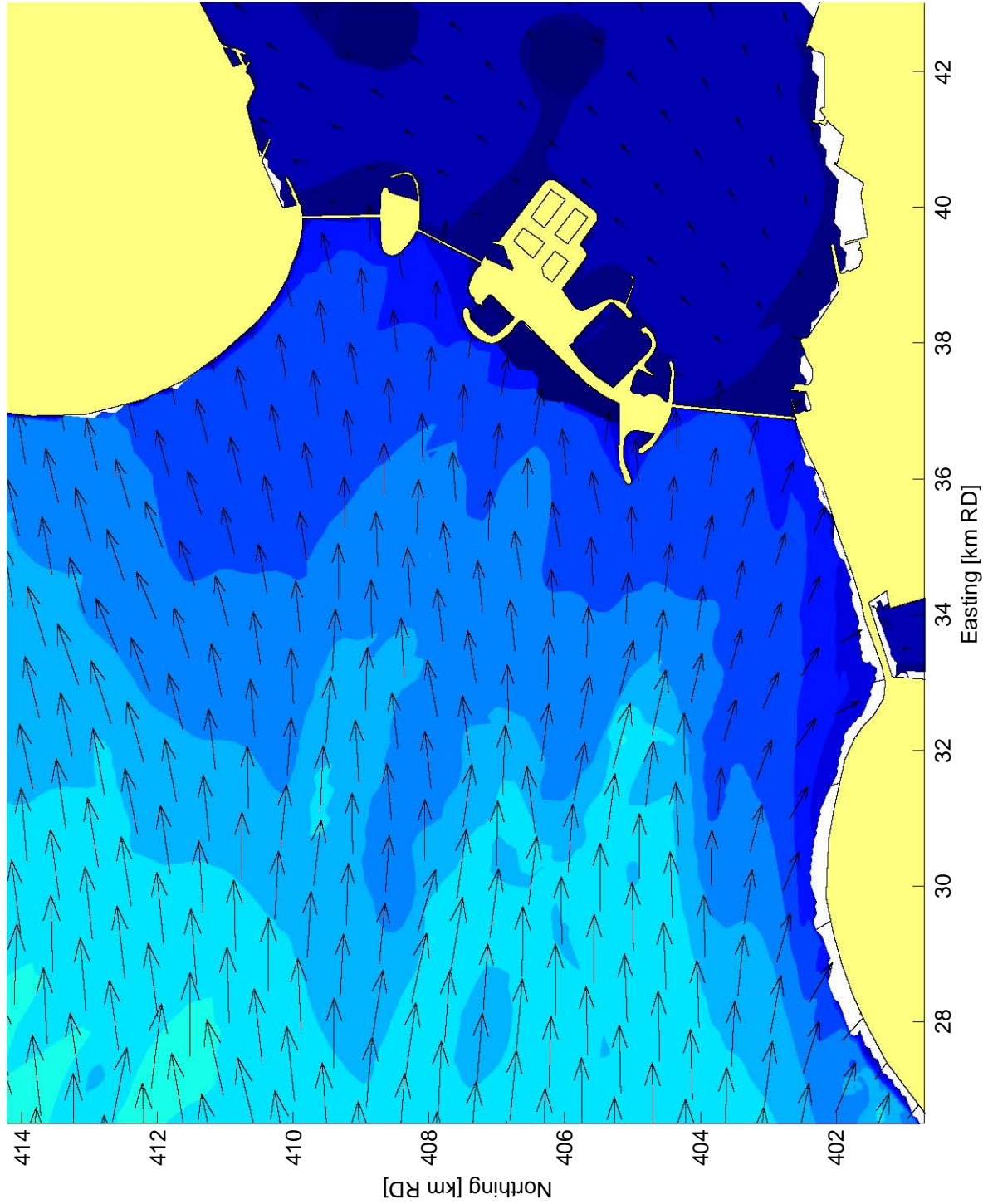
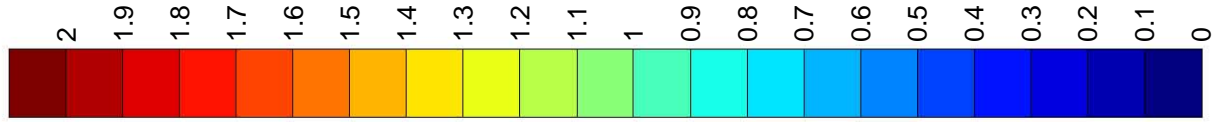
Zandhonger Oosterschelde

Deltares

z4581

Fig. 3.4a

Significant wave height (m)



Normal wave condition 45 for the Eastern Scheldt delta (bathymetry 1999)
 (offshore : $H_s = 1.8\text{m}$, $T_p = 5.7\text{s}$, $\text{dir} = 237^\circ\text{N}$, ~ 25 days/yr)

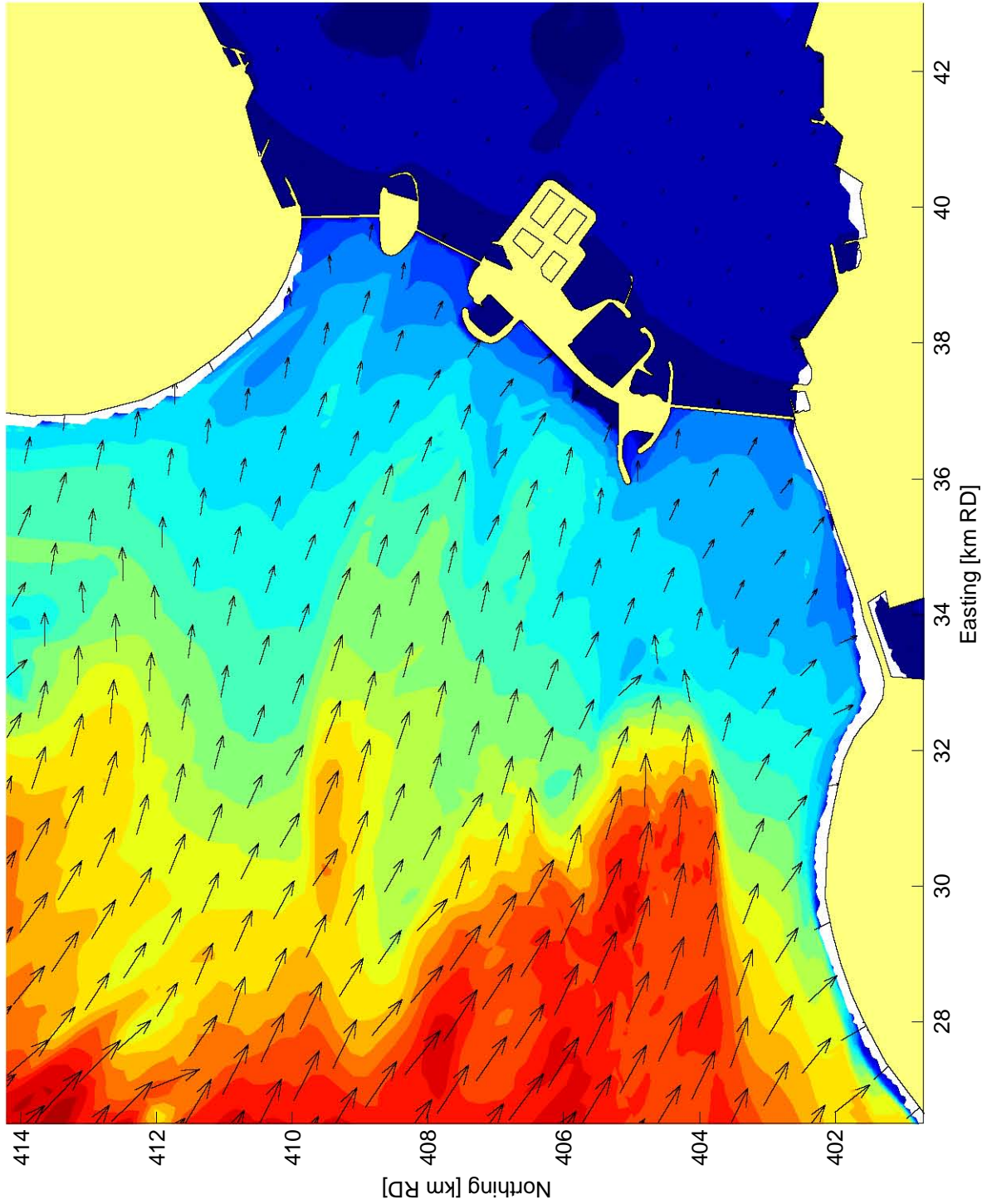
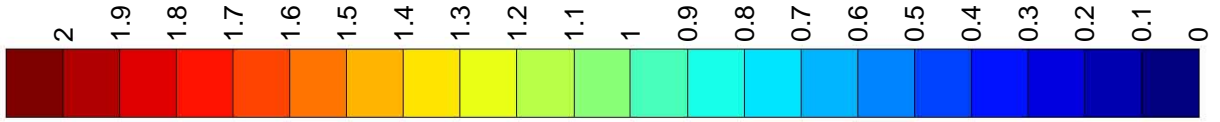
Zandhonger Oosterschelde

Deltares

z4581

Fig. 3.4b

Significant wave height (m)



Normal wave condition 69 for the Eastern Scheldt delta (bathymetry 2004)
 (offshore : $H_s = 4.4\text{m}$, $T_p = 7.8\text{s}$, $\text{dir} = 300^\circ\text{N}$, ~ 0.4 days/yr)

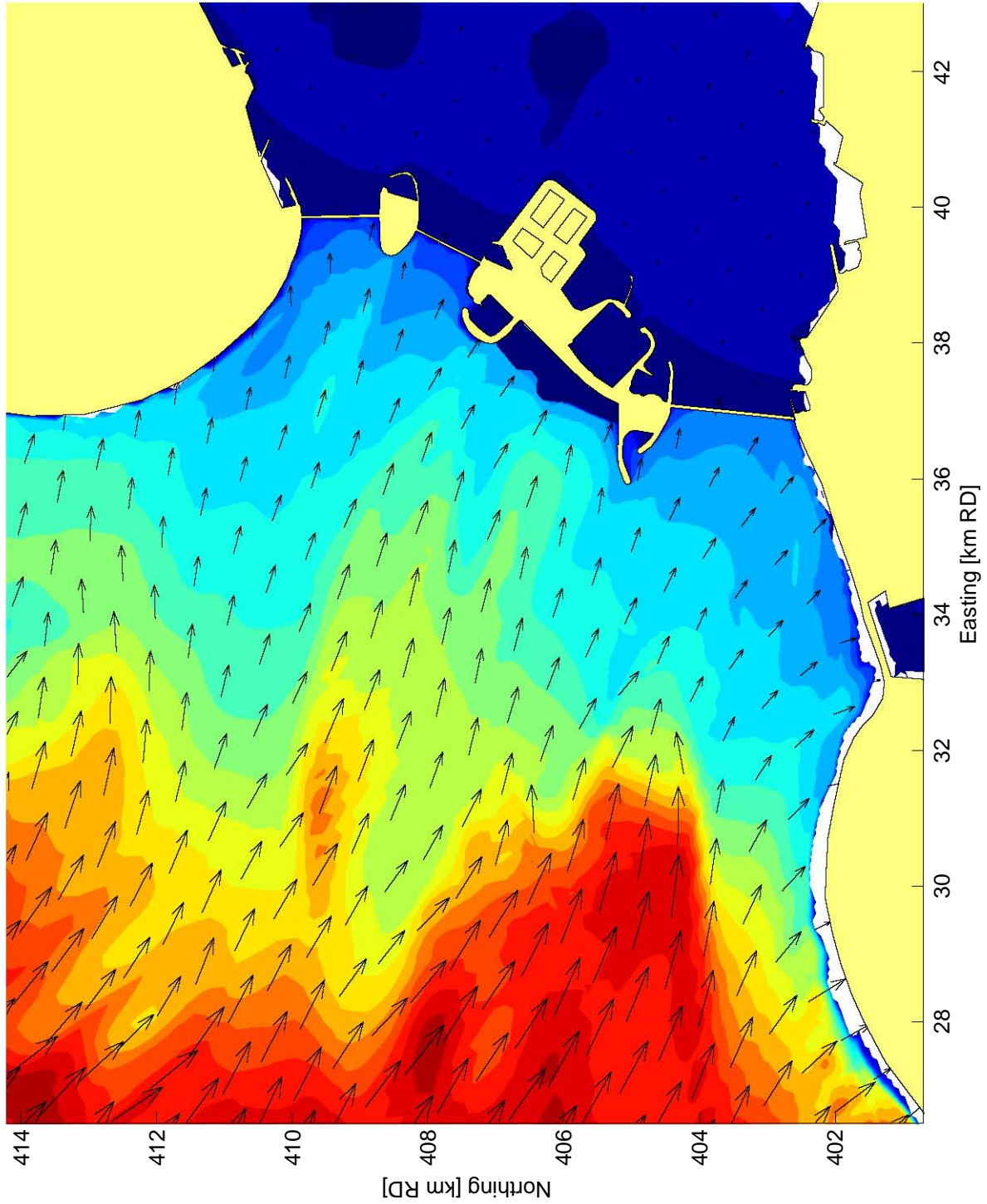
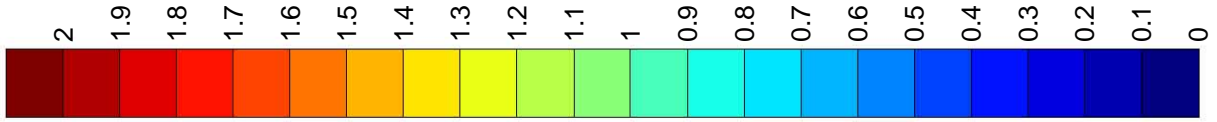
Zandhonger Oosterschelde

Deltares

z4581

Fig. 3.5a

Significant wave height (m)



Normal wave condition 69 for the Eastern Scheldt delta (bathymetry 1999)
 (offshore : $H_s = 4.4\text{m}$, $T_p = 7.8\text{s}$, $\text{dir} = 300^\circ\text{N}$, ~ 0.4 days/yr)

Zandhonger Oosterschelde

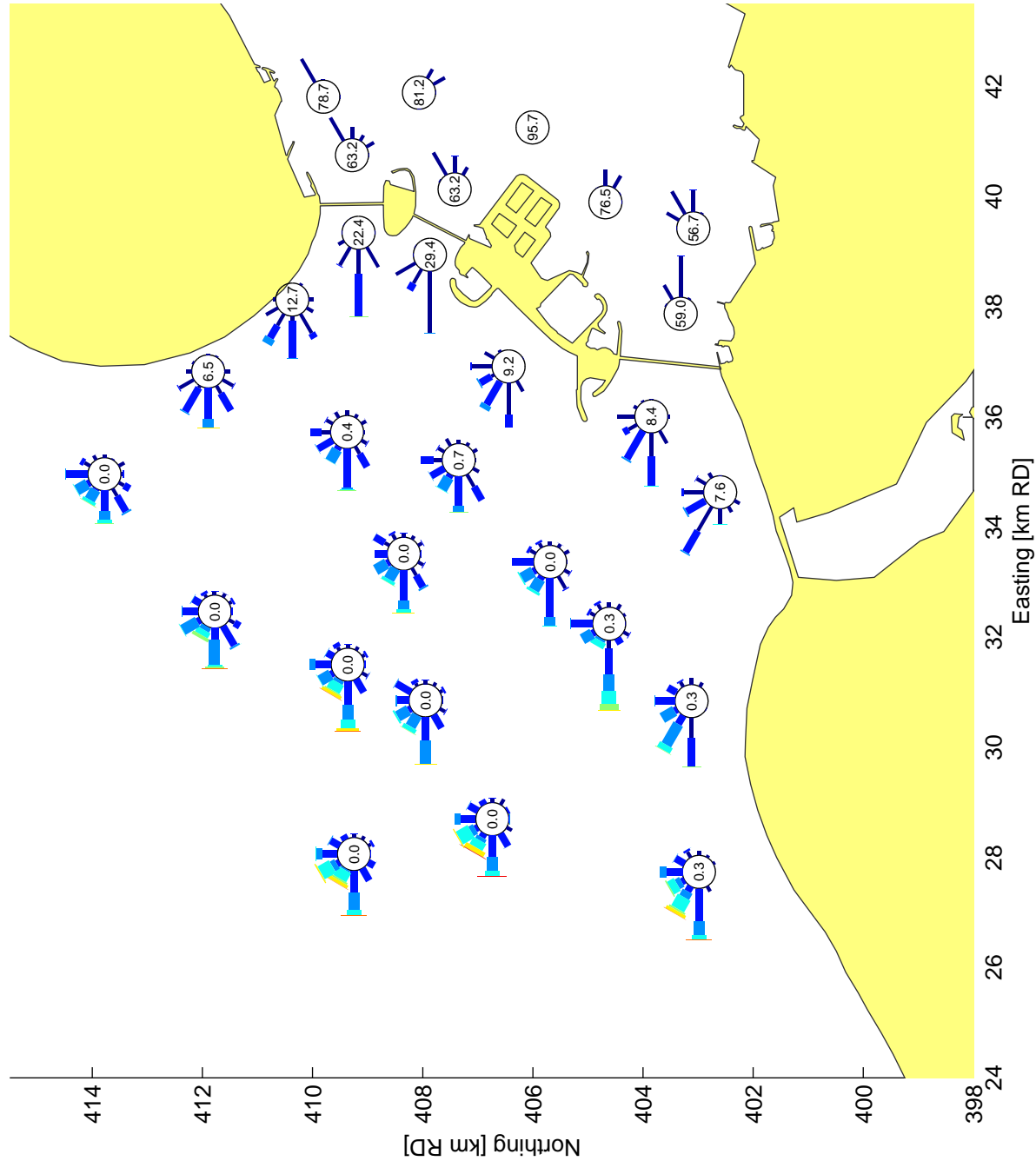
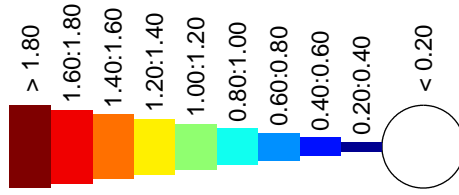
Deltares

z4581

Fig. 3.5b

EXPLANATION

Item:	Represents:
Type of bar	Hs (m)
Direction of bar (to centre of rose)	Direction
Length of bar	Occurrence (%)
Number in centre of rose	Occurrence (%) in lowest class
Undetermined data	4.31 %

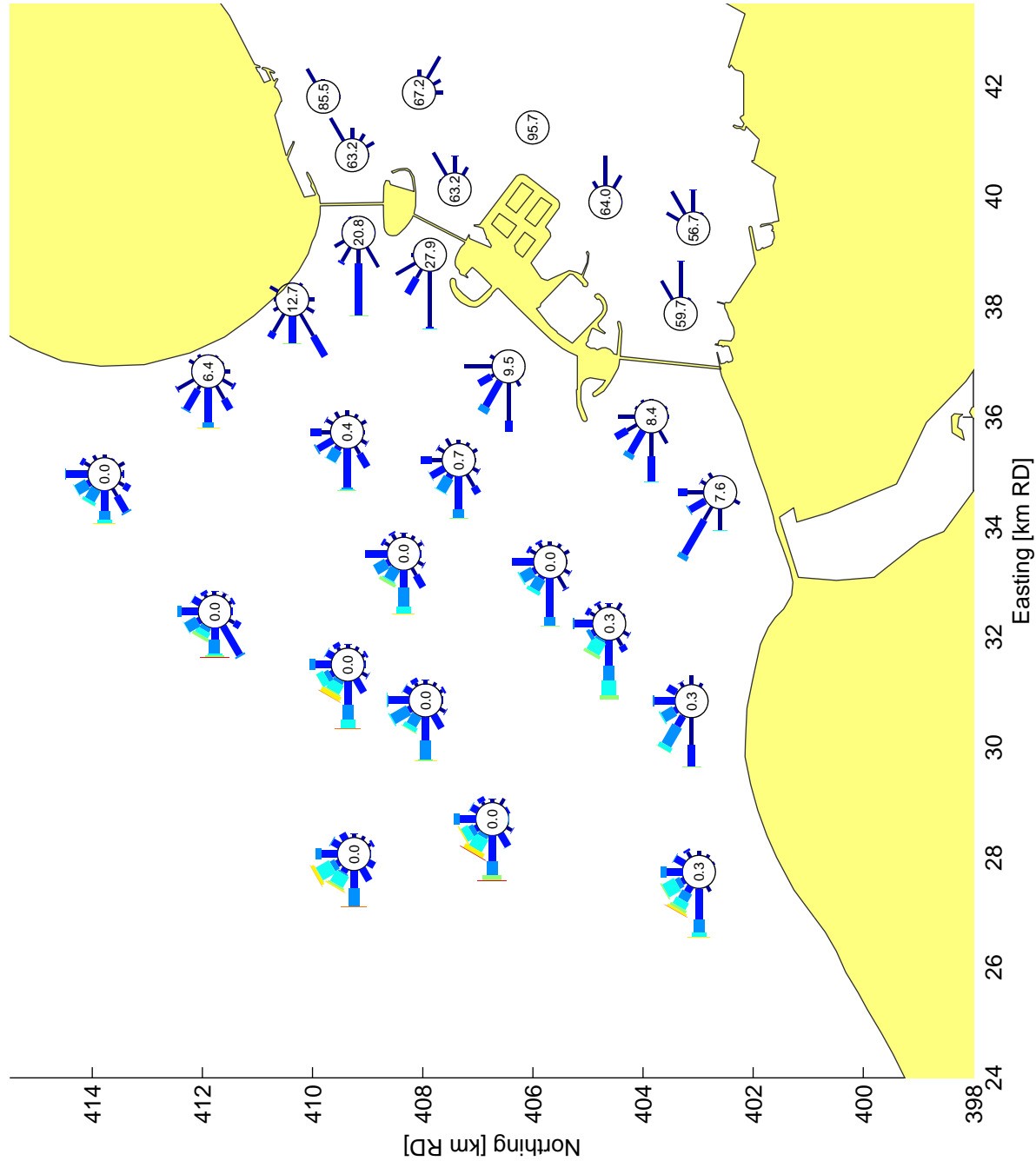
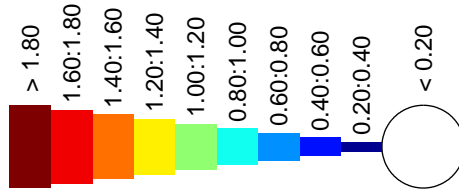


Wave height roses for the Eastern Scheldt delta (bathymetry 2004)
(used for analysis of potential sediment transport capacity in Eastern Scheldt)

Zandhonger Oosterschelde

EXPLANATION

Item:	Represents:
Type of bar	Hs (m)
Direction of bar (to centre of rose)	Direction
Length of bar	Occurrence (%)
Number in centre of rose	Occurrence (%) in lowest class
Undetermined data	4.31 %

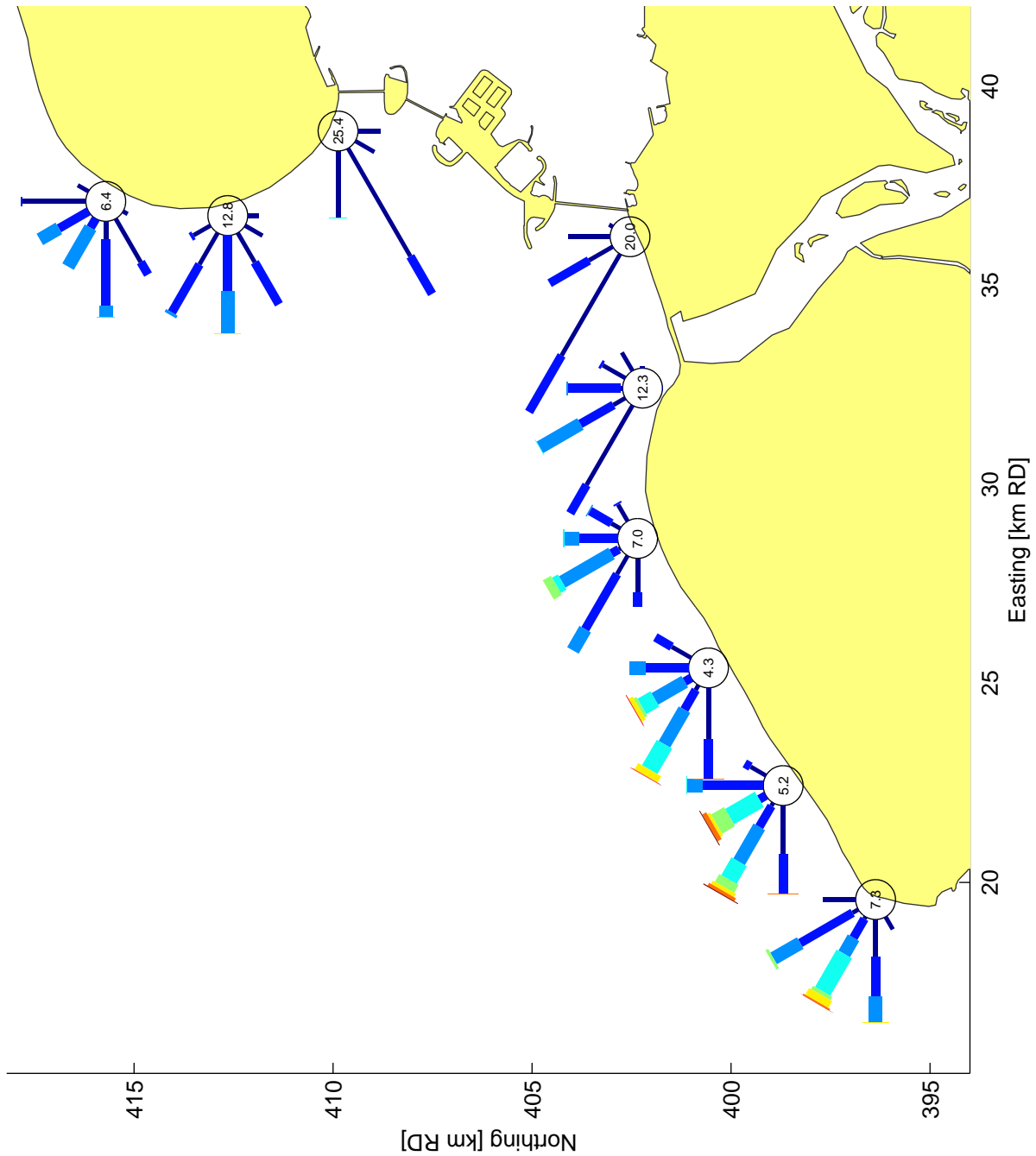
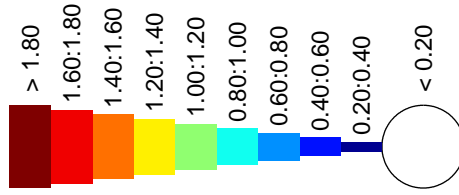


Wave height roses for the Eastern Scheldt delta (bathymetry 1999)
 (used for analysis of potential sediment transport capacity in Eastern Scheldt)

Zandhonger Oosterschelde

EXPLANATION

Item:	Represents:
Type of bar	Hs (m)
Direction of bar (to centre of rose)	Direction
Length of bar	Occurrence (%)
Number in centre of rose	Occurrence (%) in lowest class
Undetermined data	4.31 %

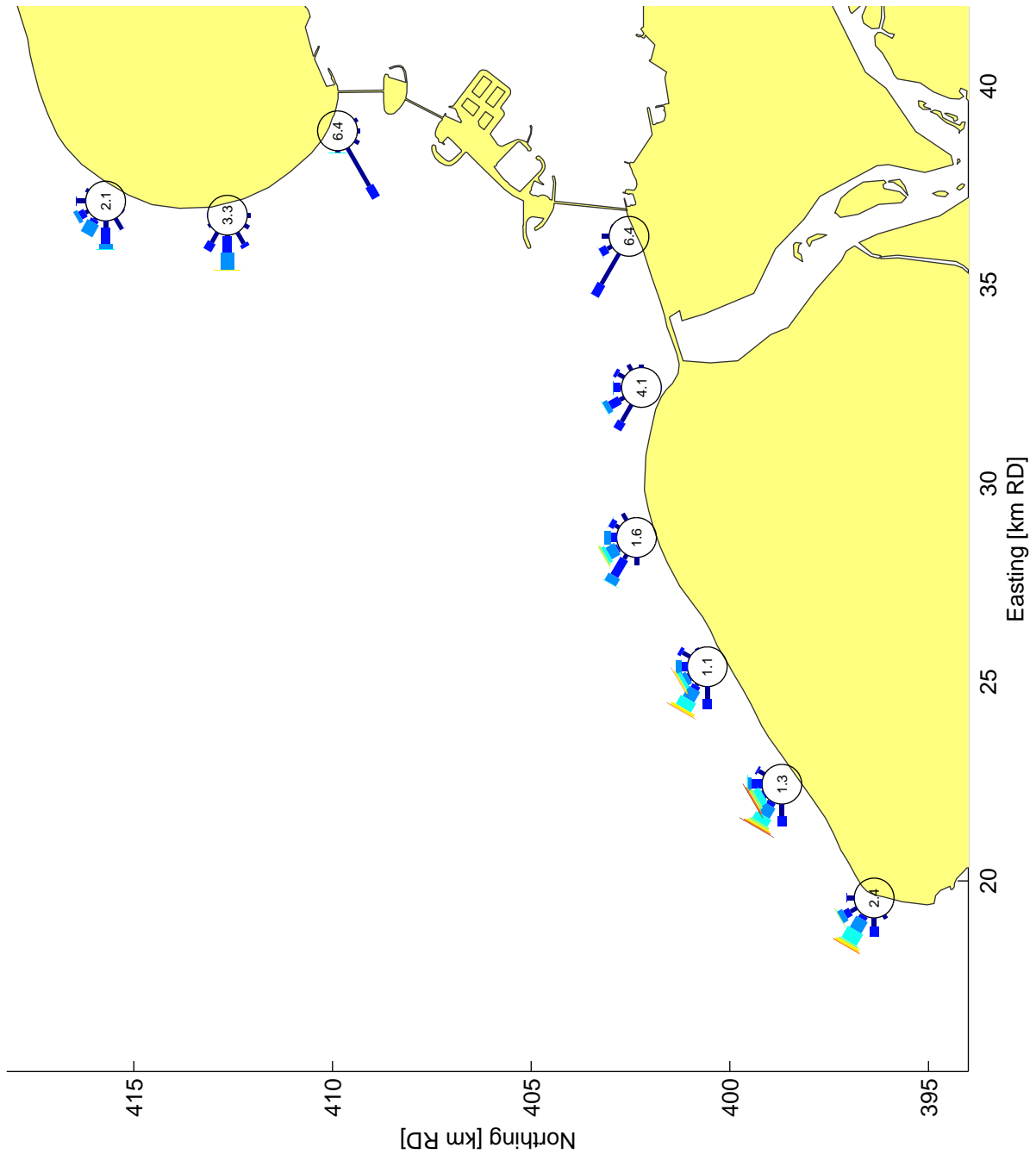
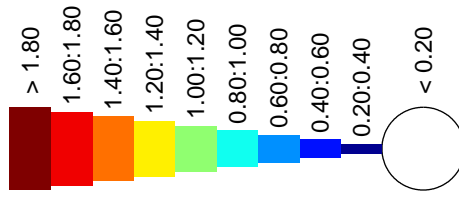


Wave height roses for the Walcheren coast for a full year
(bathymetry 2004) (located at 8m depth contour)

Zandhonger Oosterschelde

EXPLANATION

Item:	Represents:
Type of bar	Hs (m)
Direction of bar (to centre of rose)	Direction
Length of bar	Occurrence (%)
Number in centre of rose	Occurrence (%) in lowest class
Undetermined data	75.91 %

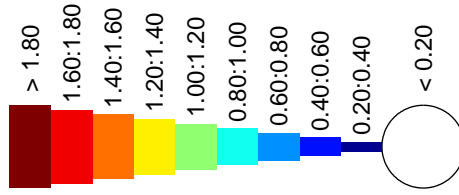


Wave height roses for the Walcheren coast for the winter season (bathymetry 2004) (located at 8m depth contour)

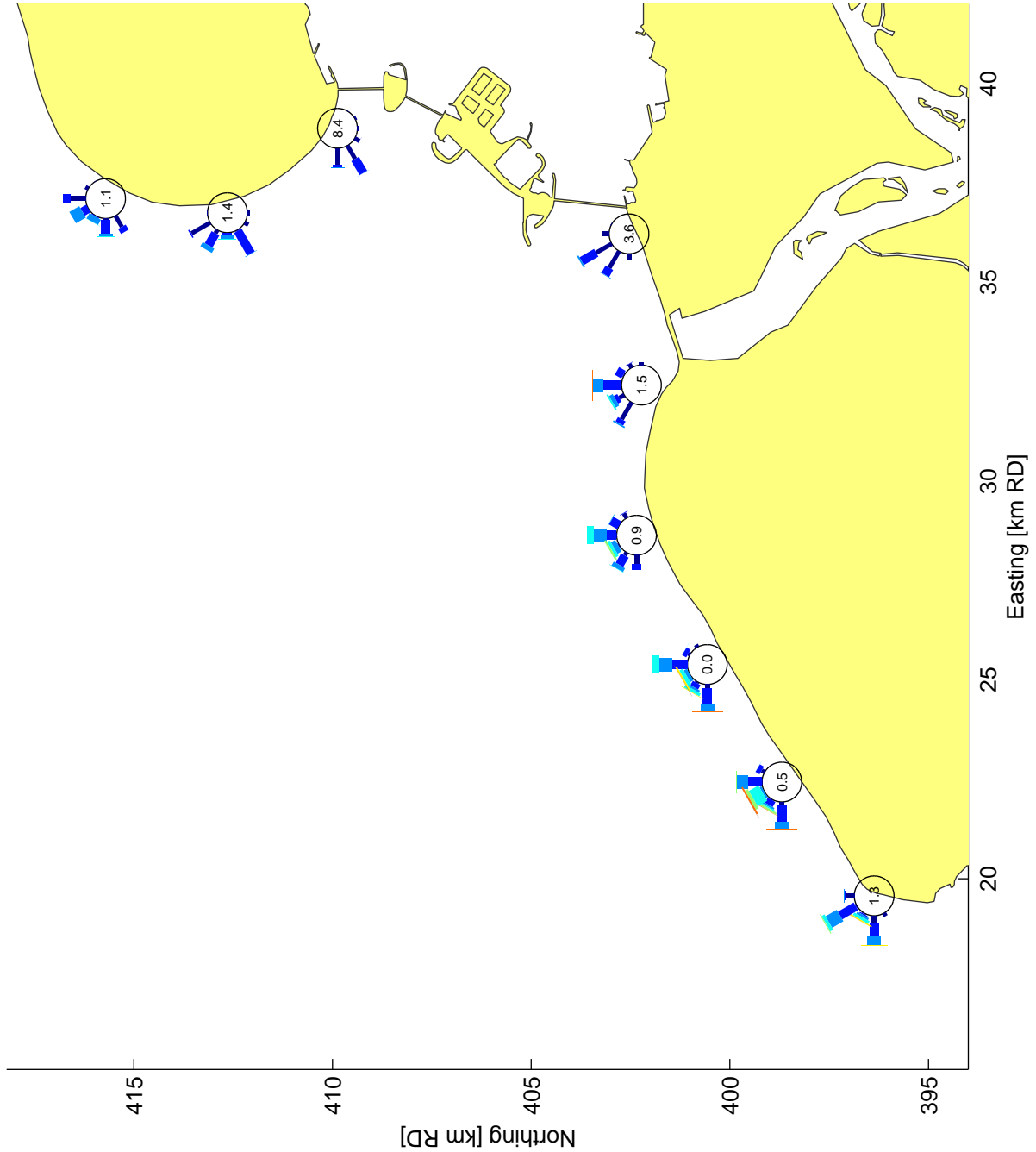
Zandhonger Oosterschelde

EXPLANATION

Item:	Represents:
Type of bar	Hs (m)
Direction of bar (to centre of rose)	Direction
Length of bar	Occurrence (%)
Number in centre of rose	Occurrence (%) in lowest class
Undetermined data	76.55 %



Hs (m)

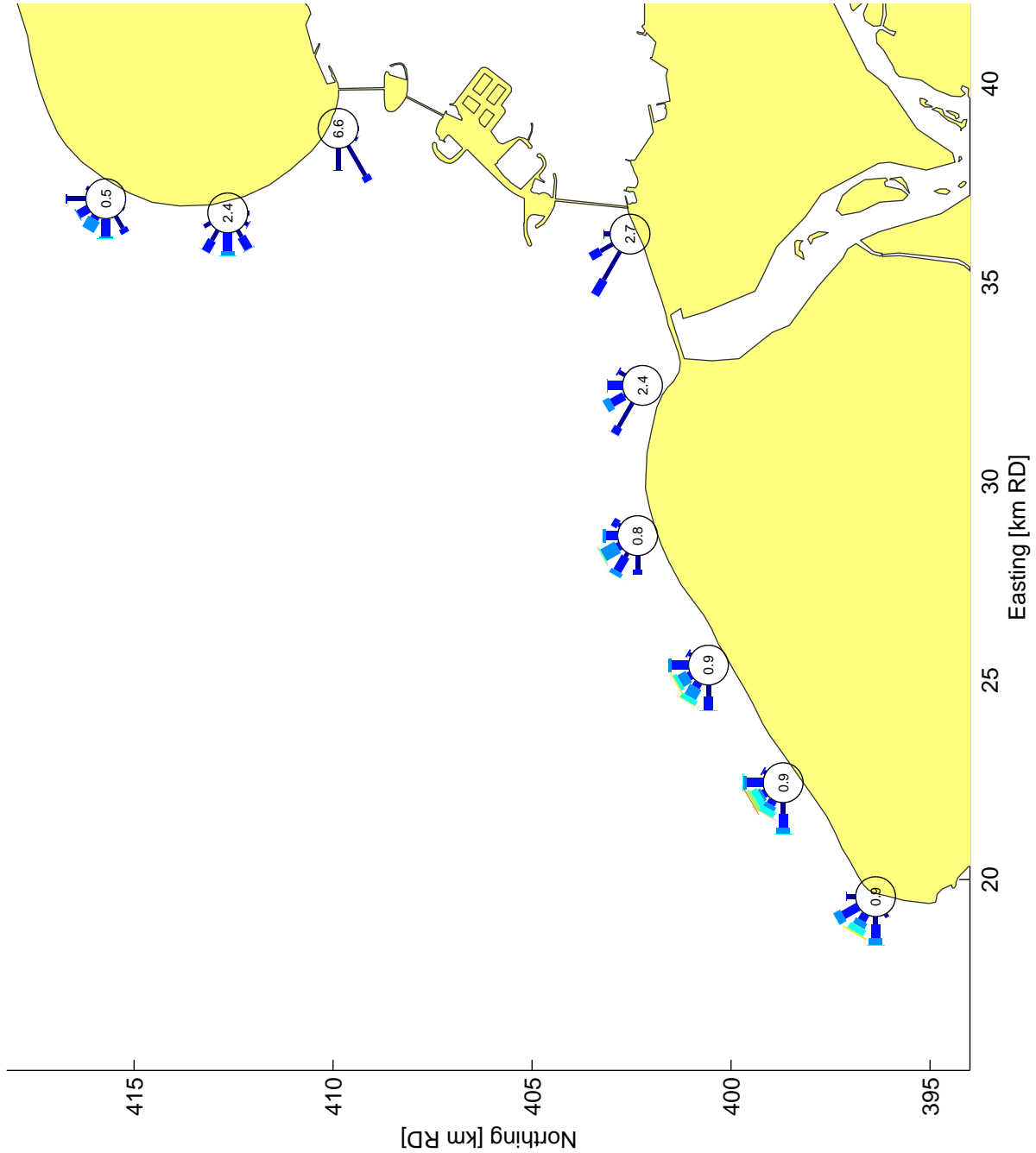
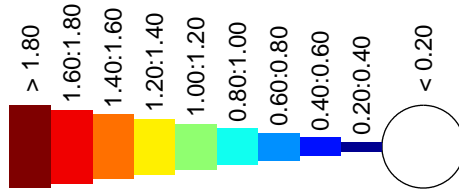


Wave height roses for the Walcheren coast for the spring season
(bathymetry 2004) (located at 8m depth contour)

Zandhonger Oosterschelde

EXPLANATION

Item:	Represents:
Type of bar	Hs (m)
Direction of bar (to centre of rose)	Direction
Length of bar	Occurrence (%)
Number in centre of rose	Occurrence (%) in lowest class
Undetermined data	76.48%

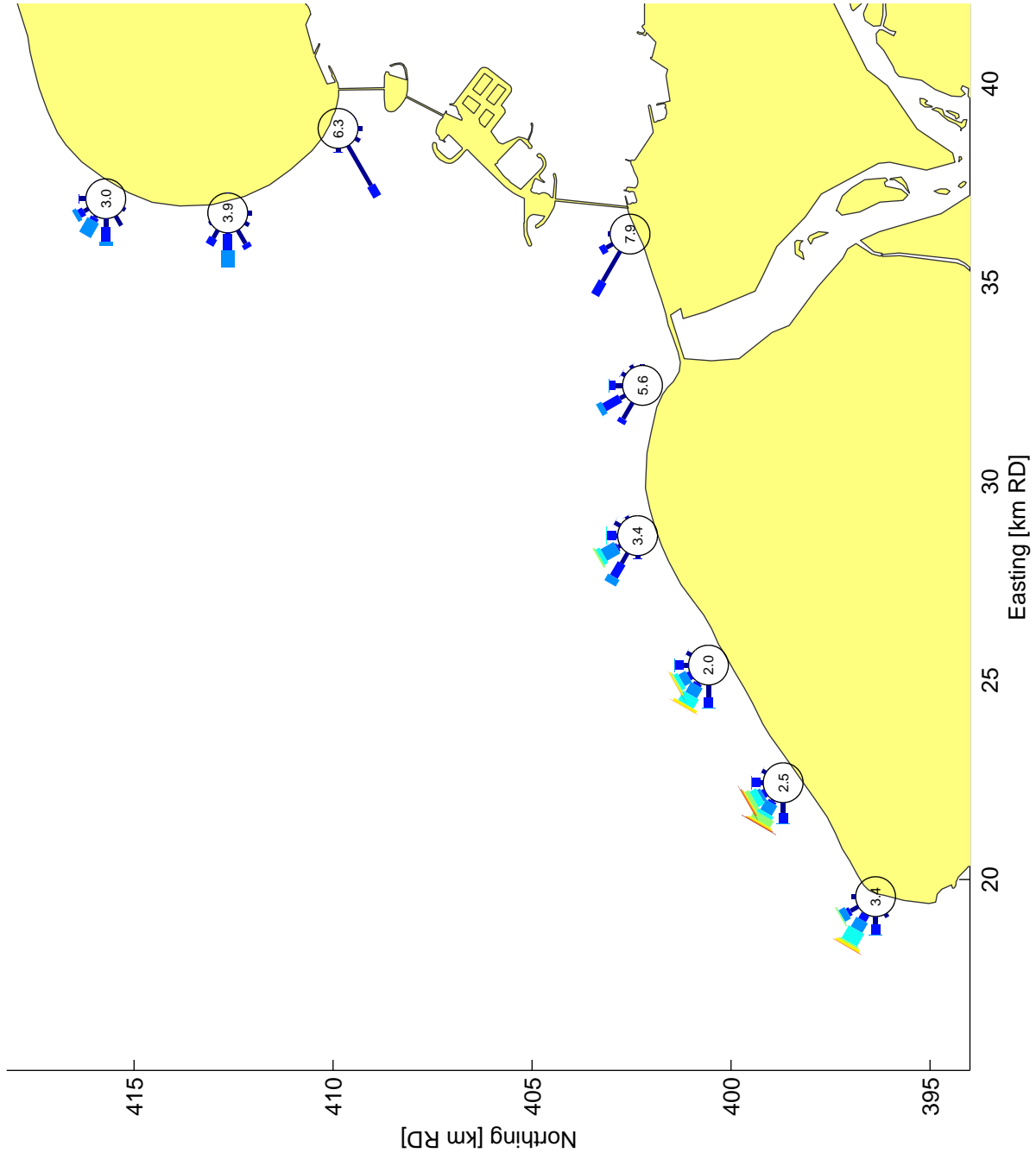
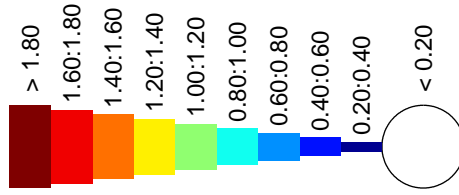


Wave height roses for the Walcheren coast for the summer season (bathymetry 2004) (located at 8m depth contour)

Zandhonger Oosterschelde

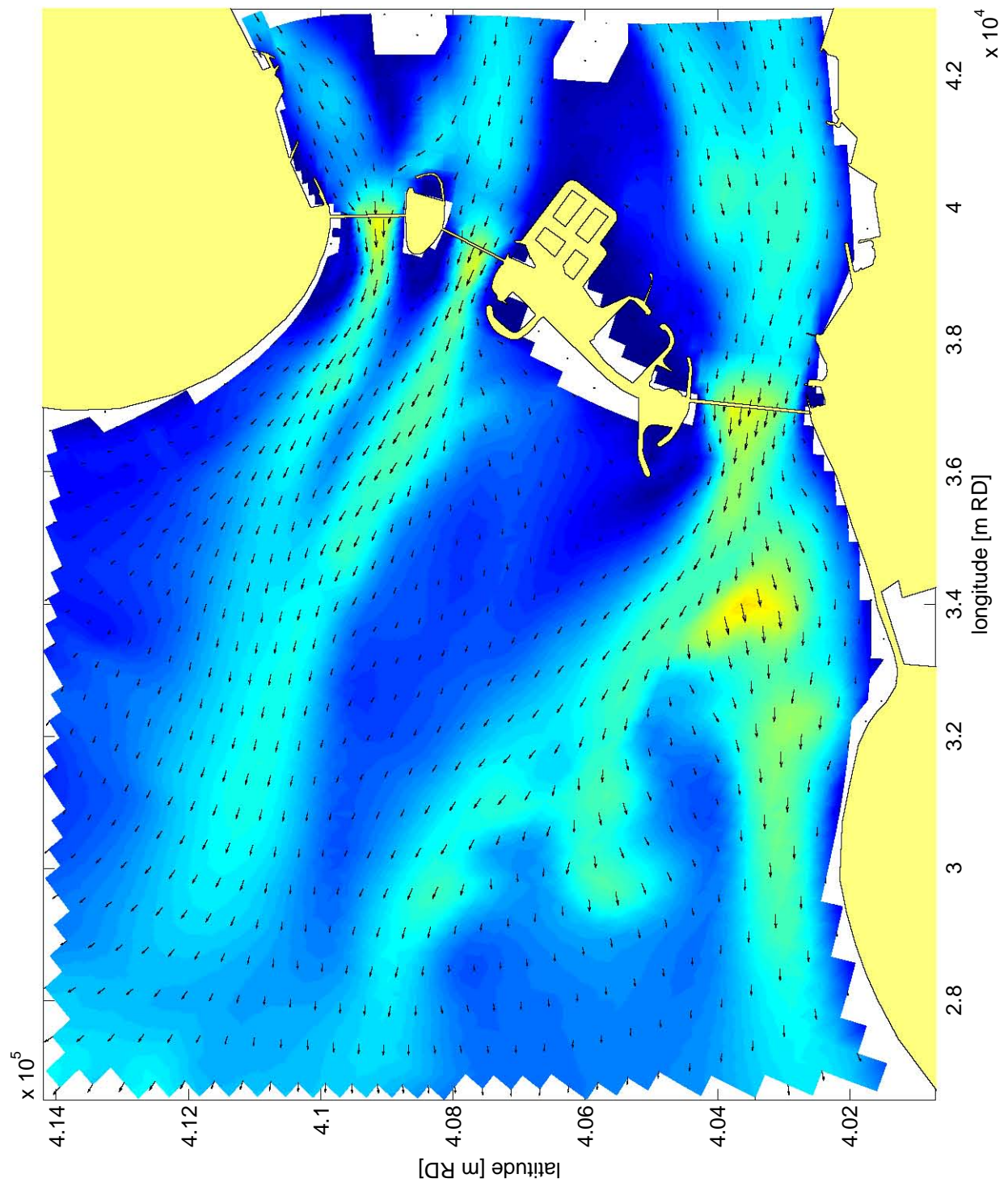
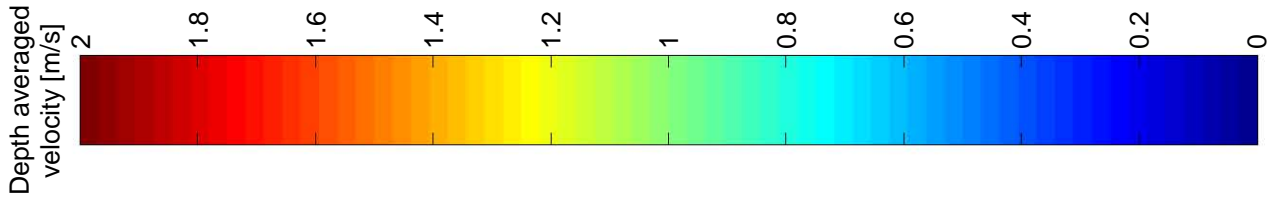
EXPLANATION

Item:	Represents:
Type of bar	Hs (m)
Direction of bar (to centre of rose)	Direction
Length of bar	Occurrence (%)
Number in centre of rose	Occurrence (%) in lowest class
Undetermined data	75.37 %



Wave height roses for the Walcheren coast for the autumn season (bathymetry 2004) (located at 8m depth contour)

Zandhonger Oosterschelde



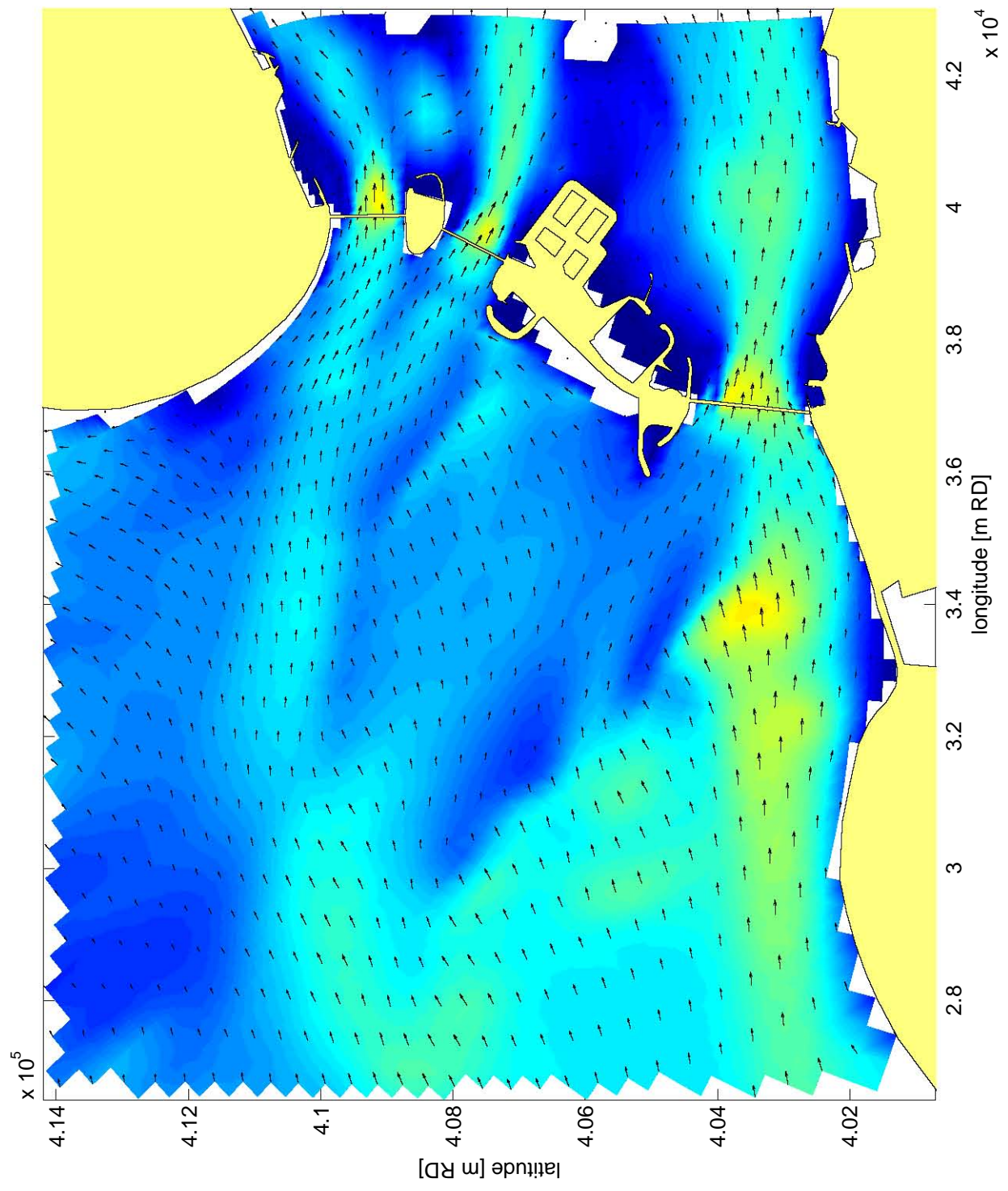
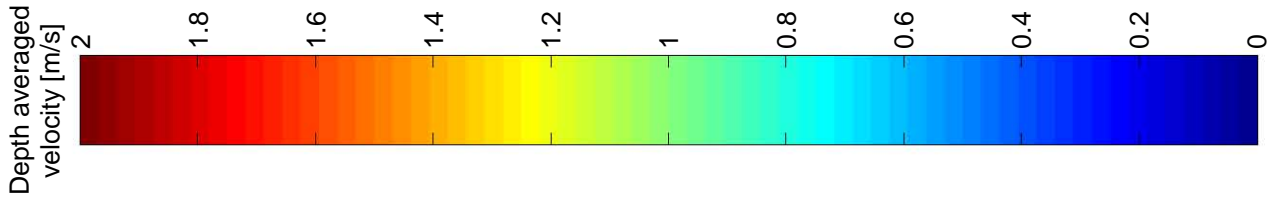
Flow velocities in MATROOS during ebb
(2008-07-01 03:00)

Zandhonger Oosterschelde

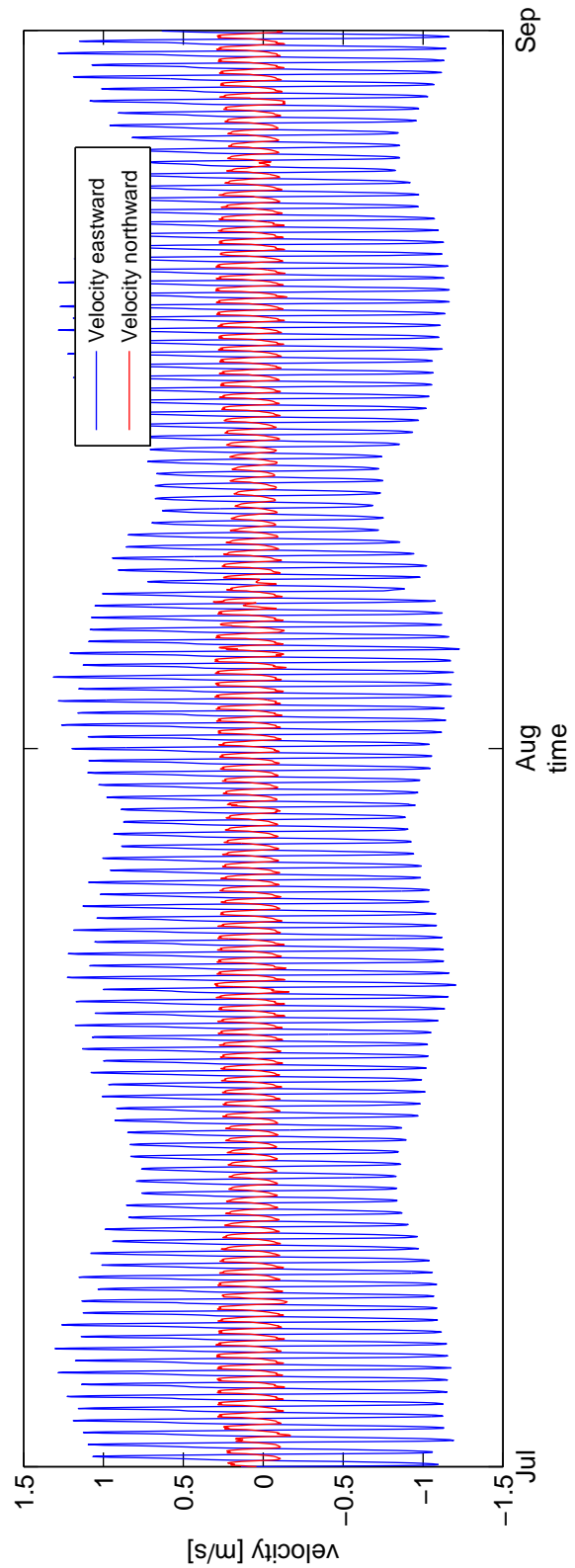
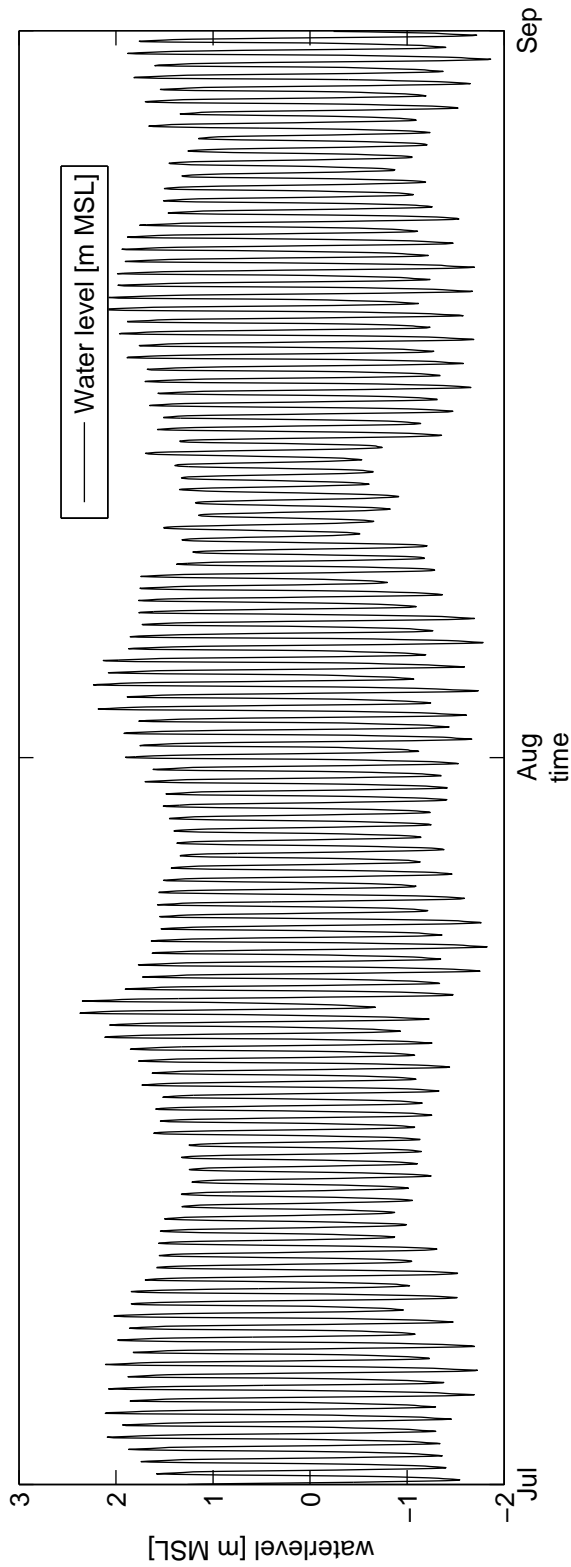
Deltares

z4581

Fig.3.8a



Flow velocities in MATROOS during flood (2008-06-30 22:00)		
	Zandhonger Oosterschelde	
Deltares	z4581	Fig.3.8b



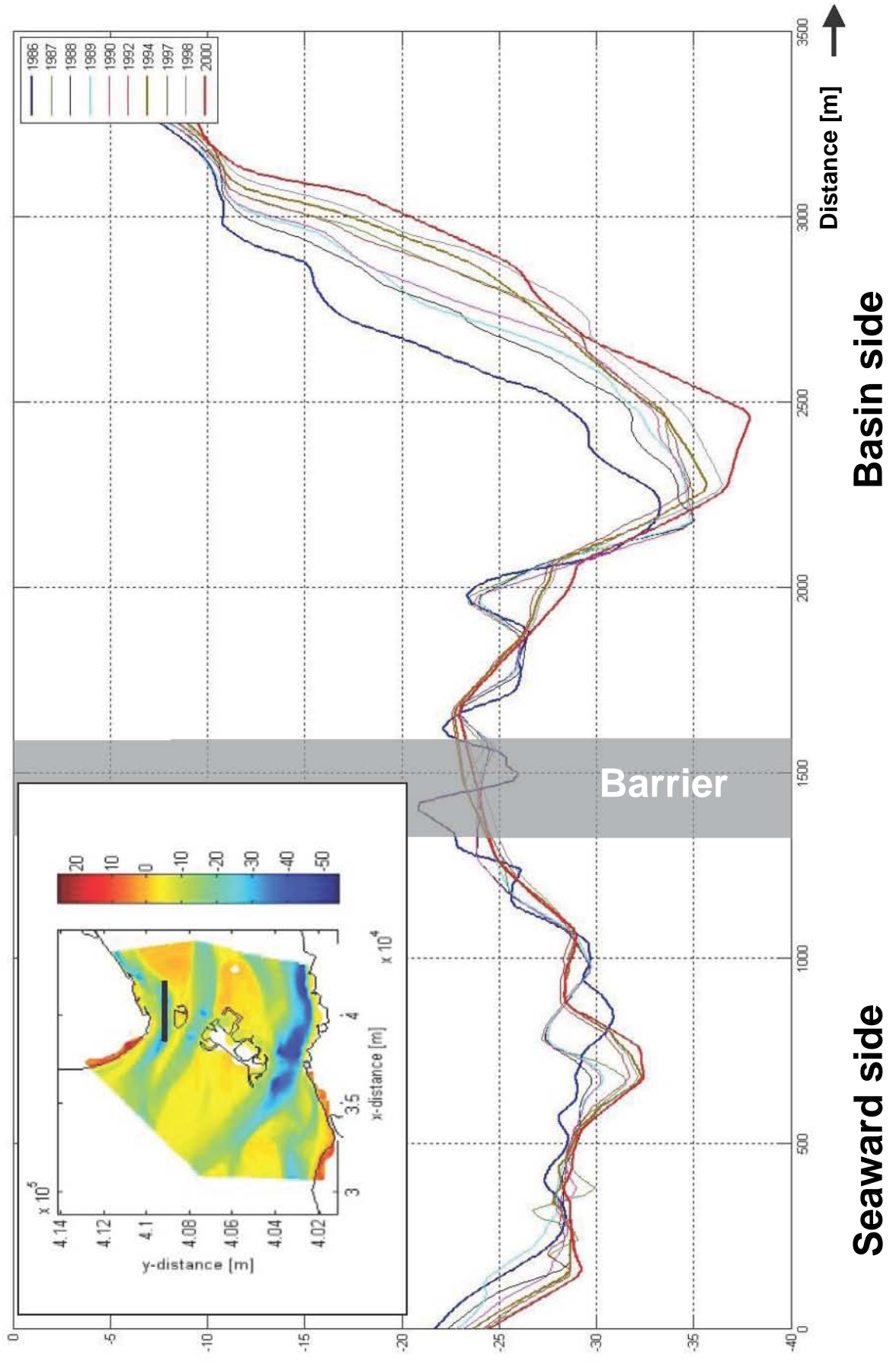
Example of timeseries from MATROOS with water levels and flow velocities
(location 1: Roompot, close to storm surge barrier; 2008-07-01 to 2008-09-01)

Zandhonger Oosterschelde

Deltares

z4581

Fig.3.9



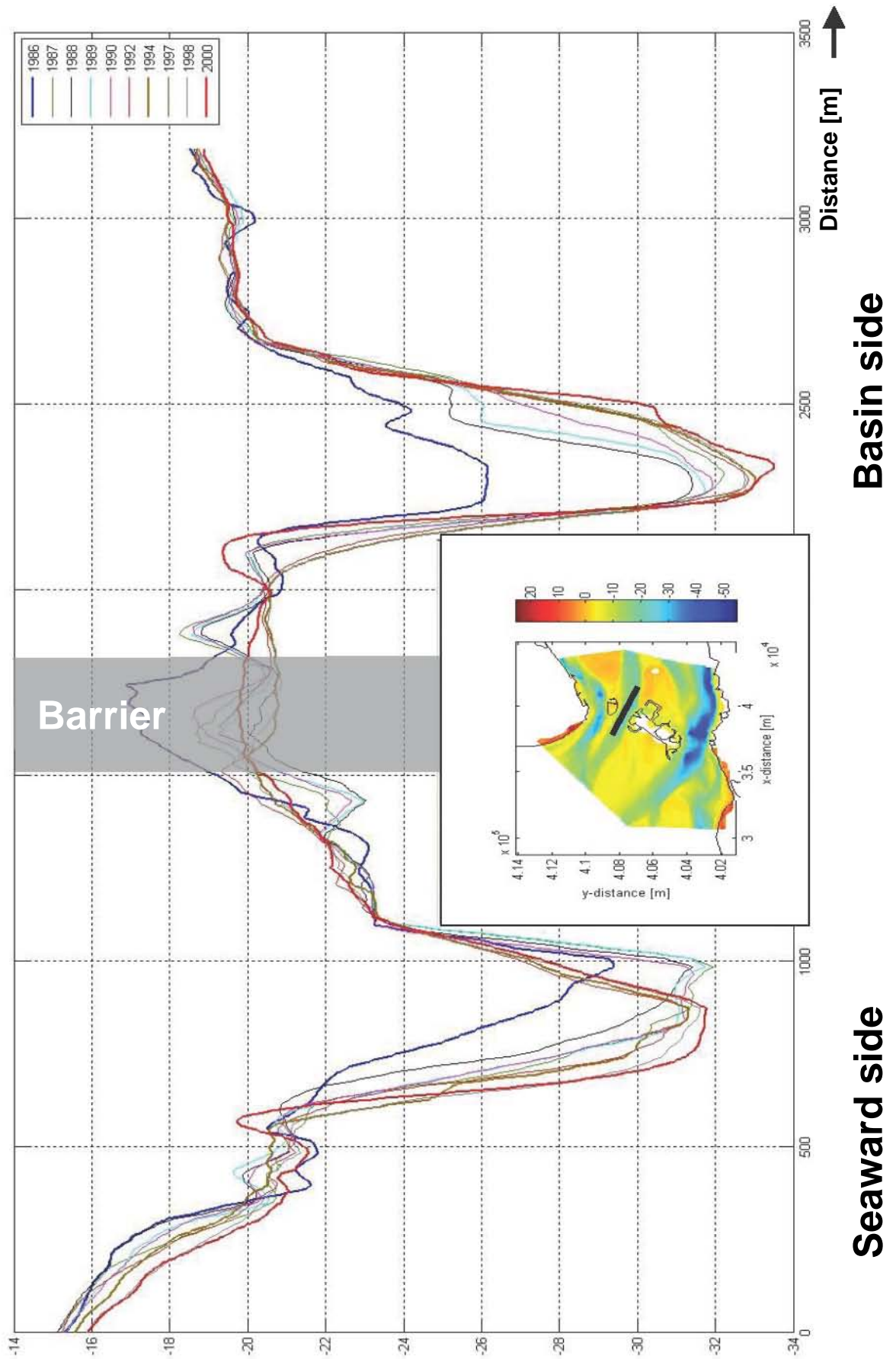
Cross-sections of the scour hole at the Hammen (Eastern Scheldt barrier in centre of figure)

Zandhonger Oosterschelde

Deltares

Z4581

Fig. 3.10



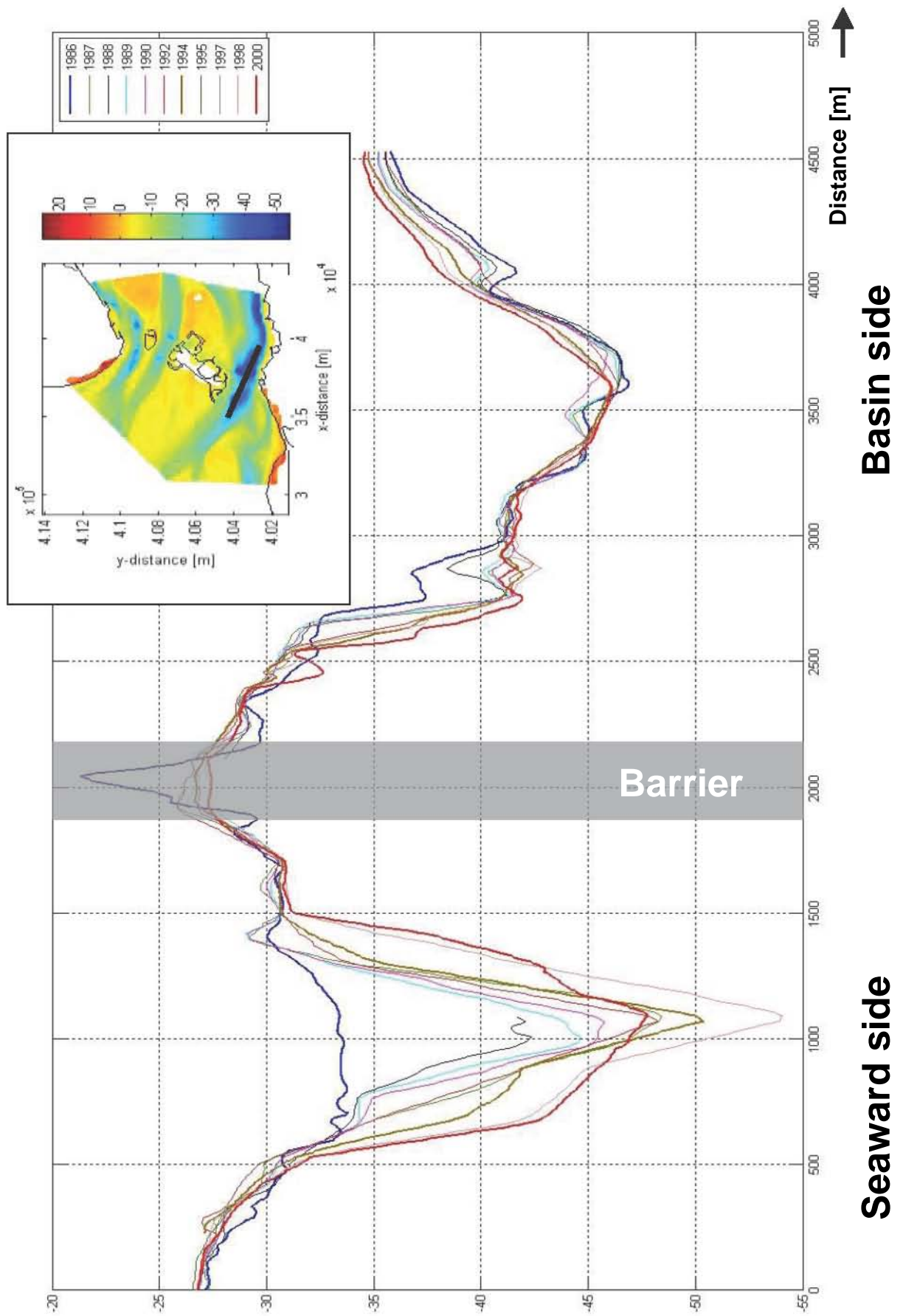
Cross-sections of the scour hole at the Schaar (Eastern Scheldt barrier in centre of figure)

Zandhonger Oosterschelde

Deltares

Z4581

Fig. 3.11



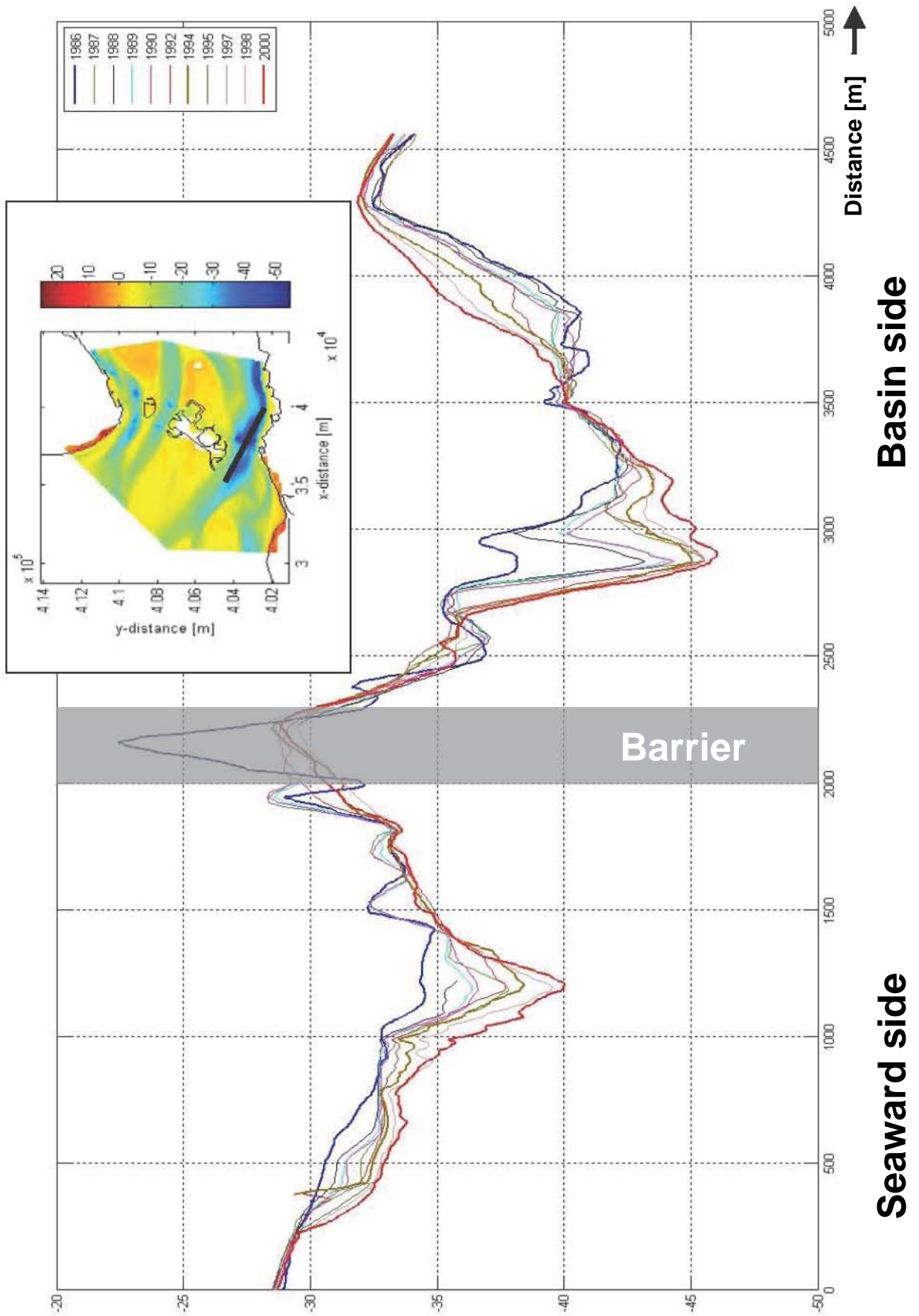
Cross-sections of the scour hole at the Roompot 1 (Eastern Scheldt barrier in centre of figure) for a ray through the centre of the Roompot scour hole

Zandhonger Oosterschelde

Deltares

Z4581

Fig. 3.12a



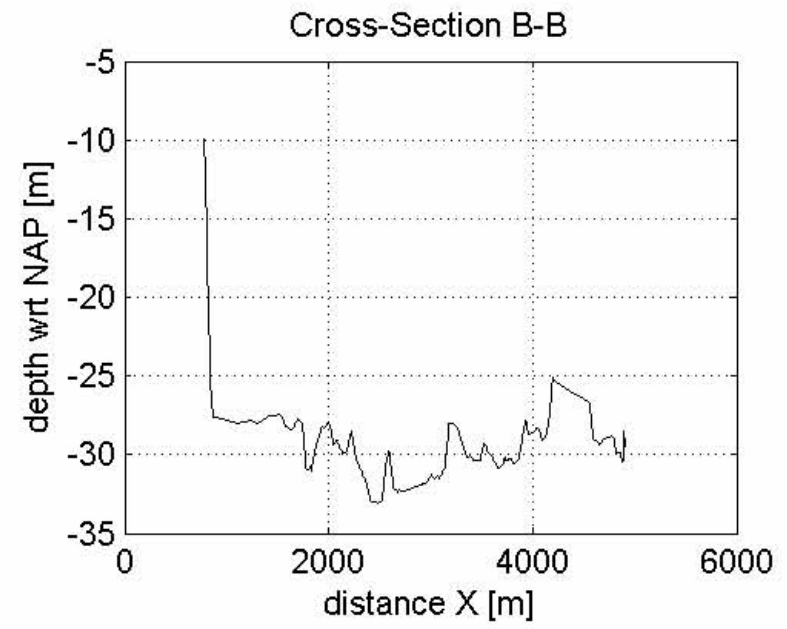
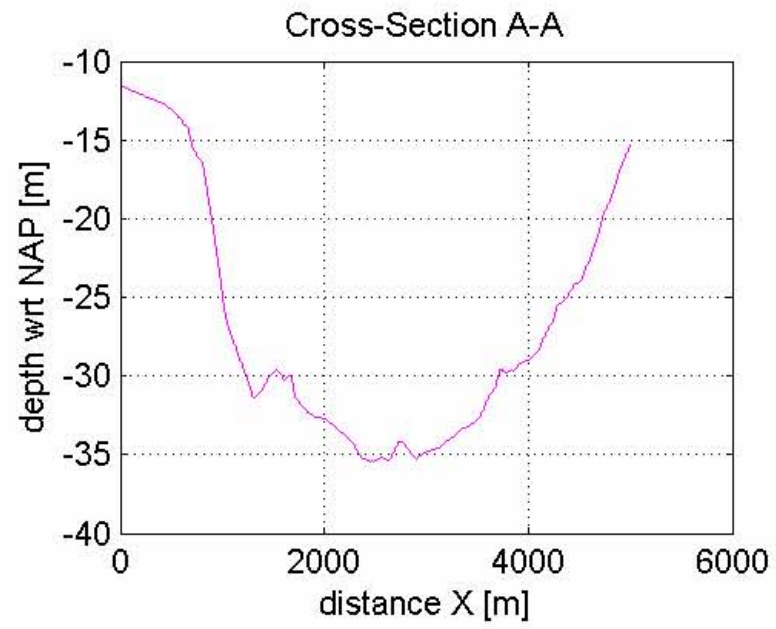
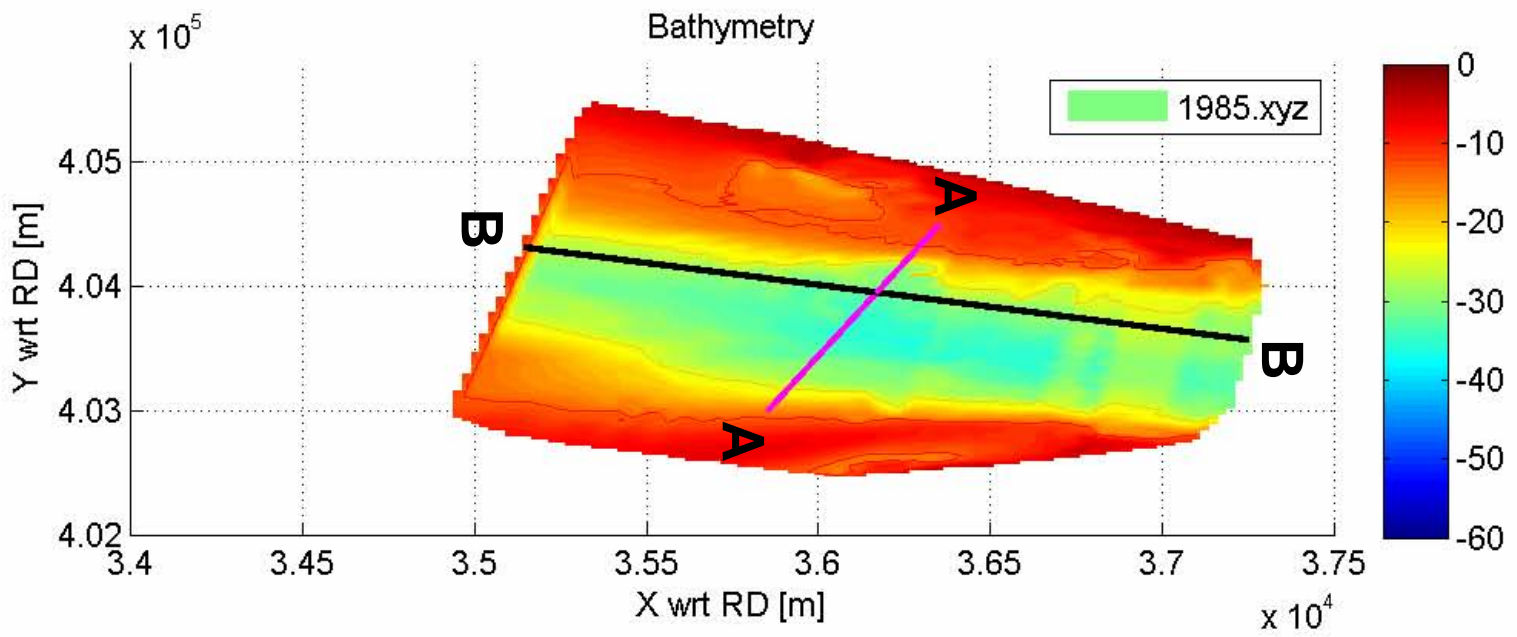
Cross-sections of the scour hole at the Roompot 2 (Eastern Scheldt barrier in centre of figure) for a ray that is slightly off the centre of the Roompot scour hole

Zandhonger Oosterschelde

Deltares

Z4581

Fig. 3.12b



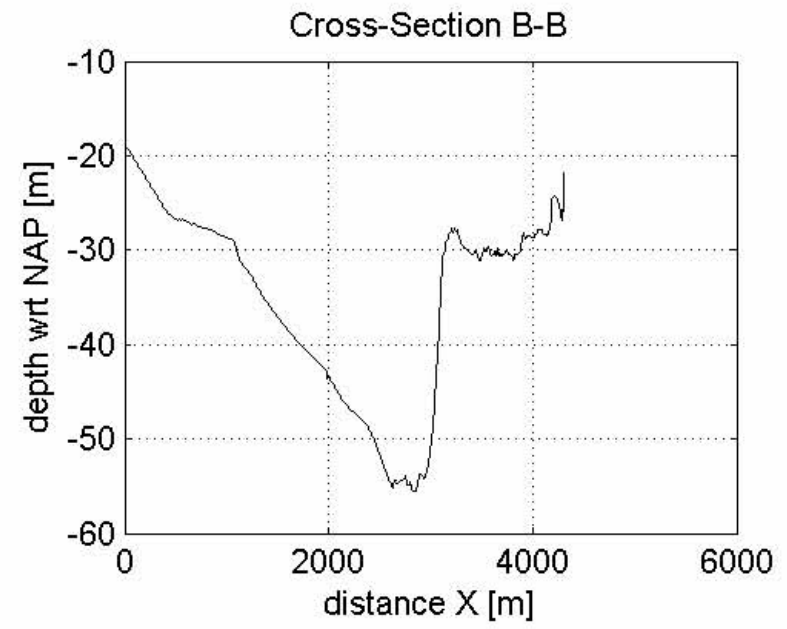
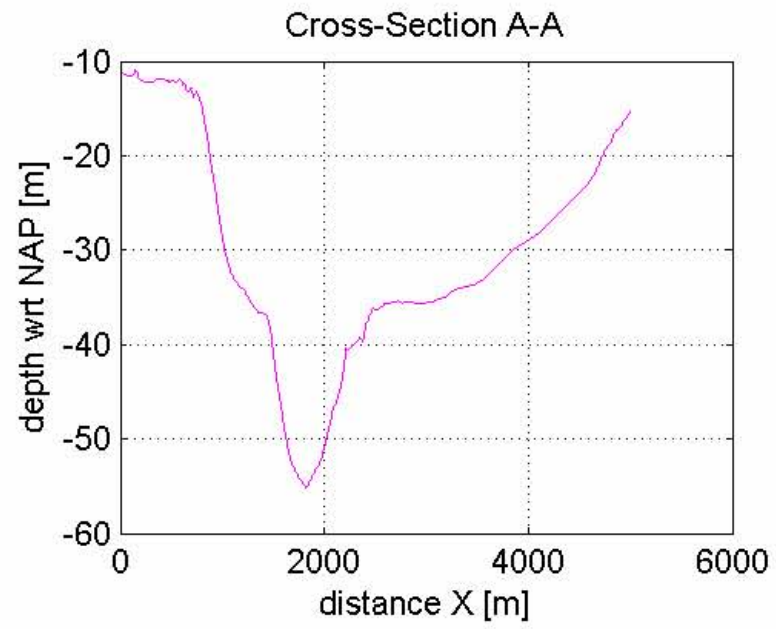
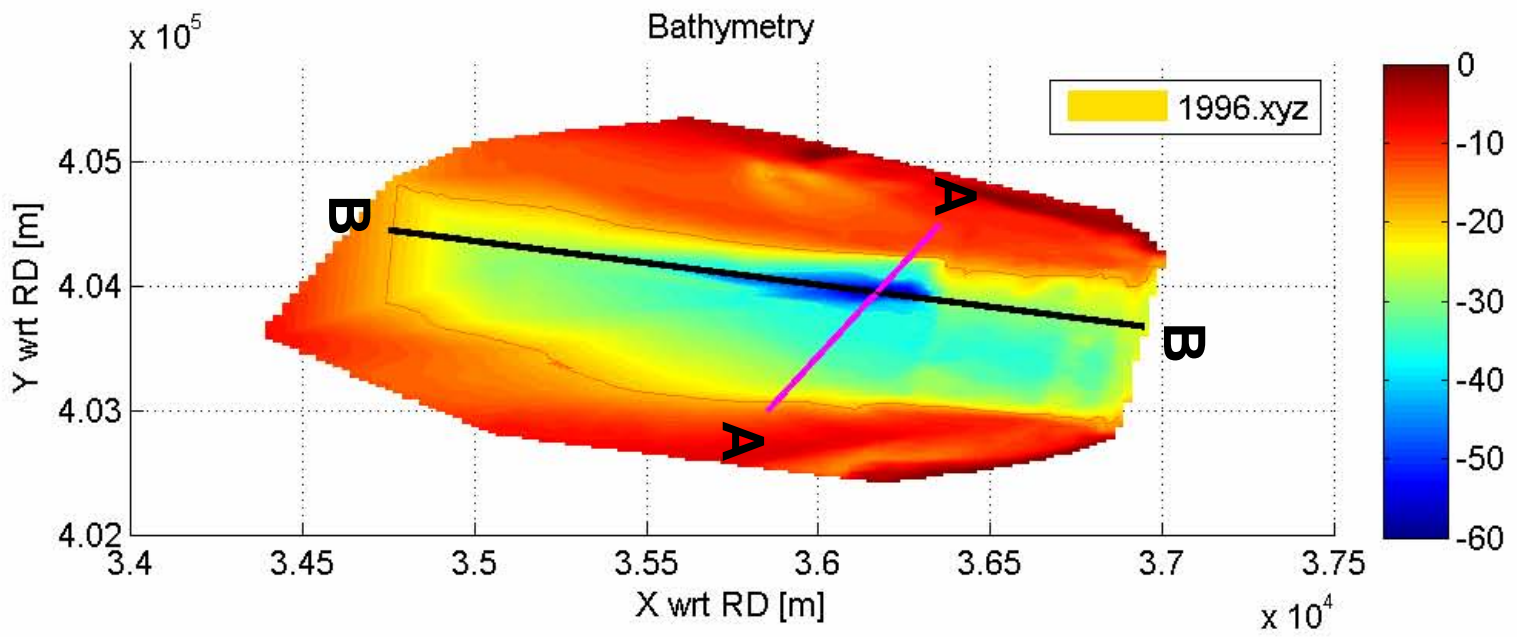
Bathymetry of the scour hole at the Roompot in 1985 (seaward of the Eastern Scheidt barrier)

Deltares

Z4581

Zandhonger Oosterschelde

Fig. 3.13a



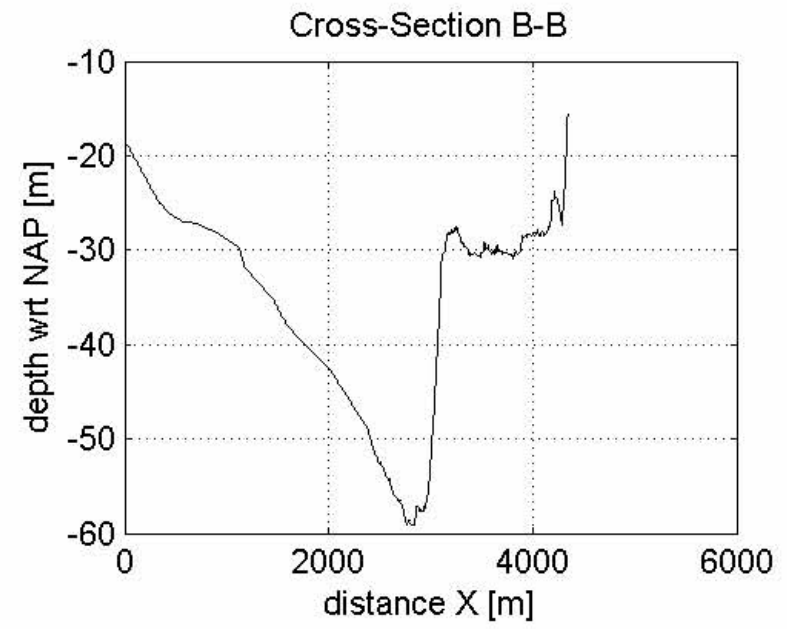
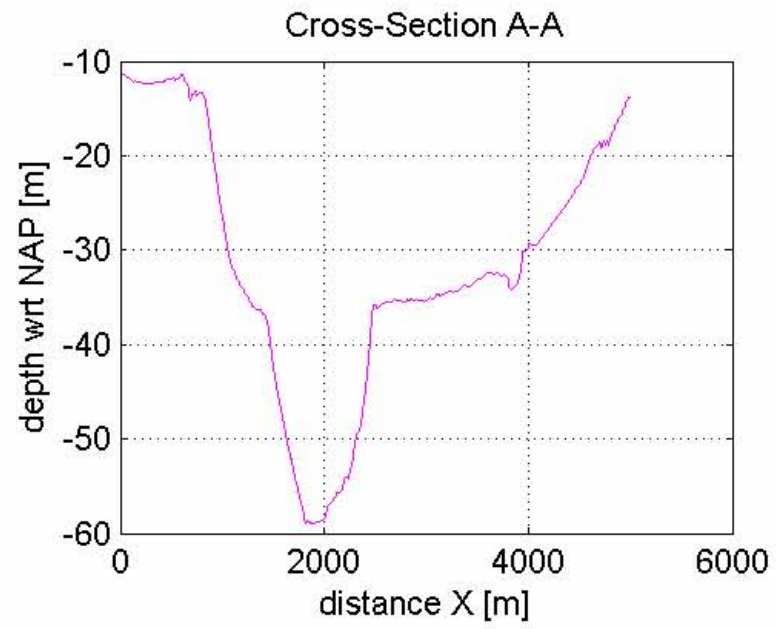
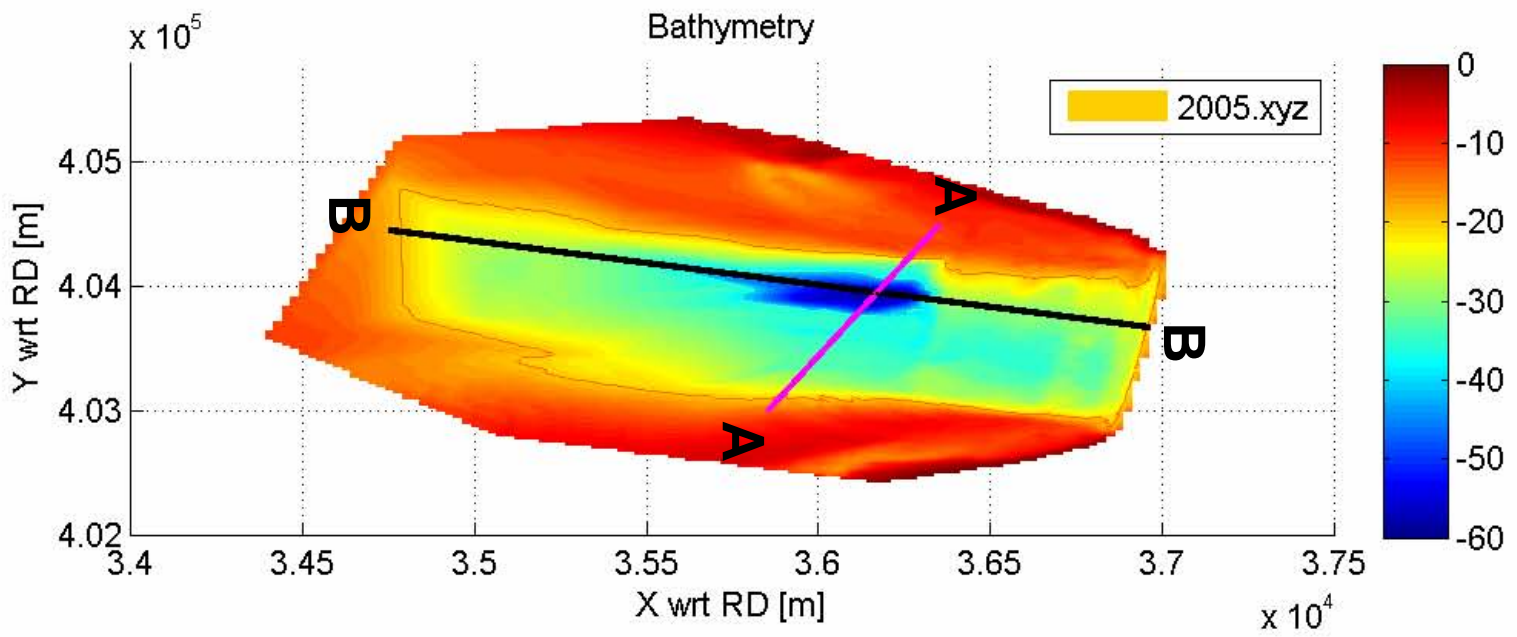
Bathymetry of the scour hole at the Roompot in 1996 (seaward of the Eastern Scheidt barrier)

Deltares

Z4581

Zandhonger Oosterschelde

Fig. 3.13b



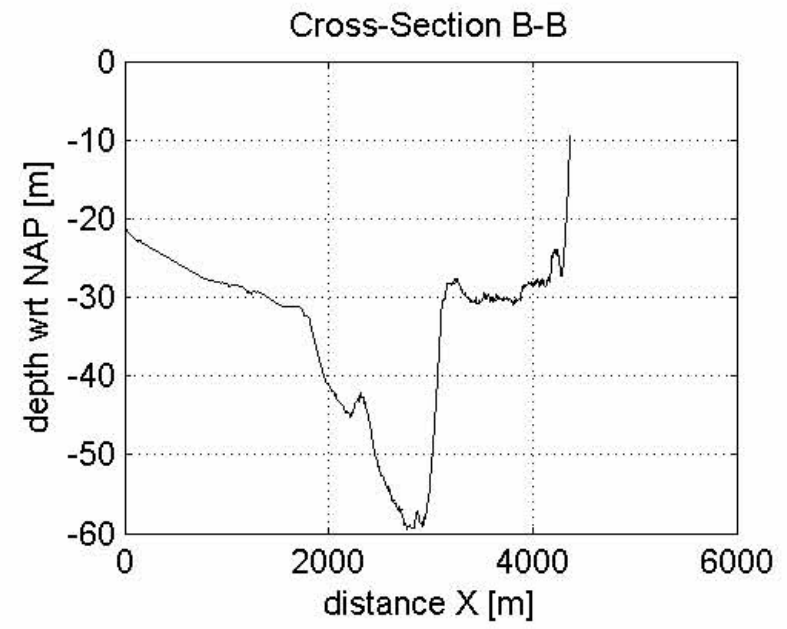
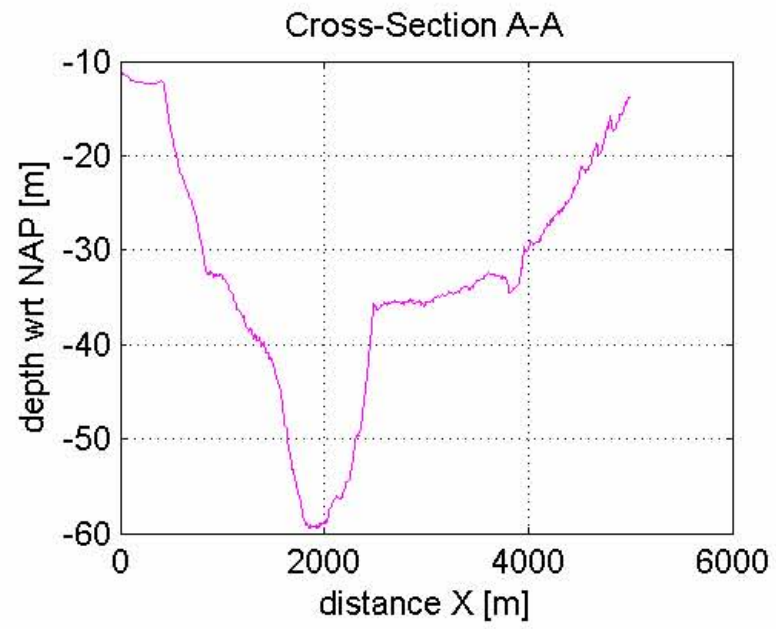
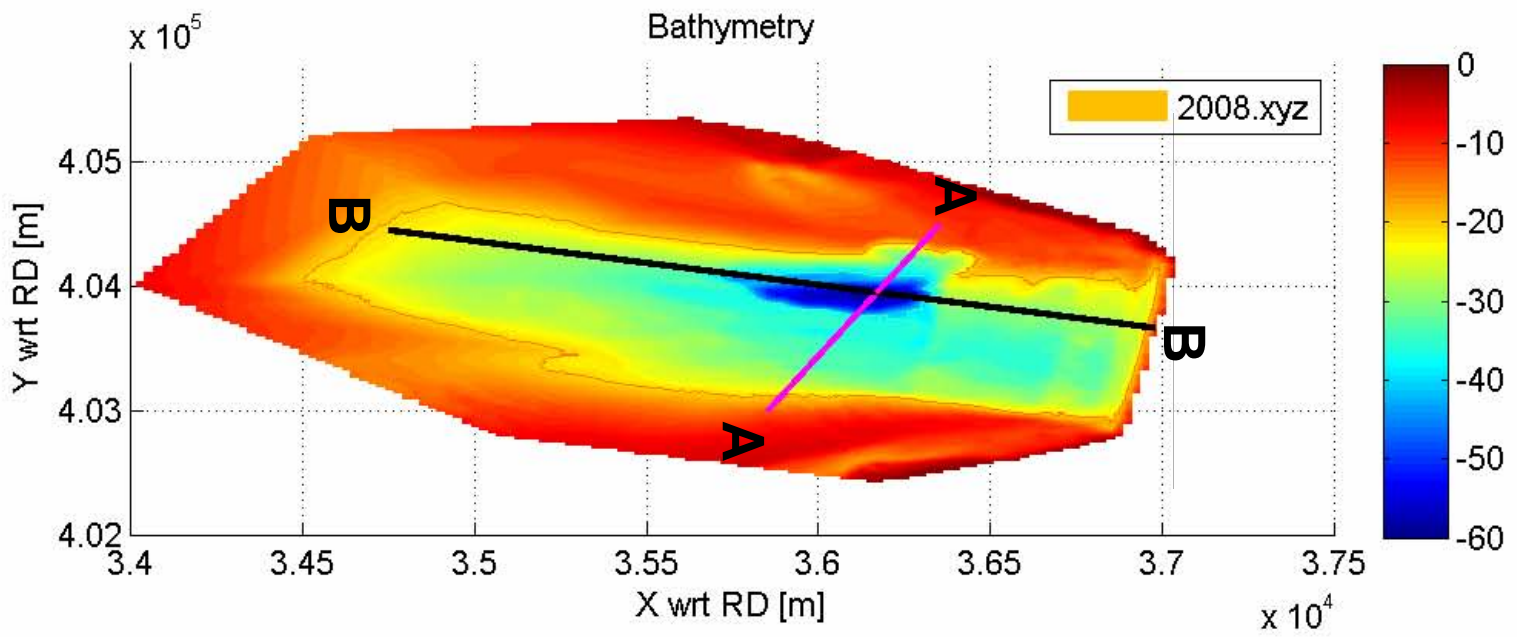
Bathymetry of the scour hole at the Roompot in 2005 (seaward of the Eastern Scheidt barrier)

Deltares

Z4581

Zandhonger Oosterschelde

Fig. 3.13c



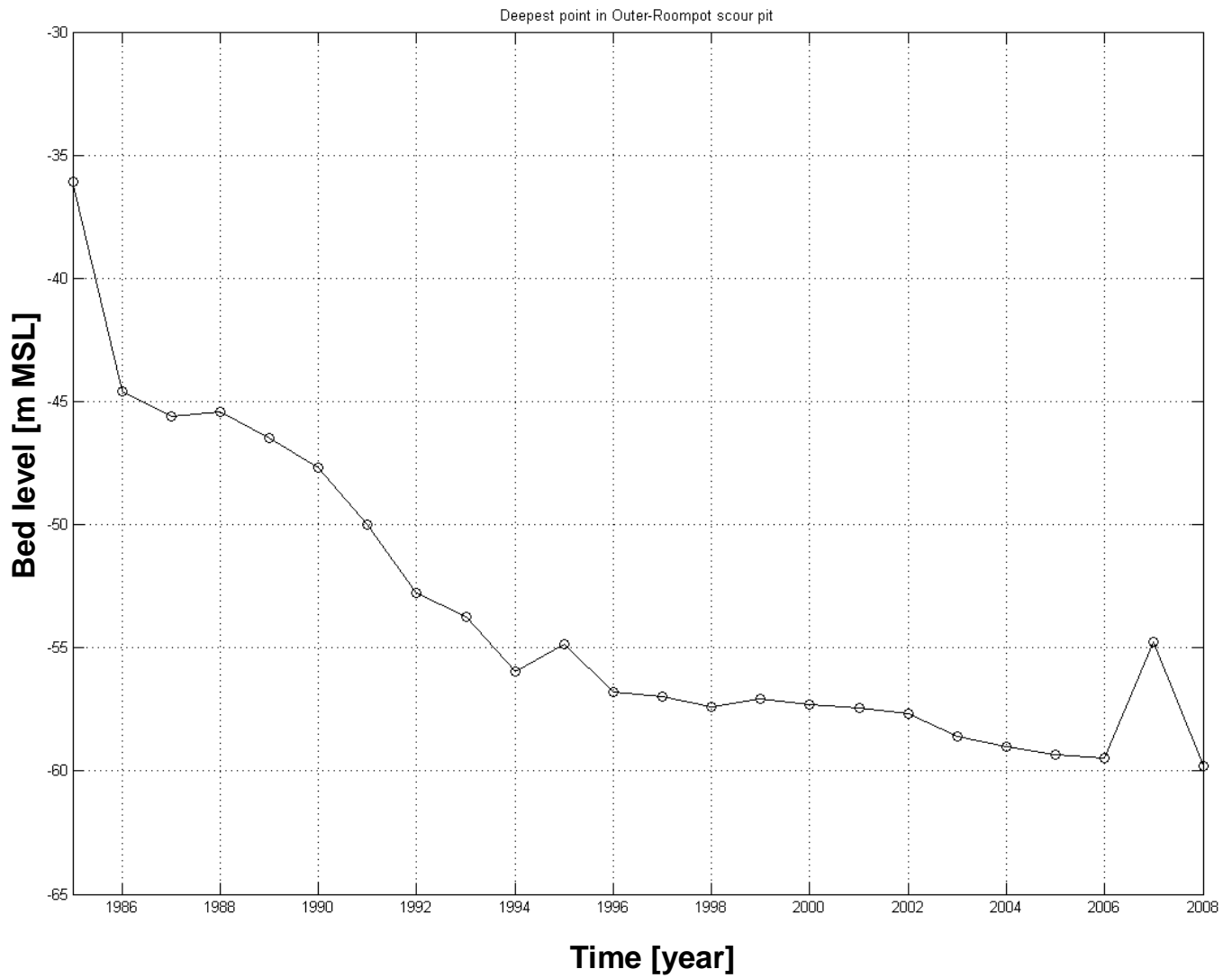
Bathymetry of the scour hole at the Roompot in 2008 (seaward of the Eastern Scheidt barrier)

Deltares

Z4581

Zandhonger Oosterschelde

Fig. 3.13d



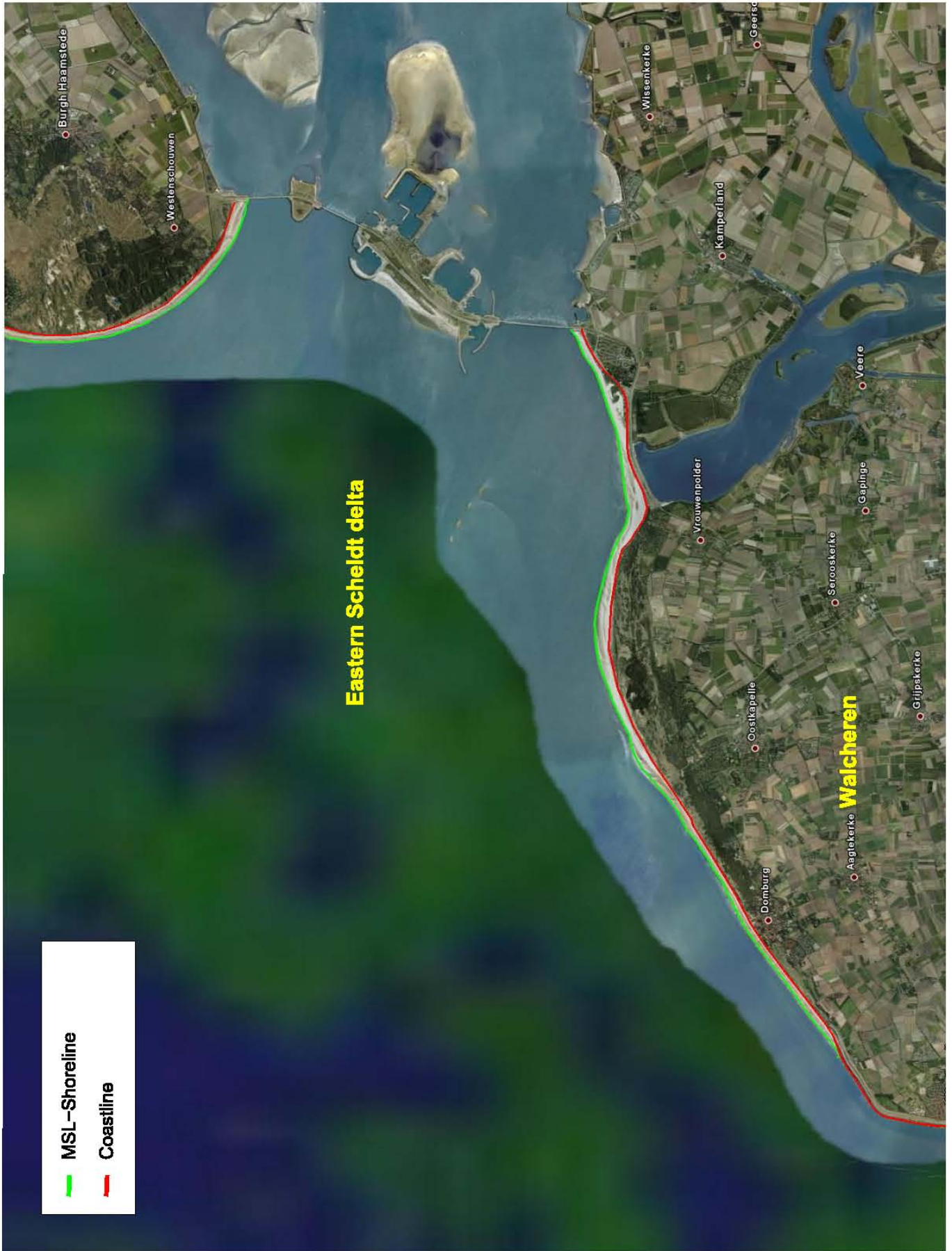
Development of scour hole (deepest point) in the Roompot after construction of the Eastern Scheldt barrier

Zandhonger Oosterschelde

Deltares

Z4581

Fig. 3.14



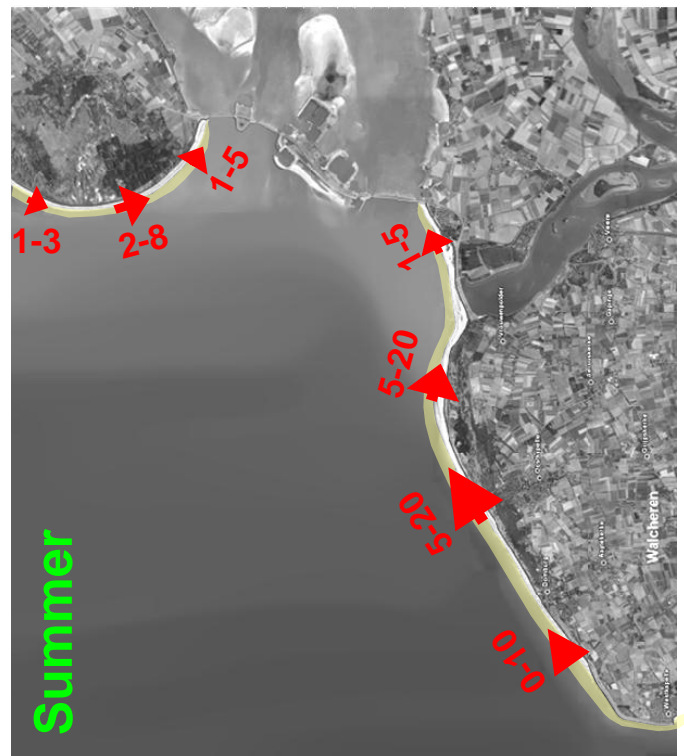
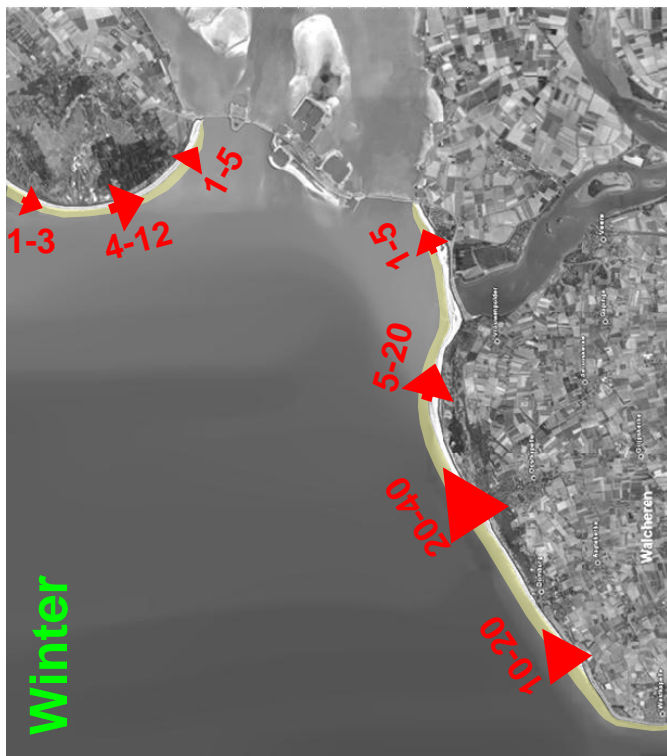
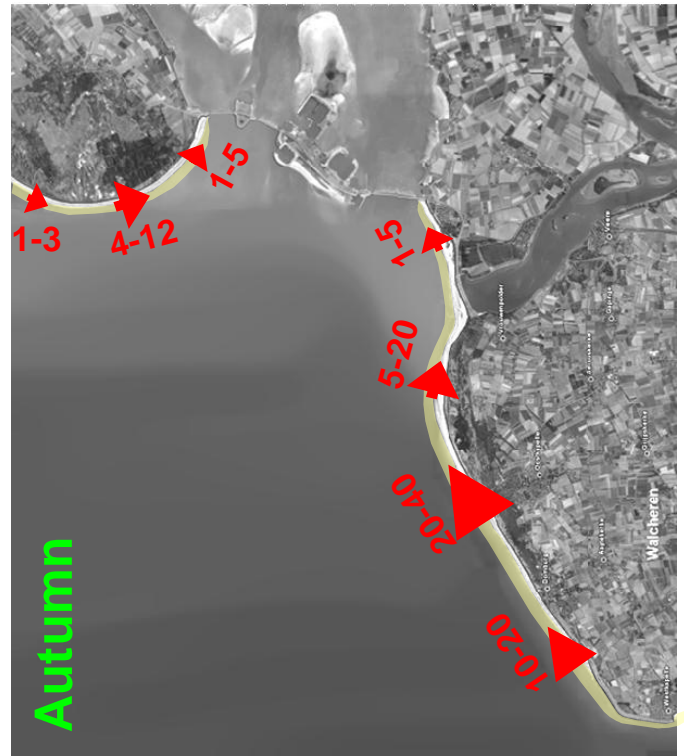
Digitised shoreline from satellite image
 (© 2008 Tele Atlas; Google Earth™ mapping service)

Zandhonger Oosterschelde

Deltares

z4581

Fig.4.1



Wave driven sediment transport along the coast of Walcheren and Schouwen for different seasons (transports are in $10^3 \text{ m}^3/\text{yr}$)

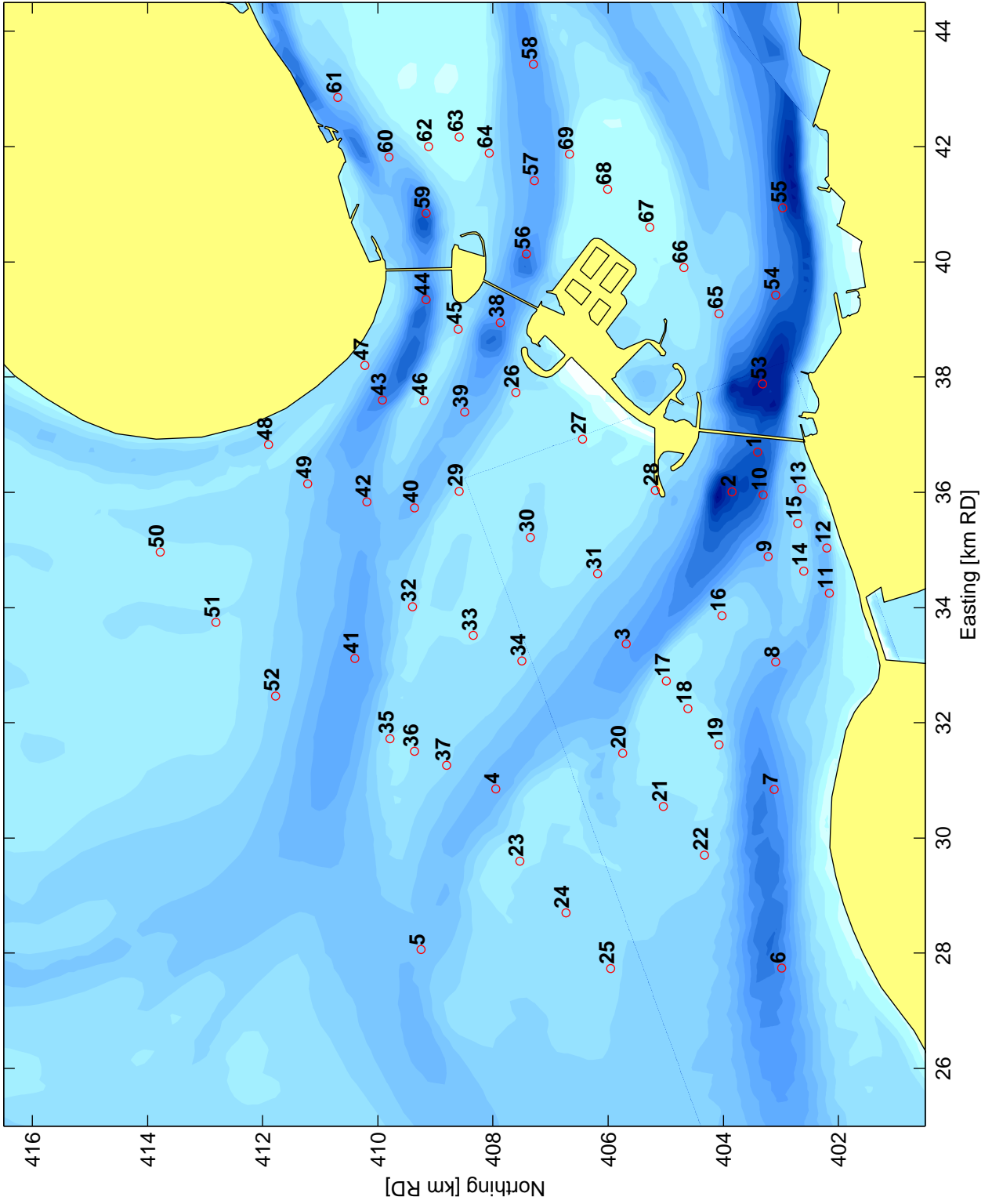
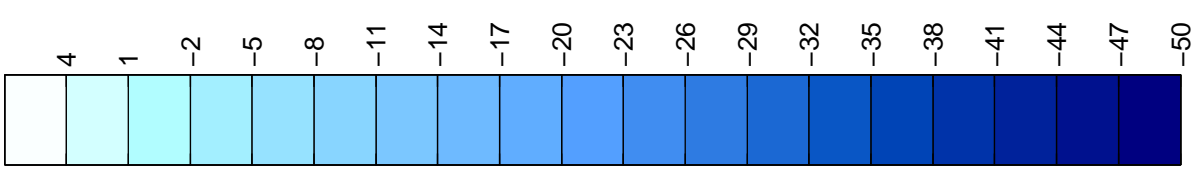
Zandhonger Oosterschelde

Deltares

Z4581

Fig. 4.3

Bed Level [m MSL]



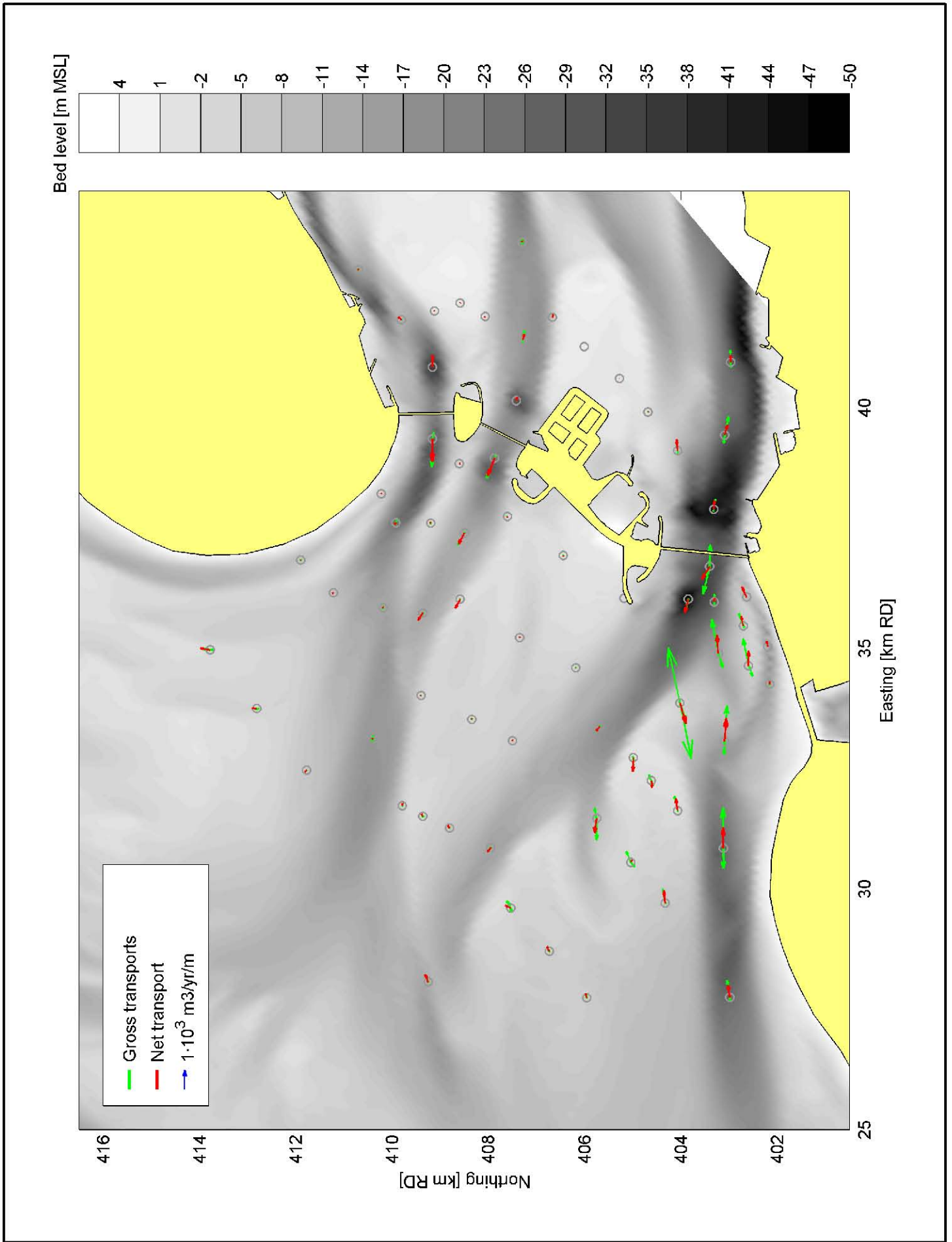
Output locations of the morphological point model
(1999 'MATROOS' bathymetry of the Eastern Scheldt delta)

Zandhonger Oosterschelde

Deltares

z4581

Fig.4.4



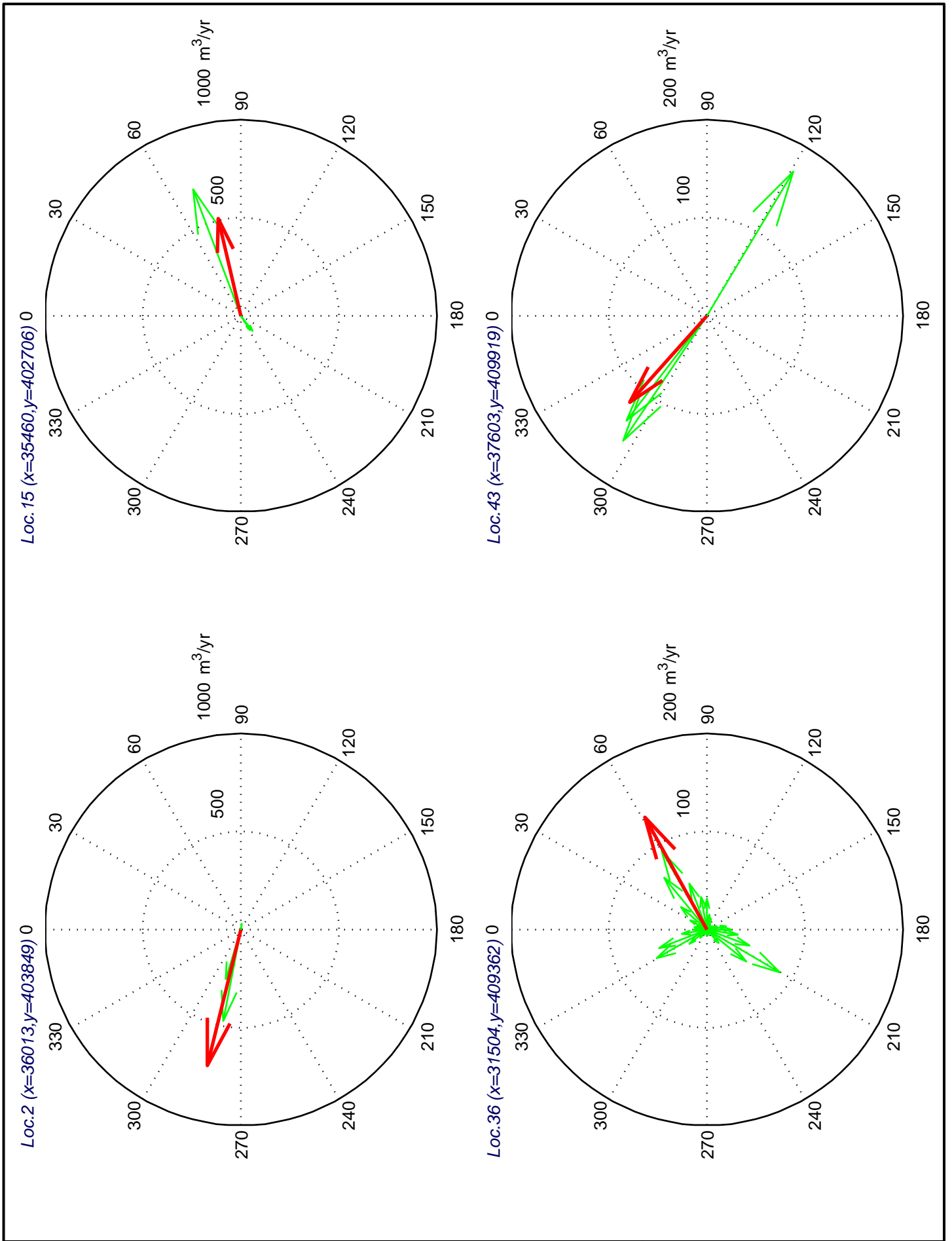
Potential sediment transport at 69 locations for 10° directional bins (1999 'MATROOS' bathymetry of the Eastern Scheldt delta)

Zandhonger Oosterschelde

Deltares

z4581

Fig.4.5a



Directional roses of the local sediment transport capacity for 10° bins (green) and net transport capacity (red) for locations 2, 15, 36 and 43

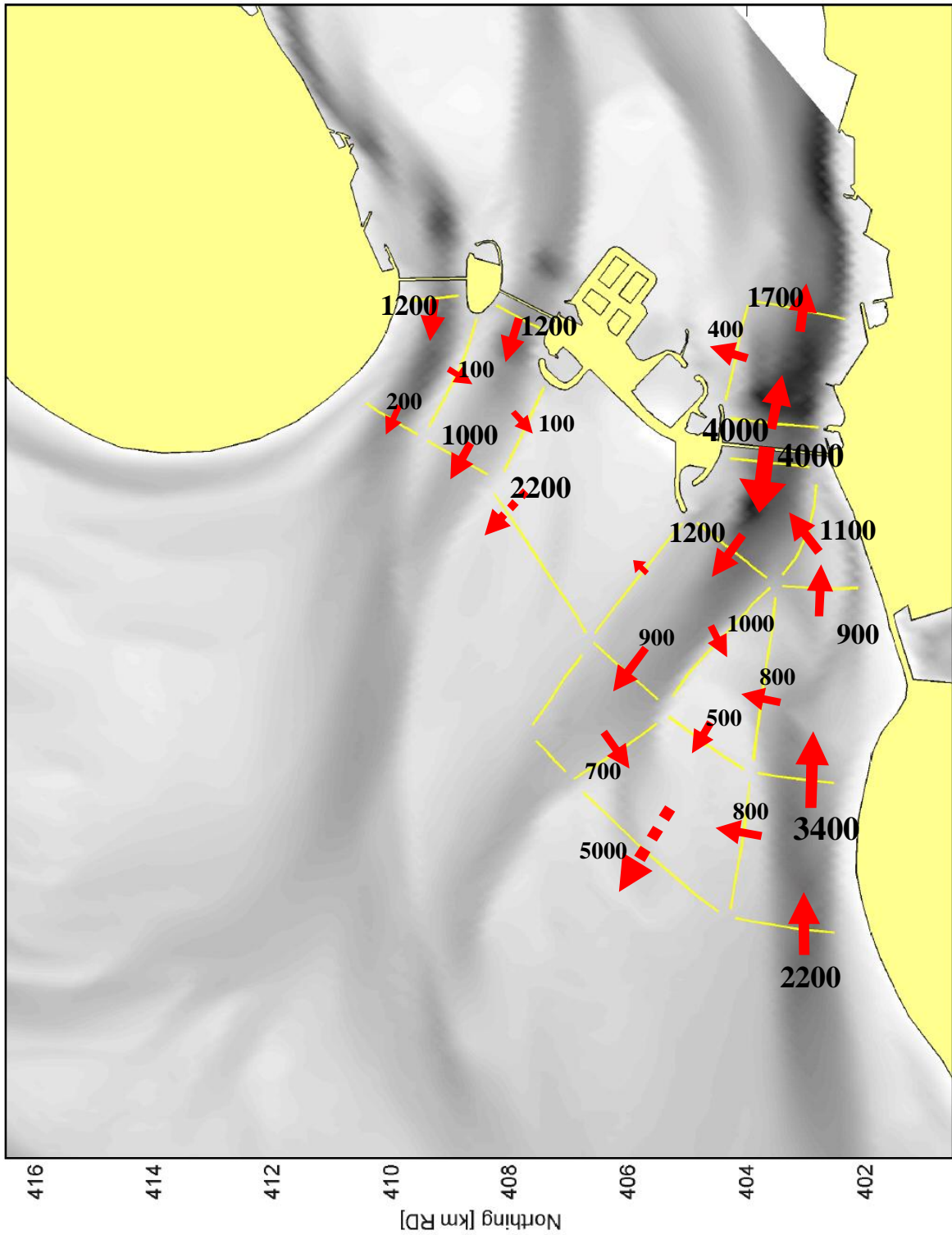
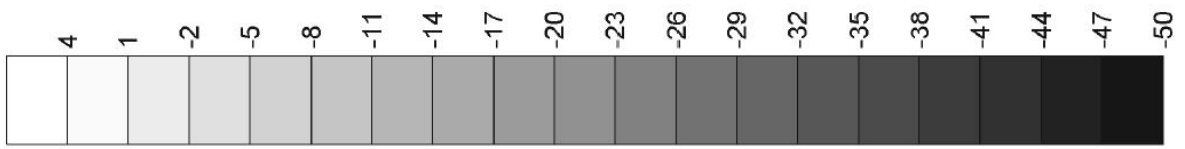
Zandhonger Oosterschelde

Deltares

z4581

Fig.4.5b

Bed level [m MSL]



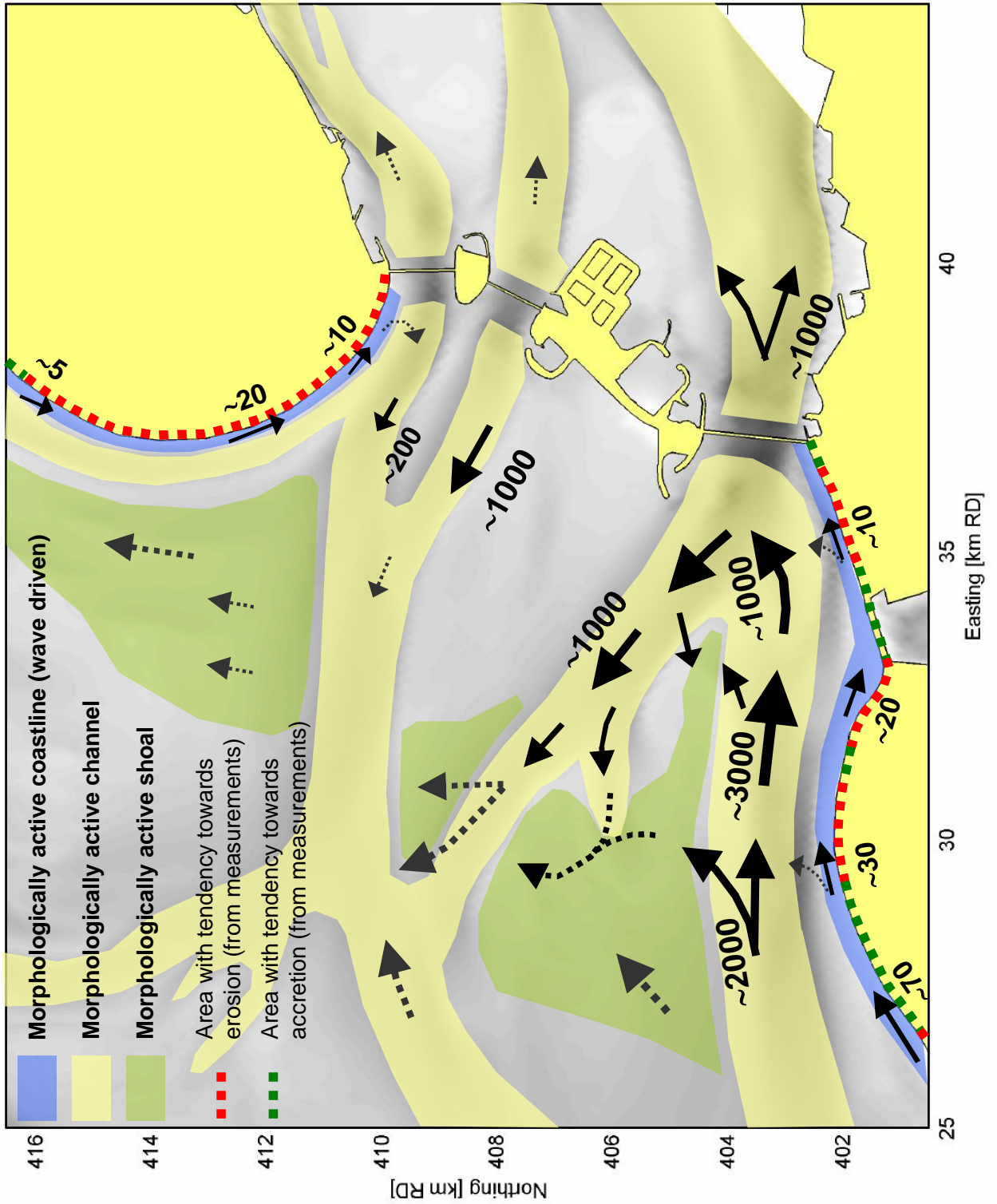
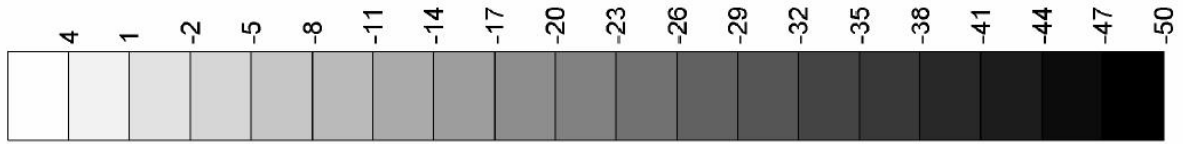
Potential net sediment transports over cross-sections (in 1000 m³/yr) after integration of sediment transport capacities over line sections

Zandhonger Oosterschelde

Deltares

Z4581

Fig. 4.6



Interpretation of sediment transport processes in the Eastern Scheldt delta (sediment transports in 1000m³/yr)

Zandhonger Oosterschelde

Deltares

Z4581

Fig. 4.7

Unibest-CL+

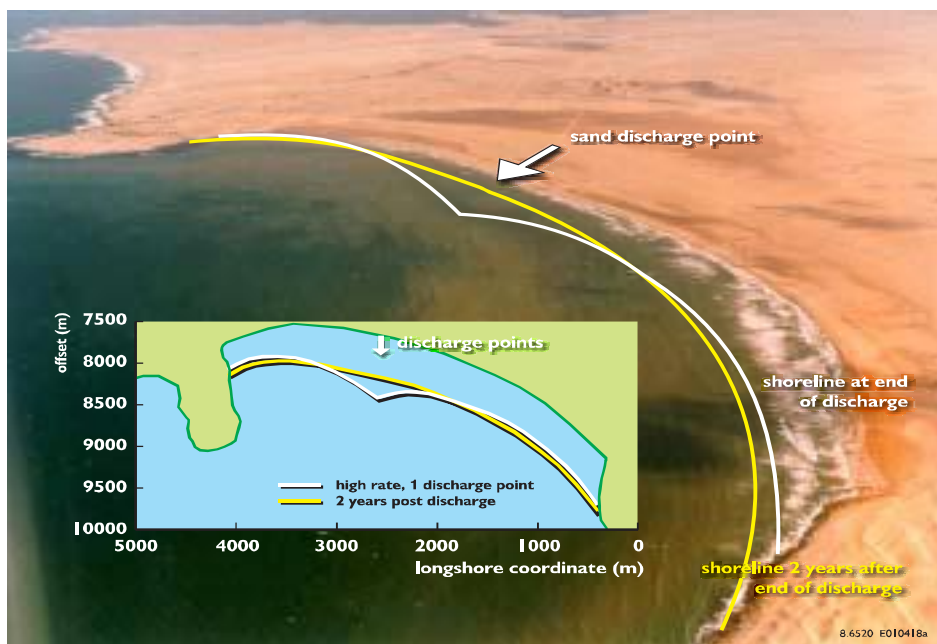
applications

UNIBEST-CL+ is a powerful tool to model longshore sediment transports and morphodynamics of coastlines. During its application on coasts world-wide it has proven to be a flexible and easy-to-access tool capable of simulating a large variety of coastal problems. UNIBEST-CL+ is a sediment balance model with which longshore transports computed at specific locations along the coast can be translated to shoreline migration. If required the effect of cross-shore phenomena can be included by importing the results of the UNIBEST modules UNIBEST-TC and / or UNIBEST-DE.

The shoreline model UNIBEST-CL+ can be used for a wide range of coastal engineering projects. A typical application is the analysis of the large scale morphology of coastal systems to provide insight in the causes of coastal erosion or to predict the impact of planned coastal infrastructure (such as a port) on the coast. But the model can also be used for considerations on a smaller scale, like the evaluation of the shoreline evolution around coastal protection works (groynes, revetments, river mouth training works and to some extent detached breakwaters). Sediment sources and sinks can be defined at any location to simulate river sediment supplies, the effect of land subsidence or sea level rise, offshore sediment loss, artificial sand bypass and beach mining. These features make it a suitable tool for the functional design of coastal defence schemes and the prediction of their impact on the coast, in the feasibility stage and in many cases also in the detailed design stage of projects.

The shoreline is defined relative to a user-defined reference line which may be curved. This enables the modelling of complex coastal areas such as deltas, bays, circular shaped beaches and even complete islands. Shoreline evolution computations can be made over a period of decades. In these computations changes in the longshore transports with time due to re-orientation of the shoreline are taken into account. Since the runs are very time-efficient, with a properly set-up model various scenarios can be evaluated and sensitivity analyses can be carried out.

The release of UNIBEST-CL+ marks a significant enhancement on its very successful predecessors UNIBEST-LT and UNIBEST-CL, and combines these two models in a windows environment. The improvements relate to the possibility of applying a curvilinear reference line, the definition of different scenarios, and the graphical output.



Example of prediction of re-distribution of discharged sand along the coast.

(courtesy of CSIR, South Africa and NAMDEB)

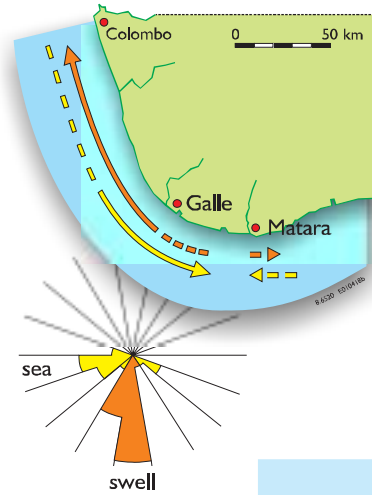
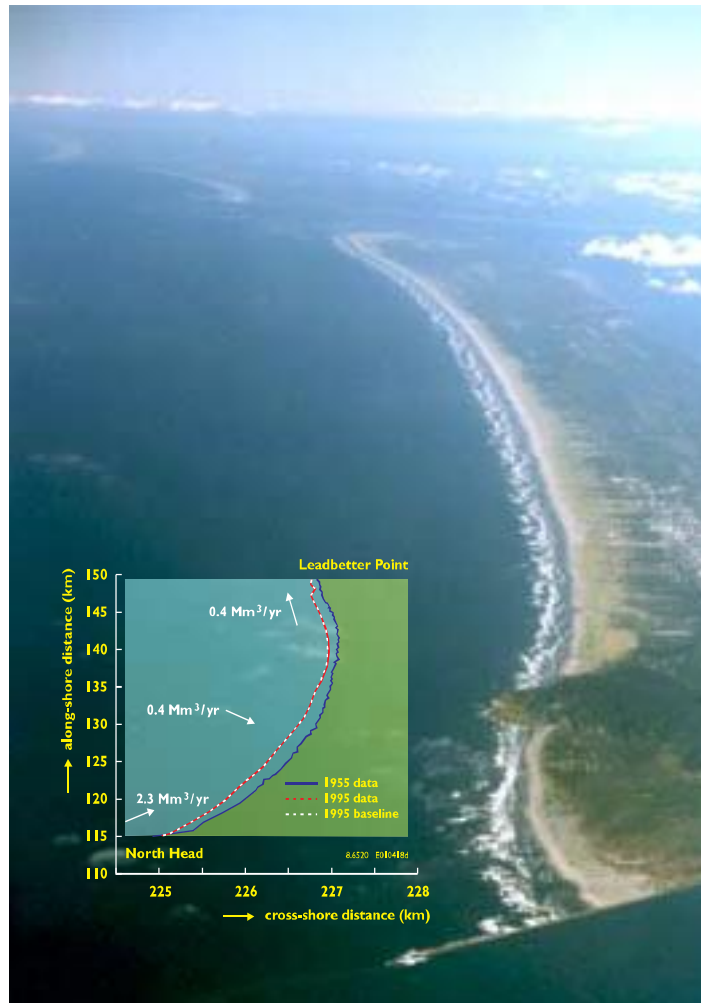


processes

Longshore currents and sediment transports generated by tidal currents and obliquely incoming waves are computed. The gradients in the (time-dependent) transports are used as input for the shoreline model.

The model includes a wave propagation module to transform the offshore wave climate to the surf zone (assuming fairly uniform depth contours) and to compute the surfzone dynamics, according to the Battjes-Stive model for wave propagation and wave decay. Principal processes are accounted for, such as changes in wave energy as a result of bottom refraction, as well as shoaling and dissipation induced by wave breaking and bottom friction.

The distribution of the longshore current along the coastal profile is derived from the depth-averaged momentum equation alongshore, where bottom friction, the gradient of the radiation stress and the tidal surface slope alongshore are accounted for.



Examples of computed distributions of longshore transport, wave height and longshore current along the profile

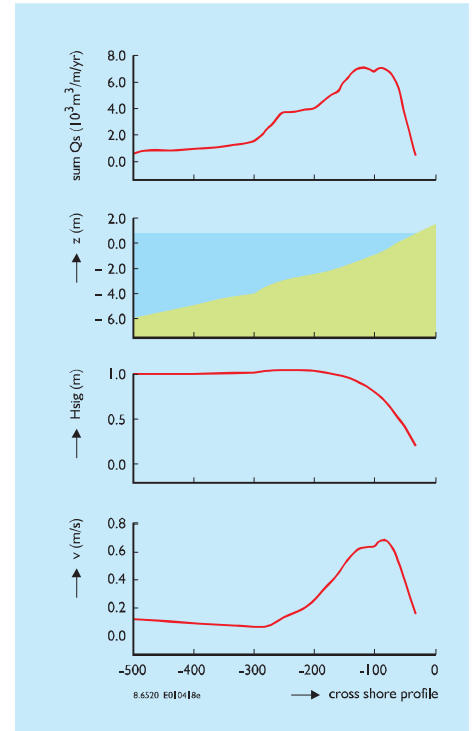
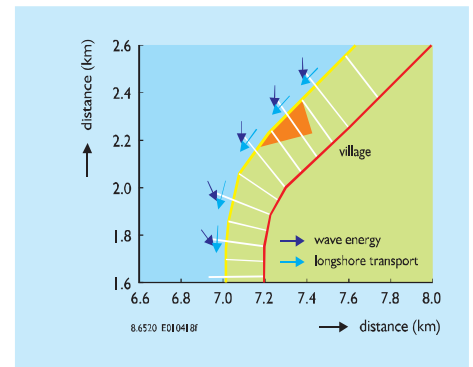


Illustration of curvilinear grid



Long Beach Peninsula, Washington, U.S.A. (Courtesy of the Washington State Department of Ecology, SW Washington coastal erosion study).

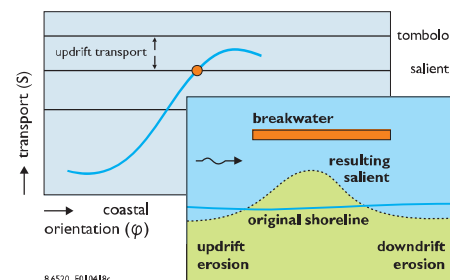
Longshore transport and its distribution along the coastal profile can be evaluated according to several total-load sediment transport formulae for sand (such as Bijker, van Rijn) or gravel (Van der Meer & Pilarczyk). The transports respond to local wave- and current conditions in an instantaneous, quasi-steady way. The net longshore transport can be computed on the basis of hundreds of combinations of wave- and tidal conditions, and the gross contributions in both directions can easily be derived.

An essential aspect in shoreline modelling is the strong relationship between the orientation of the coast and the longshore transport. In UNIBEST-CL+ this relationship is computed and presented in a so-called S- ϕ -curve. This curve forms the basis for the shoreline modelling since it provides information on transport gradients caused by a curvature of the coastline, as well as on the time-dependent response of the longshore transport on changes of the coast-orientation with time.

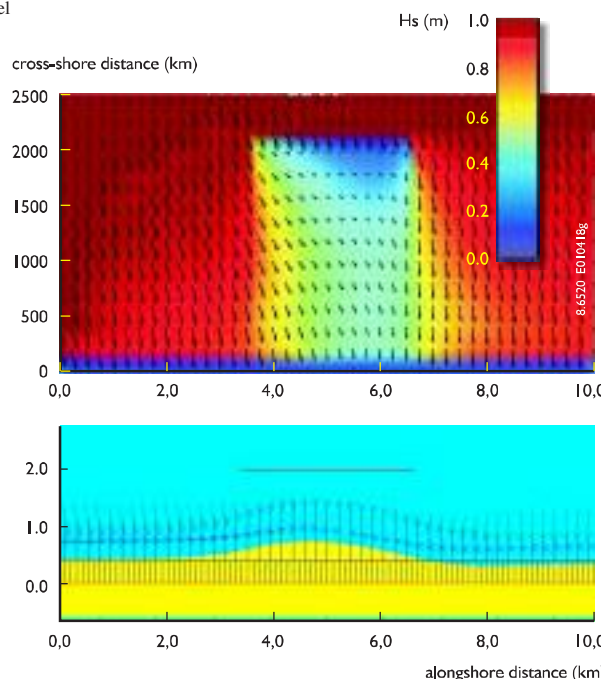
In the shoreline model the coast is represented by a single line. Given an active profile height and computed longshore transports along the coast the shoreline movement is computed on the basis of a continuity equation for sediment. Various initial and boundary conditions may be introduced so as to represent a variety of coastal situations. A non-uniform offshore or nearshore wave climate along the coast (e.g. due to structures) and resulting gradients in the longshore transport can be modelled. Different shapes of the coastal profiles can be defined along the coast and seasonal variations in the wave climate can be simulated.

The bypass of sand along structures is modelled, taking into account the cross-shore distribution of the transport and the time-dependent shoreline migration, including the effect of shoreline re-orientation updrift of the structures.

S- ϕ curve, providing insight in salient or tombolo formation



A wave field around offshore breakwater, computed with DELFT3D-WAVE model



hor. km	vert. km	erosion m/y
0.10	0.40	-5.46
0.30	0.40	-5.58
0.50	0.40	-5.82
0.70	0.40	-6.17
0.90	0.40	-6.64
1.10	0.40	-7.21

$Q_s = 1060.10 \text{ k} \cdot \text{m}^3/\text{y}$ $X = 0 \text{ m}$
 $Q_s = 1049.18 \text{ k} \cdot \text{m}^3/\text{y}$ $X = 200 \text{ m}$



Computed salient behind offshore breakwater, computed with UNIBEST-CL+

state-of-the-art wave propagation models SWAN and HISWA. With this option the development of the shoreline in and adjacent to the shadow zones of offshore islands, harbour moles and (large) detached breakwaters can be computed on the basis of detailed wave modelling in a time-efficient and flexible way. This option is especially valuable for the impact assessment or the functional design of structures, and for cases with a complex offshore bathymetry (shoals, channels, bays, non-uniform depth contours).

UNIBEST-CL+ generates output suitable for use in Geographical Information Systems (GIS) for the analysis of the effects of coastal erosion and coastal defence measures on values in the coastal zone.

link with other models

In most cases the nearshore coastal dynamics are largely determined by the waves and the wave-induced currents. A proper representation of the wave climate just seaward of the active profile is therefore essential, and translation of the offshore wave climate to nearshore locations is required. For many cases the wave propagation can be computed with the wave module of UNIBEST-CL+. However, for a complex bathymetry or for a situation with large structures the model is often applied in combination with 2DH wave propagation models. The new version of UNIBEST-CL+ offers the option to improve this procedure, by exchanging information with the sophisticated 2DH wave propagation model DELFT3D-WAVE in an efficient and user-friendly way. An interface helps the user to extract wave climates at nearshore points from computed 2DH wave fields in an interactive manner. This option is available for users who also own the model DELFT3D-WAVE. This model includes the

future developments

UNIBEST-CL+ is regularly upgraded so as to increase its scope. For the next release the graphical options for the definition of the coastline model will be improved for more accuracy and user-friendliness. On the basis of scanned maps of the area with this planned option the reference and the coastline, as well as the positions of the local wave climates and structures can be defined graphically.

model organisation

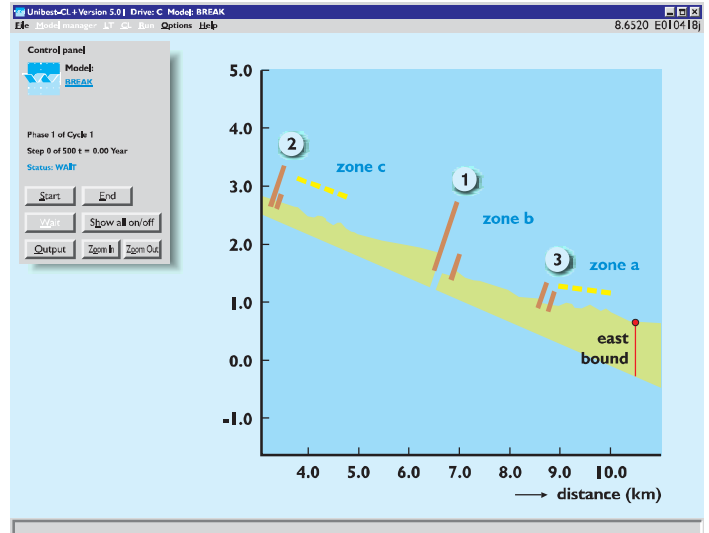
UNIBEST-CL+ runs under Windows-based systems and is controlled by a user-friendly interface in which input files can be created and edited, simulations be made and model results be graphically inspected. High-quality colour graphics can be sent to different hard copy output devices. Detailed output can be written to ASCII files. For the longshore transport computations a batch facility is provided to execute a large number of consecutive (sensitivity) runs. The various input fields are stored in different ASCII files, enabling the user to store and link different input combinations to the runs.

The main input consists of:

- the wave climate : combinations of significant wave height, wave period, wave direction and the percentage of occurrence of these combinations
- the tidal regime : combinations of current velocities and water levels and the percentage of occurrence of these combinations
- the coastal profile : any coastal profile and the active zone can be defined
- the parameters for wave propagation and sediment transport computations
- the sediment: characteristics of sand or gravel (non-cohesive sediment)
- the coastline
- the boundary conditions
- active profile heights
- grids, in the coastal profile and along the coastline
- structures (groynes, offshore breakwaters, revetments, sources/sinks)
- scenarios for combinations of above input, defining the runs

The main output (all to be graphically inspected and in ASCII files) consists of:

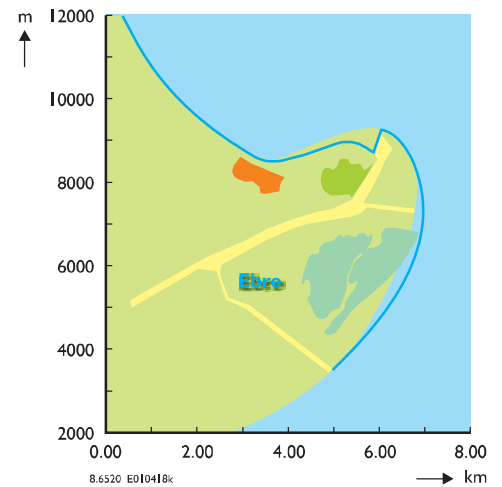
- the wave characteristics along the coastal profile
- the cross-shore distribution of the longshore currents (wave-induced and tidal)



with coastal protection schemes

- longshore transport for various coast-orientations if requested
- the cross-shore distribution of the longshore transport
- longshore transports in all profiles along the coast
- the coastline position, migration and orientation between grid points
- coastline migration rates between grid points

Example of application with strongly curved coastline



WL | Delft Hydraulics

Decisive advice: from multidisciplinary policy studies to design and technical assistance on all water-related issues.

Rotterdamseweg 185

p.o. box 177

2600 MH Delft

The Netherlands

telephone +31 15 285 85 85

telefax +31 15 285 85 82

e-mail info@wldelft.nl

internet www.wldelft.nl